

MINERALOGY AND PETROLOGY OF THE NEW IDRIA DISTRICT, CALIFORNIA

A DISSERTATION

SUBMITTED TO THE SCHOOL OF MINERAL SCIENCES

AND THE COMMITTEE ON GRADUATE STUDY

OF STANFORD UNIVERSITY

IN PARTIAL FULFILLMENT OF THE REQUIREMENTS

FOR THE DEGREE OF

DOCTOR OF PHILOSOPHY

IN GEOLOGY

By

Robert Griffin Coleman

January 1957

I certify that I have read this thesis and that in my opinion it is fully adequate, in scope and quality, as a dissertation for the degree of Doctor of Philosophy.

C. Osborne Hutton

I certify that I have read this thesis and that in my opinion it is fully adequate, in scope and quality, as a dissertation for the degree of Doctor of Philosophy.

Adolph Knopf

Approved for the University Committee on Graduate Study:

W. Steere

Dean of the Graduate Division

TABLE OF CONTENTS

	Page
Introduction	1
Purpose	3
Acknowledgements	5
Laboratory techniques	5
General Geology	7
Mineralogy	14
Perovskite	14
Benitoite	19
Neptunite	22
Joaquinite	24
Garnet Group	25
Pyroxene Group	38
Amphibole Group	46
Mica and Clay Group	51
Natrolite	58
Idocrase	61
New Mineral	62
Mineral List	63
Petrology	68
Franciscan type rocks	68
Peripheral Franciscan rocks	68
Tectonic inclusions	73
Jadeite bearing rocks	80
Origin of the jadeite	89
Serpentines	93
Intrusive rocks	100
Camptonite	101
Berkevikite soda syenite	104
Albitite and zeolite-rich rocks	113
Classification and origin of the igneous rocks	115
Metasomatic rocks	119
Chlorite rocks	120
Calc-silicate rocks	132
Titano-silicates and sodium silicate rocks	139
Origin of the metasomatic rocks	143
Minor and trace element study of rocks	146
Introduction	146
Boron	148
Vanadium	149
Gallium	149
Chromium	150
Titanium	150

TABLE OF CONTENTS

	Page
Minor and trace element study of rocks (continued)	
Columbium	151
Nickel and cobalt	152
Scandium	153
Zirconium	153
Rare earths	154
Barium and strontium	155
Silver	156
Lead	157
Copper	157
Other elements	158
Summary	159
Literature Cited	161

LIST OF TABLES

Table 1- Chemical analysis and physical properties of perovskite	18
2- Chemical and physical properties of benitoite	21
3- Chemical and physical properties of neptunite	23
4- Chemical and physical properties of joaquinite	26
5- Chemical and physical properties of titanian andradite	28
6- Determination of TiO_2 content from unit cell measurements	32
7- Refractive indices and TiO_2 content of titaniferous garnets	33
8- Chemical and physical properties of andradite garnet	35
9- Refractive indices and densities of the New Idria garnets	37
10- Chemical and physical properties of white jadeite	40
11- Comparison of optical data on jadeites	42

LIST OF TABLES

Tables (continued)	Page
Table 12- Comparisons of X-ray powder diffraction measurements of jadeite	43
13- Optical constants of pyroxenes	45
14- Chemical and physical properties of barkevikite .	47
15- Optical constants of glaucophane	49
16- Optical constants of crossite	50
17- Optical constants of New Idria chlorites and related minerals	54
18- Chemical and physical properties of kammererite .	59
19- Optical properties of kammererite compared with Cr ₂ O ₃ and Al ₂ O ₃ content	60
20- Variation in the optical constants of the idocrase with Ti content	62
21- Modal analysis of camptonite	105
22- Modal analysis of syenite	108
23- Chemical analyses of camptonite and syenite . . .	111
24- Norms of analysed camptonite and syenites	112
25- Calculation of the standard rock cell for serpentine and calc-silicate	136

LIST OF ILLUSTRATIONS

Plate I- Geologic map of the New Idria district	In pocket
II- Geologic map of calc-silicate body	In pocket
III- Geologic map of the Gem mine	In pocket
IV- Spectrographic analysis of rocks and minerals . .	In pocket
V- Photomicrographs of perovskite crystal	16

LIST OF ILLUSTRATIONS

Plates (continued)	Page
Plate VI- Photomicrographs of peripheral Franciscan schists . .	74-A
VII- Photomicrographs of schist from tectonic inclusions	81-A
VIII- Photomicrographs of the serpentines	96-A
IX- Photomicrographs of camptonite and syenite	114-A
X- Photomicrographs of metasomatic rocks	130-A
XI- Camera lucida drawings of metasomatic rocks	131
XII- Photomicrographs of metasomatic rocks	131-B
XIII- Camera lucida drawings of metasomatic rocks	141
Figure 1- Index map showing location of the New Idria district .	2
2- Relation of unit cell size and TiO ₂ content in titaniferous andradites	30
3- Relation of refractive index to density in the grossularite-tricalcium aluminum hexahydrate series .	37-A
4- New Idria chlorites plotted on Winchell's optical and chemical classification for chlorites	55
5- Camera lucida drawing of kammererite showing its formation from chromite	57
6- Sketch of lens-like jadeite body	83
7- Geologic map of tectonic inclusion containing jadeite	85
8- Polished slab of albite-glaucophane-acmite schist . .	86
9- Sketch of jadeite vein	88
10- Geologic map of syenite intrusion	106

INTRODUCTION

The area commonly referred to as the New Idria District is located in the southern extension of the Diablo Range of the California Coast Ranges. The rock complex studied is an elongate serpentine dome about 12 miles long and 4 miles wide, situated wholly within the New Idria, California quadrangle (Figure 1).

The New Idria District has long been known as the site of one of California's most productive quicksilver deposits. Cinnabar was first discovered about 1853 and since that time, up to 1944, 437,195 flasks of quicksilver have been produced. This production is valued at about \$31,000,000 (a flask of mercury now contains 76 pounds, although this weight has varied during the production history of the district). The geology of the ore deposits has been described by many writers, including Becker (1888), Eckel and Myers (1946), Lake (1929), Schutte (1931), and Yates and Hilpert (1945). These reports and accompanying maps have been consulted frequently and in part have been incorporated into the present study. Since this present investigation is not concerned directly with the cinnabar deposits, the reader is referred to the above references for a complete description, particularly Eckel and Myers.

The district is situated in a rugged and isolated portion of the Diablo Range trending about N 40° W. The serpentine dome is characterized by soft rounded hills, excepting San Benito Mountain (Elev. 5248) and Santa Rita Peak (Elev. 5164) which are prominent peaks of more resistant serpentine. Flanking the serpentines are resistant

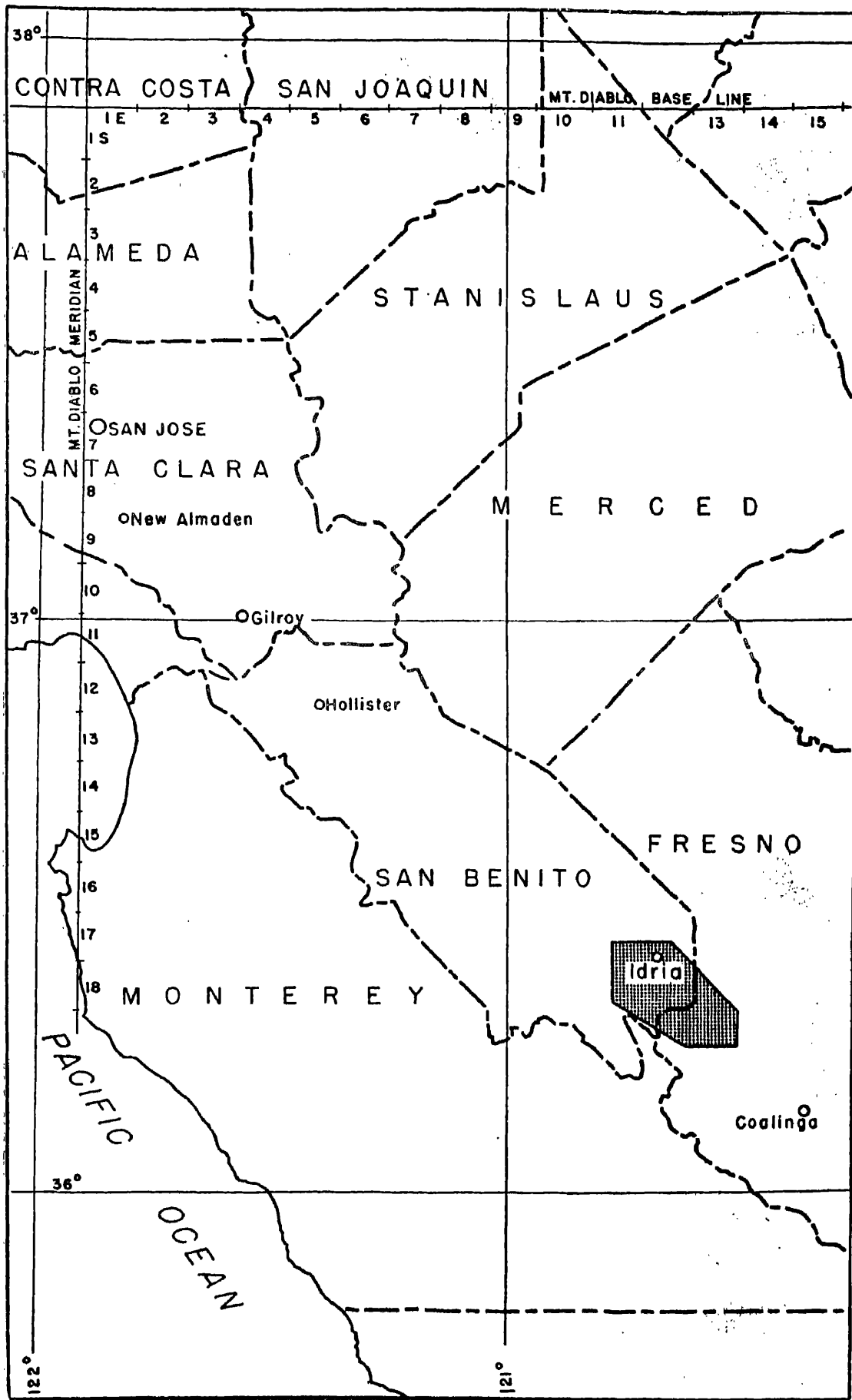


FIGURE 1. Index map showing location of the New Idria district.

sedimentary ridges marked by Sampson Peak (Elev. 4900), San Carlos Peak (Elev. 4843), and Wright Mountain (Elev. 4560). To the south, the serpentine dome assumes a sharp ridge form which branches to the east from the main Diablo Range and is here called Joaquin Ridge. The relief within the serpentine is somewhat subdued as a result of the peculiar way in which the serpentine weathers. In contrast, the relief is sharply increased in the more rugged sedimentary rocks. The total relief of the area studied is about 3,000 feet.

The headwaters of the San Benito River lie in the central and western portions of the serpentine. The river drains to the SW where it cuts a deep canyon through flanking sedimentary rocks. The northern part of the serpentine is drained by Clear Creek which also flows SW through sedimentary rocks and joins the San Benito River at Hernandez, whereas the southern part of the dome is drained by White Creek which joins Los Gatos Creek to the south. The drainage divide of the area is described by a line through San Carlos Peak to the north and Santa Rita Peak and Joaquin Ridge to the south. All of the east flowing streams are small and intermittent.

The serpentine area is marked by poor soil development and an almost complete lack of grass and much of the area is completely bare of vegetation. In contrast, the ground cover in the sedimentary rock area is marked by well developed grass and open oak groves.

PURPOSE

This investigation was undertaken to study a peculiar suite of minerals found within the serpentine and the associated rock types; it is a well known area for the variety of minerals found within the serpentine, and the discovery of benitoite (Louderback, 1907) was the first report on

the peculiar and distinct type of local mineralization. Since this first account many additional discoveries of small bodies containing calc-silicates and titano-silicates have been recorded, and recently several outcrops that contain jadeite were discovered along Clear Creek, increasing the already complex variety of minerals present in this interesting area. An attempt was made to correlate these small isolated mineral complexes with the surrounding and enclosing rocks in order to ascertain if all of these deposits were related to a single stage of mineralization within the serpentine or if they represented several distinct periods of mineral introduction. In conjunction with the problem of origin, detailed mineralogical studies are herein reported for many of the individual mineral species to establish their exact chemical and physical character.

Field work and mineral collecting extended through 1950 to 1952; no long periods of time were spent in the field although the aggregate time spent doing field work was about three months. Considerable time was spent in the laboratory purifying and analyzing the mineral species; the methods used in the laboratory investigation will be described in detail. All of the rock and mineral samples collected are now in the Stanford University collection. The samples are labeled with the author's initials (RGC) followed by the sample number and the year collected, i.e., RGC-32-50. These sample numbers are used in the text to identify the specimen and also for location. On plate I the sample numbers are plotted at points of collection in order that the reader may ascertain the geologic location of each specimen.

ACKNOWLEDGEMENTS

The author wishes to acknowledge the helpful guidance and counseling provided by Professor C. O. Hutton during the course of this investigation. Laboratory facilities and equipment were provided at various stages throughout the investigation by Louisiana State University, Atomic Energy Commission, and the U. S. Geological Survey, these are gratefully acknowledged. I am indebted to Hatten Yoder and George Switzer who reviewed the manuscript and have given me many helpful suggestions.

LABORATORY TECHNIQUES

Those minerals which were studied in detail were carefully separated from the enclosing rock by various techniques to ensure a pure mineral phase. Since these methods are not standard, they are described below.

The Franz Isodynamic Separator proved to be the most useful device in effecting a preliminary concentration of a desired mineral. The rock is crushed to the desired size to ensure that the individual fragments were free from inclusions, and the sized fraction is then elutriated to remove the finer dust. The coarse sized material is then passed through the magnetic separator to effect a preliminary concentration, which was then centrifuged with appropriate heavy liquid until a relatively pure concentrate was obtained. All of the mineral species analyzed in this paper were purified in this manner and in all cases the analyzed material was 95% or greater in purity.

It was found that for the complex calc-silicate and titano-silicate rocks, the various minerals could be isolated and grouped by a generalized

separatory procedure. The various steps follow:

1. Rock crushed to pass through 100 mesh sieve and then elutriated to remove fine dust particles. Further sizing was carried out so that the material used for magnetic separation was between 100 and 200 mesh.
2. About 50 grams of the sized material was passed through the magnetic separator at settings from 0.2 amps to 1.3 amps in steps of 0.2 amps.
3. Each fraction was then inspected under the binocular to determine the number of minerals present.
4. Those fractions which showed two or more minerals present were centrifuged first in bromoform and the heavies thus obtained were further centrifuged in methylene iodide. The methylene iodide heavies were further centrifuged in Clerici solution if additional separation was necessary.
5. Routine optical and micro-chemical methods followed.

This method of determining the minerals present has many advantages over thin section study, since those minerals present in minor quantities may be completely overlooked in thin section; whereas in a 50 gram sample, systematic separation almost invariably produces enough of these minor minerals for a positive identification. Further, by magnetic and density fractionation, identification of the minerals is facilitated as the minerals are placed in definite ranges according to their density and magnetic properties. Tabulated below are the minerals commonly found to be susceptible at a range of field strengths as determined during this investigation. The separator was set at a tilt of 5° and a slope of 10° .

Amperage

< 0.2	ilmenite - chromite.
0.2 - 0.4	Fe-chlorite - stilpnomelane - barkevikite - andradite - melanite.
0.4 - 0.6	Mg-chlorites - idocrase - sphene.
0.6 - 0.8	idocrase - apatite - calcite - diopside.
> 0.8	apatite - perovskite - zeolites - calcite.

Analyses of the minerals completed by the author followed the procedures recommended by Hillebrand and Lundell (1929). These analyzed minerals posed no particular problems and the procedures followed were strictly those recommended for the elements desired.

Density determinations on purified mineral powders were made with a micro-pycnometer and CCl_4 as the liquid. Other density determinations were made on the Berman Balance.

Determinations of refractive indices were made by the immersion method and the combination of 'oils' which matched most closely the desired optical direction was measured directly by the Abbe' refractometer using sodium light. For those minerals which have indices greater than the immersion liquids, a small prism was made along the desired optical direction and the refractive index was determined on a single stage goniometer by the minimum deviation method. The universal stage was used to relate the optical direction with crystallographic direction, and also for determination of feldspar compositions using the method described by Turner (1947).

The semi-quantitative spectrographic analyses of the rocks and minerals were done on 10-mg samples following the method of Waring and Ansell (1953).

GENERAL GEOLOGY

The general geology of the New Idria District will be discussed very briefly in order to establish the geologic situation in which these peculiar metasomatic rocks occur. The geology of the region has been described in more detail by several writers: Eckel and Myers (1946), Anderson and Pack (1915), Mielenz (1939), and Phillips (1939). Their maps and discussions

have been consulted freely and in part incorporated into this discussion. The geologic map of the area (Pl. I) is essentially the same as that of Eckel and Myers, although the author has added or subtracted data where there was a difference of interpretation. All the major contacts were walked out and as much of the serpentine area as possible was carefully investigated by walking out all of its drainage system.

Serpentines, which make up the largest areal unit of the mapped area, lie between the San Andreas fault on the west and the Great Valley of California on the east. The rocks in this area are folded in a series of anticlines and synclines trending about N. 70° W. This folding is somewhat oblique to the general trend of the San Andreas fault which trends N. 40° W. The serpentine is an elongate oval body which is flanked by the Franciscan formation of Jurassic age and the upper Cretaceous Panoche formation. Serpentine and flanking rocks form an asymmetric anticlinal dome. Eckel and Myers have shown that the northeast flank of the dome is marked by overturned beds and by the irregular New Idria thrust fault which follows along or near the Franciscan-Panoche contact. The remainder of the contact around the dome is marked by a shear zone which is expressed by topographic lows and where the contact can be inspected it is marked by high angle faults or shear zones. The fault bounded serpentine seems to have moved upward in relation to the Franciscan and Panoche formations.

The rocks which crop out in the area investigated are divided into six types: (1) Franciscan formation of Jurassic age, (2) serpentine, (3) Panoche formation of Upper Cretaceous age, (4) younger Cretaceous and Tertiary sedimentary rocks, (5) syenite intrusives, and (6) superficial deposits. These have been listed in their apparent chronological order and

will be discussed briefly in that order.

The Franciscan formation has been considered as Jurassic in age by Reed (1933) and Taliaferro (1943) and in this particular area no fossil evidence is present to support or disprove this age. Since the Franciscan is the basement rock here, as it is in many areas, the pre-Jurassic geologic history is obscure. The Franciscan consists mainly of greywacke sandstone with some interbedded conglomerate and shales. Minor in volume but characteristic of the Franciscan formation are thin bedded lenses of chert associated with basaltic lavas. The basaltic rocks are discontinuous and are largely altered to greenstones which are spilitic in character. The Franciscan formation is at least 5000 feet in thickness and the most extensive exposures are along the southwestern part of the dome; elsewhere it appears as a discontinuous rim around the serpentine. Large and small tectonic inclusions within the serpentine may have been formerly part of the Franciscan formation; these have been mapped as Franciscan (Pl. I). Metamorphism of the Franciscan formation has been irregular and spotty in the district and has produced a grade of metamorphism similar to that of the green schist facies; glaucophane schists of the Franciscan formation are found within these metamorphosed zones. The Franciscan in other parts of the Coast Ranges is generally overlain unconformably by Cretaceous and Tertiary rocks, although in the New Idria District the contacts between the Franciscan and younger formations are usually faulted. The Franciscan formation, therefore, seems to have gained its present position by tectonic movements and a direct stratigraphic sequence with the younger sedimentary rocks cannot be established. A more

complete discussion of the rock types within the Franciscan is given later in the section on petrology.

The serpentine in the New Idria District as well as those serpentine bodies 'intrusive' to the Franciscan formation in the Coast Ranges have been considered as part of the Franciscan formation and tentatively are called Jurassic in age. Detrital serpentine within the lower beds of the upper Cretaceous rocks in this district shows that some of the serpentine is at least older than upper Cretaceous. The serpentine forms the entire central part of the district and Eckel and Myers report small elongate bodies of serpentine along the New Idria and other faults where these separate the Franciscan and Panoche rocks. An important feature of the serpentine is the nature of its contact with the surrounding sedimentary rocks. This contact is most certainly faulted around the entire serpentine body and evidence of intrusive contact action is completely lacking. These faulted contacts suggest that the serpentine has been brought into its present position by tectonic movement and not by intrusive forces; therefore, the age of the primary ultrabasic rock cannot be determined by the present exposed contact relationships. The original movement of the ultrabasic 'magma' (probably a crystalline mush) into the earth's crust may well have been during the period of maximum downwarping of the Franciscan geosyncline. Tectonic movements following the original emplacement of the ultrabasic rocks have probably resulted in the serpentinization and upward squeezing of the rock into its present position. The emplacement of the serpentine may have been accomplished in several distinct stages, and this view is supported by the presence of abundant serpentine debris in nearby sediments of three widely different ages; in the upper Cretaceous (Panoche formation),

the late middle Miocene (Big Blue member of the Vaqueros formation), and the Pliocene (Tulare formation) as pointed out by Eckel and Myers. A more detailed description of the petrology of the serpentine is given later in the text.

The Panoche formation, of upper Cretaceous age, consists of shaly beds and sandstones. It completely surrounds the body of serpentine and Franciscan rocks, extending to the northwest and southwest away from the mapped area. The Panoche formation is 20,000 feet thick at the type section, (Anderson and Pack, 1915), although in the southern portion of the district only 10,000 feet are present and near the New Idria mine it thins to 5,000 feet. As mentioned earlier, the contacts between the Panoche formation and the older Franciscan formation are faulted and it is presumed that the pre-faulting relationships were unconformable. The basal layers of the Panoche formation are conglomeratic and contain abundant serpentine and Franciscan debris cemented with magnesite. The basal conglomerate grades upward into shale and concretionary sandstone in about equal proportions. Most of the sandstone is in the upper half of the formation although sandstone lenses are commonly interbedded in the lower shaly member. The Panoche formation is important with respect to the cinnabar deposits of the district as most of the larger ore deposits are found within the Panoche formation.

The Panoche formation is overlain conformably by the Moreno shale of upper Cretaceous age. The Moreno crops out in a continuous belt near the north edge of the area and is 3,000 feet in thickness in the northwest corner of the district but thins to about 1,000 feet near New Idria. The

Moreno is characterized by chocolate-brown to maroon or purple platy organic shale which generally serves to distinguish it from the Panoche formation and the overlying Tertiary beds. The Moreno formation is made up of clay shale of clastic origin, organic siliceous shale with foraminifera and diatoms, and some lenses of arkosic sandstone. Large scale calcareous concretions with megascopic fossils are commonly found in the shales.

The Tertiary beds range in age from Eocene to Pliocene and represent several thousand feet of thickness. The beds are undivided since they have little bearing on the present investigation. These beds shown only in the northern part of the map (Pl. I), consist largely of soft gray clay which have been interpreted as lake deposits by Melenz (1939) and Eckel and Myers (1946).

Within the serpentine three small intrusive bodies of syenite and camptonite are located in the southeastern portion of the dome. Two of these bodies are clearly intrusive into the serpentine and the third body along the extreme southern border at the headwaters of White Creek is part of a large landslide mass which pushed out over the Panoche formation obscuring the original relationships. Eckel and Myers (1946, p. 91) state that the syenite is intrusive into the Panoche shales at this locality, but there is no field evidence to support this. The syenite has actually arrived at its present position across the serpentine-Panoche contact by landslide action and not by intrusive action. The age of these intrusions can only be inferred, although they are definitely later than the serpentine and by their lack of deformation appear to be of late Tertiary age. These intrusive rocks

are unique in that they have no correlatives in other parts of the Coast Ranges. Tertiary volcanic and intrusive rocks are common in the Coast Ranges but none of these rock types bear any resemblance to these syenites and camptonites.

The plastic nature of the serpentine and its deep weathering in the district combined with rather sharp relief have produced large landslide masses within the serpentine; the largest of which is in the southern portion of the area where about four square miles of it have been mapped (Pl. I). These masses are composed of the same serpentine material that is found along the ridges at their heads. The larger ones have traveled several miles crossing the serpentine-sedimentary rock contacts and filling valley bottoms of the streams draining away from the dome. Some of the older landslides show considerable erosion of the original hummocky surface. Several have forced streams to cut new valleys along their edges producing a peculiar topography, with the stream valleys having double drainage around the center filled in by serpentine debris. Many of these slides are still active, moving slowly during the rainy seasons and probably more rapidly when triggered by local earthquakes which are common in this region.

MINERALOGY

The New Idria District has an extensive suite of rare and peculiar minerals, and this study has attempted to investigate and describe systematically the species present, exclusive of the mercury deposits. The minerals characteristic of the metasomatic bodies within the serpentine were studied in the greatest detail in addition to those from other rock types which were poorly known or exhibited exceptional development.

PEROVSKITE

Perovskite was first reported from the New Idria District by Bolander (1950a) and later by Pabst (1951) and Murdoch (1951). The locality for the original discovery is given as the SE 1/4 of sec. 25, R. 12 E., T. 18 S. Four additional locations have been discovered in this study, all of them within section 25. These localities are numbered 34, 37, 56 (original discovery), 57, and 83: see Plate I.

In these five localities perovskite assumes several habits and exhibits a range of color and crystallinity. Perfect euhedral crystals are found at locality 56 and here perovskite, associated with black euhedral melanite and reddish prisms of idocrase, forms drusy surfaces and veins within a chlorite rock. Perovskite from localities 34, 37, and 37 crystallized as anhedral grains or as distinct veins within chlorite rocks, and is sometimes completely surrounded by melanite or forms discontinuous veins mixed with melanite. Localities 56 and 83 are the only two exposures which produced euhedral crystals of perovskite.

Euhedral perovskite is dominantly shiny black grading to dull yellow, and forms crystals up to one centimeter square. The crystals show cubic form and are commonly modified by (011) and (111) faces. Occasional single octahedra are noted, particularly from locality 83, and Pabst (1951) and Murdoch (1951) report additional forms; (023), (034), (045), (311). The following interfacial angles were determined on a picked crystal from locality 56.

$$100 \wedge 010 = 89^{\circ}59'30''$$

$$111 \wedge 110 = 35^{\circ}07'00''$$

$$100 \wedge 110 = 45^{\circ}00'00''$$

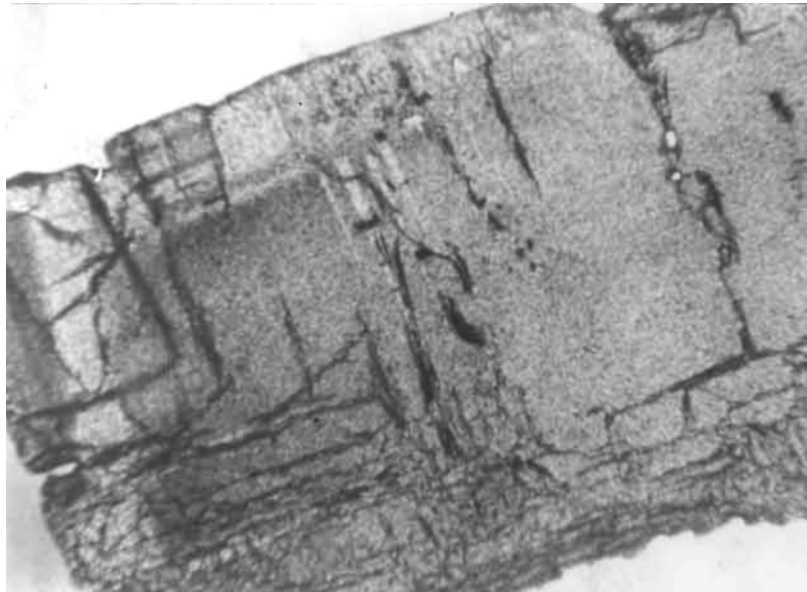
Some question regarding the symmetry of perovskite has been raised by Bowman (1908), Zedlitz (1939) and Murdoch (1951), since the external symmetry of perovskite conforms to the isometric system, although X-ray study and the optical character suggest either orthorhombic or monoclinic symmetry. Interfacial angles measured on the New Idria perovskite certainly suggest an isometric character, although optical examination shows it to be anisotropic with biaxial optics. Perovskite is listed as pseudo-cubic in Dana's seventh edition (Palache, et al., 1944) and comparison of unit cell dimensions (calculated on the basis of isometric structure) of the New Idria perovskite with the cell edge of other occurrences shows fair agreement.

$$\text{New Idria} - 7.63 \text{ \AA} \pm 0.01$$

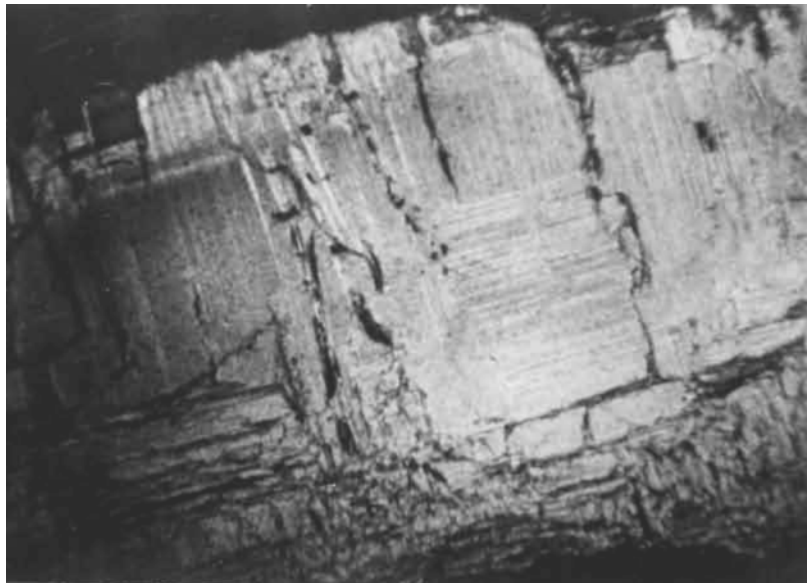
$$\text{Urals} - 7.645 \text{ \AA} \pm 0.015$$

$$\text{Zermatt} - 7.590 \text{ \AA} \quad ?$$

$$\text{Crestmore} - 7.64 \text{ \AA} \pm 0.01$$



1



2

PLATE V. Photomicrographs of perovskite crystal cut perpendicular to the c-Axis. (X 40)

Figure 1. Plain light

Figure 2. Crossed nicols.

Murdoch (1951) has suggested that perovskite crystallizes in the isometric form and on lowering of temperature inverts to a lower symmetry. This view is supported by Megaw (1946) who has shown that synthetic double oxides of the perovskite type assume different symmetries as a result of changing temperature. Controlled heating accompanied by X-ray studies could possibly show that the inversion in perovskite may be a function of temperature.

Optical determinations by universal stage show that perovskite from locality 56 is biaxial positive with an optic axial angle of 90° and extreme dispersion, $r > v$. Following Bowman's (1908) interpretation of orthorhombic symmetry, $Y = c$ and $X = a$. Two types of twinning were noted, polysynthetic with lamellae parallel to $\{001\}$ and the composition plane parallel to $[110]$. The twin lamellae show extinction at 45° to the lamination. The second type is also polysynthetic with broader lamellae parallel to $\{001\}$ and the composition plane parallel to (111) , with parallel extinction to the lamination. Plate V shows the twinning of perovskite on a section cut perpendicular to the c -axis. Pleochroism is marked in the darker varieties by $Z > X$.

A quantitative chemical analysis was made on purified perovskite from locality 56 using both light and dark material, since there was no apparent difference in their physical makeup. The analysis is set out in Table 1 with density and refractive index data and it shows that New Idria perovskite is almost pure CaTiO_3 . A semi-quantitative spectrographic analysis reveals the presence of Ce and La in the range 0.1-0.5% and Nb and Nd in the range 0.01-0.05%. Zirconium was also detected in the range of 0.005-0.01%, the complete spectrographic analysis is given in Plate IV. The lack of extensive substitution for Ca or Ti suggests that

Table 1.--Chemical analysis and physical properties of perovskite
(RGC-56B-51).

	Weight percent	Metal atoms	
TiO ₂	58.16	.985	} 1.01
SiO ₂	0.53	.010	
Al ₂ O ₃	0.43	.010	
CaO	40.73	.985	} .99
MgO	0.06	.001	
FeO	0.13	.003	
	<u>100.04</u>		

Analyst, W. H. Herdsman.

Calculated density = 4.08 ($a_0 = 7.625$).

Density = 4.18 ± 0.005 (Berman Balance).

$N = 2.385 \pm 0.002$ (minimum deviation on prism cut parallel to c-axis).

Birefringence = 0.002.

the titanium bearing solutions were derived from a magma of basic nature rather than an alkalic type since Nb may become strongly enriched in the acid alkalic rocks. Perovskites from alkalic rocks such as those at Magnet Cove, Arkansas, and Kaiserstuhl, Baden, Germany contain several percent Nb.

BENITOITE

Benitoite was first described by Louderback (1907) and (1909) and since then no additional work has been reported on the genesis of this singular occurrence. Furthermore no other reports of benitoite, in place, have appeared, since the original naming and description. Reed and Bailey (1927) recognized benitoite as a detrital mineral in oil-well cuttings from wells located in the Great Valley of California, and it is assumed that the source was probably the New Idria locality. Benitoite is found in a single mineralized vein within a rather large tectonic inclusion within the serpentine (Pl. III). The vein is variable in width, shows numerous bifurcations, and is composed essentially of natrolite impregnated with fibrous hair-like bluish amphiboles varying in composition from crossite to glaucophane (Pl. XIII).

Benitoite accompanied by neptunite and joaquinite is always found implanted or imbedded in a natrolite gangue in open cavities of veins as drusy surfaces projecting inward to the central cavity. The vein walls are composed of pure white cockscomb natrolite which varies in thickness from fractions of an inch to several inches. The zeolite grades imperceptibly into a bluish-green wall rock which is composed of intergrown natrolite and fibrous blue amphibole.

The mineral forms euhedral ditrigonal-dipyramidal crystals with $\{0\bar{1}1\}$ prominent and $\{0001\}$, $\{10\bar{1}1\}$, $\{10\bar{1}0\}$, $\{0\bar{1}10\}$ common. The largest crystal reported is about two and a half inches across, although the average crystal is less than an inch. Color varies from sapphire-blue to light blue; occasionally benitoite is colorless. A strong bluish fluorescence is produced in benitoite under ultra-violet light using both long and short wave sources.

Benitoite is unique in that it is known to occur at only one locality in the world and it is the only naturally occurring example of a mineral in the ditrigonal-dipyramidal symmetry class. The unit cell and space group of benitoite have been worked out by Zachariasen (1930) as follows:

$$\text{space group: } D_{\frac{2}{3}}^6 = C_{\bar{6}}^2 c$$

$$Z = 2$$

$$\text{Trigonal } a - 6.60 \text{ \AA} \pm 0.01$$

$$c - 9.71 \text{ \AA} \pm 0.01$$

$$c:a - 1.471 : 1$$

Louderback (1909) had duplicate analyses of benitoite made but minor or trace elements were not determined. A purified concentrate of benitoite was analyzed by spectrographic (Pl. IV) and gravimetric (Table 2) methods. The optical constants, determined on the material used for analysis, are given in Table 2, where it will be noted that Al and some Ti must be apportioned to Si in order to give six metal atoms for this group. Ferrous iron is grouped with Ti and the Ca with Ba. In general this analytical data agrees with that given by Louderback except for those additional elements determined in the most recent analyses. It was suggested that the color variation might be due to small amounts of some unrecognized element which

TABLE 2. CHEMICAL AND PHYSICAL PROPERTIES OF BENITOITE FROM THE GEM MINE.

	1	2	3	4	METAL	ATOMS
SiO ₂	43.56	43.79	43.61	43.40	5.93	} 6.00
Al ₂ O ₃	-	-	-	0.11	.01	
TiO ₂	20.18	20.00	19.50	20.04	2.06	} 2.02
FeO	-	-	-	0.22	.02	
BaO	36.34	36.31	37.01	36.60	1.96	} 1.97
CaO	-	-	-	0.04	.01	
H ₂ O +	-	-	-	nil		
H ₂ O -	-	-	-	0.19		
	<u>100.08</u>	<u>100.10</u>	<u>100.12</u>	<u>100.60</u>		

PROPERTIES OF NUMBER 4

Omega = 1.755 ± .002

Epsilon = 1.800 ± .002 (minimum deviation on cut prism)

UNIAXIAL POSITIVE, (2V of 20° noted in strained crystal)

X = colorless

Z = light to deep blue

DENSITY = 3.67 ± .003 (Berman Balance)

1, 2, and 3 - Analyses taken from Louderback (1909), analyst Blasdale.
 4 - Analyst, R. G. Coleman.

could produce the coloration. Spectrographic analysis of the blue material shows 0.001-0.005% V, 0.01-0.05% Nb, and 0.001-0.005% Cu and it would seem that the blue coloration might result from these trace elements. Further investigation along spectrographic lines to determine what trace elements are characteristic of the different colored varieties should be carried out.

NEPTUNITE

Neptunite is the most abundant Ti-silicate in the natrolite veins of the Gem mine, where it forms single, elongate crystals with distinct prismatic habit, embedded or implanted on natrolite and associated with benitoite and joaquinite. Neptunite prisms are usually attached at one end only and have grown outward with complex terminations on the projecting end. The dominant forms developed on these crystals are $\{100\}$, $\{110\}$, $\{001\}$, and $\{111\}$. Ford (1909) has completely described the crystallography of neptunite from this locality. The neptunite is black to dark reddish-brown with a splendid luster and makes a striking specimen when implanted on the pure white cockscomb natrolite. The neptunite is found in the same relative position in the natrolite veins as the benitoite, that is, forming drusy surfaces projecting inward to the central vein cavity. Along parts of the mineralized natrolite veins, neptunite completely covers the surface of the vein walls to the exclusion of other minerals. Neptunite has been found only within the mineralized veins of the Gem mine. Louderback's (1909) analysis of neptunite together with optical data determined on other than analyzed material are presented in Table 3. A

TABLE 3. CHEMICAL AND PHYSICAL PROPERTIES OF NEPTUNITE
FROM THE GEM MINE

	WEIGHT %
SiO ₂	53.44
TiO ₂	17.18
FeO	11.23
MgO	1.82
CaO	0.25
MnO	1.78
Na ₂ O	9.14
K ₂ O	5.34
	<u>100.18</u>

ALPHA = 1.692 ± .002

GAMMA = 1.708

OPTIC ANGLE = 66° ± 2° (+)

EXTINCTION ANGLE, Z ∩ c = 16°

OPTIC PLANE IS PARALLEL TO (010) WITH Y = b

DENSITY = 3.21 ± .005 (Berman Balance)

Chemical analysis from Louderback (1909), analyst, Blasdale.
Optical and density determinations (by Coleman) were not made
on the analyzed material.

semi-quantitative spectrographic analysis for optically studied material is listed on Plate IV.

A perfect prismatic cleavage is developed parallel to $\{110\}$ forming an intercleavage angle of 80° ; this can be seen in sections cut normal to c-axis. X-ray crystallography by Gossner and Mussgnug (1931) shows neptunite to be monoclinic with unit cell dimensions given below:

$$a_0 - 16.54 \text{ \AA}$$

$$b_0 - 12.64 \text{ \AA}$$

$$c_0 - 10.04 \text{ \AA}$$

$$\text{beta} - 115^\circ 24'$$

Further notes on neptunite from the Gem mine have been published by Arnold (1908, p. 312), Schaller (1911, p. 55), and Buttgenbach (1937-38, p. 325).

JOAQUINITE

Joaquinite is one of the rarest minerals found within the New Idria District and like benitoite its occurrence here is unique. Louderback (1909) described joaquinite as a new mineral from the Gem mine and Palache and Foshag (1932) restudied it. No later work on joaquinite has appeared in the literature.

Joaquinite is sparingly associated with benitoite and neptunite as small euhedral crystals (up to 2 mm), honey yellow to brown in color and with pyramidal and flat tabular forms predominating.

A second locality for joaquinite was discovered during this investigation along the southeastern flank of Santa Rita Peak, where it occurs

as extremely small crystals (less than 1.5 mm) implanted on natrolite druse within a large tectonic inclusion (see locality RGC-81-51) in serpentine. Benitoite and neptunite were not found associated with joaquinite, although the mineralization of the host rock is similar to that found at the Gem mine. The chemical and physical properties are summarized in Table 4.

GARNET GROUP

Garnet is quantitatively an important mineral in many of the metasomatic bodies within the serpentine, and in restricted parts of the serpentine garnet is an important mineral locally. Titanian andradite (melanite as used by some authors), is the most abundant garnet in those metasomatic rocks which have a high titanium content, where it is associated with perovskite, sphene, apatite, idocrase, and chlorite. Andradite is commonly found in the unaltered serpentine or in the periphery of the metasomatic rocks where the Ti content is low. Uvarovite is commonly associated with small pods of chromite within the serpentine and may be intergrown with kammererite. Grossularite and hydrogarnet are found associated with the jadeite bodies, and spessartite is present in the syenite as euhedral crystals. The low-grade metamorphic rocks peripheral to the serpentine contain garnets in some facies.

A detailed study was carried out on a jet black titanian andradite from RGC-42-50 (see Plate I for location), a metasomatic rock within the serpentine. The titanian andradite occurs as euhedral dodecahedra (0.1 to 0.5 cm) implanted on chlorite (rumpfite). In thin section, the

TABLE 4. CHEMICAL AND PHYSICAL PROPERTIES OF JOAQUINITE
FROM THE GEM MINE.*

WEIGHT PERCENT	
SiO ₂	36.4
TiO ₂	30.5
FeO	3.5
BaO	24.7
Na ₂ O	4.6
MgO	0.3
	<u>100.0</u>

ANALYST - W. F. Foshag

ALPHA = 1.748

Z>Y>X ABSORPTION IN YELLOW

BETA = 1.767

OPTIC SIGN = (+)

GAMMA = 1.823

2V = 50°

DISPERSION - R<V PERCEPTIBLE

DENSITY = 3.89

* All data in this table taken from Palache and Foshag (1932).

garnet shows a strong zoning manifested by a change in color from core to periphery of the crystals. The core is usually very light brown and grading outward the absorption increases to deep reddish-brown in steady progression although in some cases the zoning is strongly banded which suggests an oscillatory process during growth (see Pl. XII, Fig. 3). Zoning is common in titanian andradite from other localities. Some variation of the refractive indices was noted between the rims and core material (Becke line) but not enough to measure; however, other physical and chemical properties of these zones were measurable. All of these garnets are anisotropic with a birefringence of about 0.004 and, occasionally, dodecahedral twinning as described by Winchell (1951) was observed. The titanian andradite was purified by centrifuging and the darkest peripheral zones of the garnet were used for the analysis (Table 5).

The analysis of the New Idria titanian andradite when compared to published analyses of andradite shows excess titanium and a deficiency in silica and ferric iron. This deficiency appears in all cases where titanium has entered the lattice of the andradite molecule to form titaniferous garnets. All published analyses of titanian andradites and schorlomites are found to be deficient in both Fe^{3+} and Si^{4+} when recalculated to fit the standard garnet formula. If the excess Ti is apportioned between silica and ferric iron most of the titanian andradite and schorlomite analyses fit the standard garnet formula $\text{R}_3\text{R}_2(\text{SiO}_4)_3$. Thus it would appear that if Ti is introduced into the andradite lattice it may occupy either the Si^{4+} or Fe^{3+} positions. When the analysis of the New Idria titanian andradite is calculated on the basis of 12 oxygens per unit cell, the excess Ti was

TABLE 5. CHEMICAL AND PHYSICAL PROPERTIES OF TITANIAN ANDRADITE
(RGC-42-50).

	Wt. %	METAL	ATOMS		IDEAL
SiO ₂	30.74	2.55	} .45	} 3.00	3.00
Al ₂ O ₃	4.78	.47			
Fe ₂ O ₃	17.67	1.10	} .02	} 1.85	2.00
TiO ₂	11.36	.71			
FeO	.99	.07	} 3.12	} 3.00	
MnO	.76	.04			
CaO	33.51	2.98			
MgO	.25	.03			
H ₂ O +	nil	-			
H ₂ O -	.08	-			
	<u>100.14</u>				

$N = 1.857$ to $1.860 \pm .002$

DENSITY = 3.625 ± 0.003 (pycnometer, 23°C)

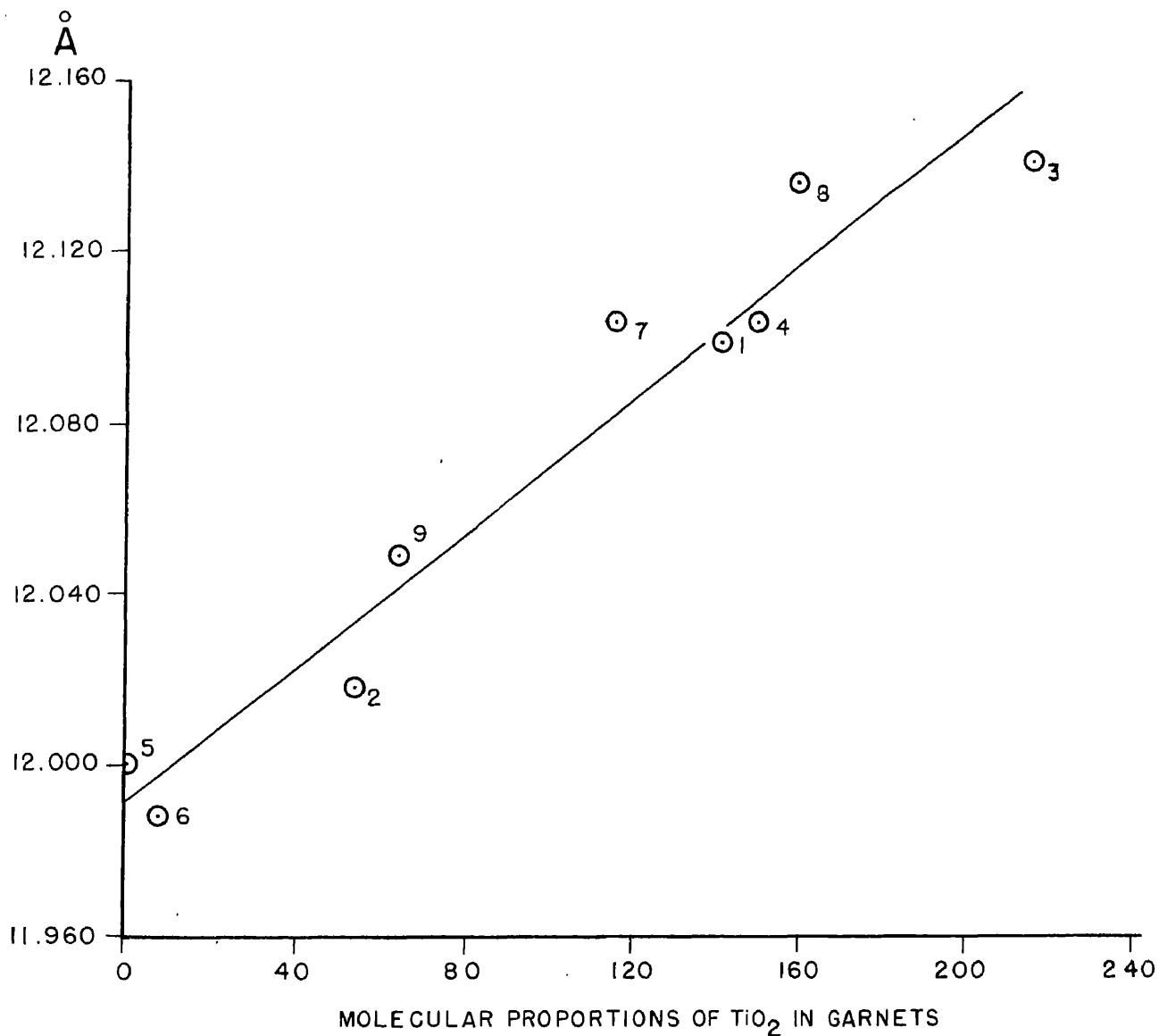
LATTICE CONSTANT = a_0 $12.10 \text{ \AA} \pm .01$

ANALYST .. R. G. Coleman

placed in the octahedral positions and most of the Al was apportioned to the Si positions in order to balance the excess positive charge produced by Ti in the Fe³⁺ positions. If the excess Ti is considered to replace Si a satisfactory balance is found, although reasons for the present apportionment will be discussed later.

A titanian andradite (schorlomite) analyzed by Zedlitz (1953) contained 17.50 percent TiO₂ and only 26.85 percent SiO₂, thus in this garnet much of the titanium must be in tetrahedral coordination. In calculating the formula for this garnet it is necessary to apportion 0.75 of the Ti for Si to bring the amount of metal atoms in tetrahedral coordination up to the theoretical value of 3.00. Since the size of the Ti ion is 0.64 Å and that of Al is 0.57 Å, both larger than Si (0.59 Å), there must be some increase in the cell edge of the garnet lattice to accommodate Ti and/or Al in the Si positions.

Zedlitz (1955) has shown that this is truly the case in those titaniferous garnets analyzed by him. Zedlitz plotted the unit-cell dimensions of the analyzed garnets against the molecular percent of TiO₂ and it was shown that there was an almost straight line increase of unit cell size with increasing TiO₂. In the present study, Zedlitz's values have been supplemented with additional garnet analyses and all are plotted in a similar fashion (see Figure 2). In order to determine if only Ti apportioned to the tetrahedral Si positions was responsible for the lattice expansion, another plot was made (not shown) using the Ti apportioned to the Si positions plotted against the unit cell size. This plot shows a stronger divergence from a straight line function than that in Figure 2, and it seems that the total titanium in the



SOURCE	TiO %	UNIT CELL IN Å
1-NEW IDRIA	11.36	12.10
2-MAGNET COVE, ZEDLITZ (1933, 1935).	4.60	12.019
3-JIVAARA, " "	17.30	12.143
4-KAISERSTUHL, " "	12.10	12.104
5-REZBANYA, MACKOWSKY (1939).	NIL	12.001
6-SPARTA, " "	0.75	11.988
7-OBERBERGEN, " "	9.38	12.104
8-IIWAARA, " "	12.77	12.139
9-IRON HILL, LARSEN (1942).	5.08	12.05

FIGURE 2. RELATION OF UNIT CELL SIZE AND TiO₂ CONTENT IN TITANIFEROUS ANDRAD

structure controls the expansion of the garnet unit cell.

The titanium content of several garnets from the New Idria District was determined indirectly by measuring the unit cell and estimating the TiO_2 content from Figure 2. The TiO_2 content determined in this manner suggests that all the garnets found in the replacement veins must carry ranging amounts of titanium (Table 6). The first two garnets listed are from different zones within the same garnet. The core is a lighter color than the rim with an apparent increase in TiO_2 from the core outward. The titanium andradite (RGC-56-51) is associated with perovskite, chlorite, and idocrase. The last two garnets in Table 6 are from the same metasomatic rock (RGC-54-50) and a spectrographic analysis of the light green andradite shows 1.5% Ti, or 2.8% TiO_2 . This value agrees satisfactorily with the TiO_2 content determined from Figure 2 and it would appear that the color of the New Idria garnets is not a true index of smaller quantities of Ti substituting in the garnet structure.

Comparison of the refractive index of analyzed New Idria titanian andradite with that of other titaniferous garnets from the literature shows that the former has a lower refractive index than that ordinarily found and it is suggested that in this instance the excess Ti^{4+} mainly replaces Fe^{3+} and not Si. Thus the refractive index would remain about the same as that of andradite. From the data presented in Table 7 it is apparent that the refractive indices of titaniferous garnets are not necessarily a function of their titanium content, although a more complete study of these garnets could possibly produce a satisfactory explanation for the anomalies produced by Ti substitution in the andradite lattice.

TABLE 6. DETERMINATION OF TiO_2 CONTENT FROM UNIT CELL MEASUREMENTS.

SAMPLE No.	MINERAL	UNIT CELL IN Å	TiO_2 %
RCC-42-50	TITANIAN ANDRADITE, BLACK (RIM)	12.12	14
RCC-42-50	TITANIAN ANDRADITE, BROWNISH BLACK (CORE)	12.08	10
RCC-56-51	TITANIAN ANDRADITE, BLACK	12.11	13.5
RCC-34-50	TITANIAN ANDRADITE, BROWNISH BLACK	12.06	8.5
RCC-34-50	ANDRADITE, LIGHT GREEN	12.06	8.5

Unit cell measurements made by A. Fabst.

TABLE 7. REFRACTIVE INDICES AND TiO_2 CONTENT OF TITANIFEROUS GARNETS.

LOCALITY	N	TiO_2 %
1- NEW IDRIA, CALIF.	1.86	11.36
2- IRON HILL, COLO.	1.907	5.08
3- TURGA, FINLAND	1.90	6.34
4- ROCCA, ITALY	1.94	8.70
5- MAGNET COVE, ARK.	1.94	16.90
6- JIVAARA, FINLAND	2.01	19.00

2- Larsen (1942), 3- Kranck (1928), 4,5,6- Winchell (1951).

The close similarity of the optical and physical properties of the dark garnets to the light colored andradite garnets led to a more detailed study of the andradite garnets found in the metasomatic bodies. In the contact zone of one of these bodies (RGC-109-52) a colorless to light green andradite was found that showed well developed dodecahedral form up to 0.1 cm in diameter. Diopside, idocrase, and chlorite are associated with the garnet. The light colored andradite grades into a dark titaniferous garnet in the central portion of the metasomatic calc-silicate body. An analysis of the andradite is presented in Table 8 together with the physical properties.

This andradite shows weak birefringence similar to that in titanian andradite described earlier but does not exhibit the twinning characteristics of that mineral. The analysis shows excellent agreement with that of other analyzed andradites found in the literature. In comparing this analysis with the analyzed titanian andradite from New Idria, it can be readily seen that ferric iron was replaced to a greater extent than silica in the formation of the titanian andradite. Therefore, if the excess alumina replaces silica and all of the titanium replaces ferric iron, the physical constants of the titanian andradite, i.e., density, refractive index, should not be radically different from andradite; as the atomic weights of titanium and iron are comparable as are their ionic refractivities. If this generalization holds true, it might well explain the similarities (optics and density) between the andradite and titanian andradite of the New Idria District. On the other hand if the titanium enters the andradite structure and replaces silicon in preference to ferric iron it should be expected

TABLE 8. CHEMICAL AND PHYSICAL PROPERTIES OF ANDRADITE
GARNET (RGC 42-50).

	Wt. %	METAL ATOMS		IDEAL
SiO ₂	35.33	2.96	} .04 } .26	3.00
Al ₂ O ₃	2.98	.30		
Fe ₂ O ₃	25.48	1.60		
TiO ₂	.57	.04	} 1.96	2.00
FeO	.52	.04		
MnO	.22	.02	} 3.11	3.00
CaO	33.76	3.02		
MgO	.74	.09		
H ₂ O+	nil			
H ₂ O-	.38			
	<u>99.98</u>			

$N = 1.879 \pm .002$

DENSITY = 3.717 ± 0.003 (pycnometer, 24°C)

ANALYST - W. H. Hardsman

that the density and the refractive indices would be radically different as the atomic weight and ionic refractivities of silicon and titanium are not similar. On this basis, the titanium in the titanian andradite was apportioned to ferric iron because the refractive index indicated very little substitution of titanium for silicon. When the indices and densities of the garnets from the metasomatic and serpentine rocks are compared, their constant nature is remarkable considering the amount of substitution (Table 9).

Grossularite has been reported from the New Idria District by Pabst (1951, p. 482) and Yoder and Chesterman (1951, p. 3). Although the author was unable to find grossularite, minor concentrations of hydrogarnet were found associated with the jadeite pods in a prehnite-rich rock. The hydrogarnet makes up to 10% of the rock and occurs as granular masses intergrown with prehnite. Individual grains of the hydrogarnet show distinct zoning which is manifested by differences in refractive index. From the core outward the refractive indices increase in value. A portion of the rock showing a high concentration of hydrogarnet was ground to minus 500 mesh and centrifuged in liquids of known densities and the refractive index of each density fraction was determined in order to establish the compositional range of the zoned hydrogarnet. The determinations show that the zones of hydrogarnet fit nicely into the grossularite-tricalcium aluminum hexahydrate series as described by Hutton (1943, p. 174) and by Yoder (1950b, p. 243). These data plotted on the diagram (Figure 3) published by Yoder indicate that the composition of the inner cores extends below that of plazolite and hibschite

TABLE 9.--REFRACTIVE INDICES AND DENSITIES OF THE NEW IDRIA GARNETS.

SAMPLE No.	MINERAL	N	DENSITY
RGC-34-50	LIGHT GREEN ANDRADITE	1.83	4.00*
RGC-109-52	DARK BROWNISH BLACK MELANITE $\frac{1}{2}$	1.863	-
RGC-109-52	ANDRADITE (ANALYZED)	1.879	3.717
RGC-67-51	ANDRADITE, LIGHT GREEN	1.863	-
RGC-92-52	ANDRADITE, LIGHT GREEN	1.863	-
RGC-37-50	MELANITE, BROWNISH BLACK	1.863	-
RGC-42-50	MELANITE, BLACK (ANALYZED)	1.857	3.625
RGC-56-51	MELANITE, BLACK	1.866	3.72
RGC-34-50	MELANITE, BROWNISH BLACK	1.866	3.71
RGC-14-50	ANDRADITE, LIGHT YELLOW	1.869	3.68
RGC-27-50	ANDRADITE, LIGHT GREEN	1.862	3.78

* High density may be due to chromium, spectrographic analysis shows 1-5% Cr.

$\frac{1}{2}$ /Melanite is used here as a synonym of titanian andradite.

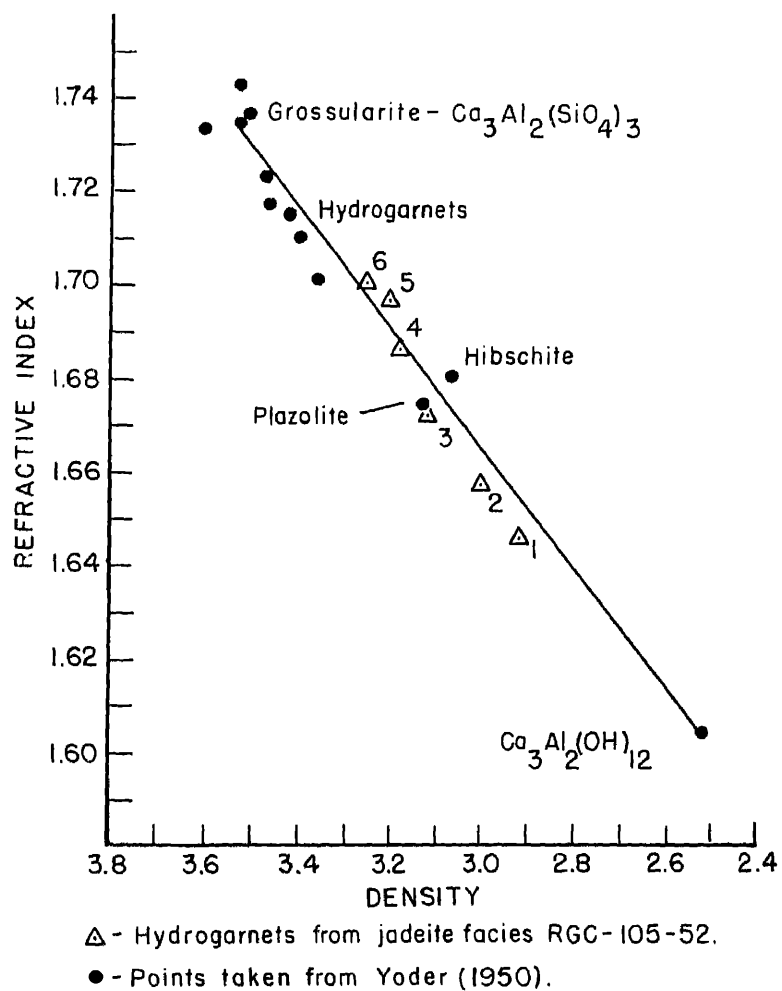


FIGURE 3. RELATION OF REFRACTIVE INDEX TO DENSITY IN THE GROSSULARITE - TRICALCIUM ALUMINUM HEXAHYDRATE SERIES. SIX SEPARATE ZONES OF NEW IDRIA HYDROGARNETS PLOTTED; NUMBER ONE, INNER ZONE GRADING OUTWARD TO NUMBER SIX, THE PERIPHERAL ZONE.

and the peripheral zone extends up to hydrogarnets. According to Hutton no natural minerals of the series more hydrous than plazolite have been found, and therefore this appears to be the first recorded case of a natural hydrogarnet containing almost 14% H₂O.

Yoder (personal communication) has found that synthetic hydrogarnets assume a zoning similar to the naturally occurring material described. Since this synthetic material was produced in open tubes at constant temperatures and pressures there may have been some leaching of silica, therefore, the zoning of the hydrogarnets cannot, as yet, be explained experimentally.

PYROXENE GROUP

The New Idria District is particularly noteworthy for the variety of pyroxenes present in the different rock types. The serpentine is characterized by the orthopyroxenes, the dynamothermal metamorphic rocks by jadeite-acmite, the metasomatic rocks by diopside, and the late stages of the syenite intrusion by aegirine-augite. In many cases, pyroxene is the dominant mineral and therefore is quantitatively important in the petrology of the district.

The first authenticated outcrop of jadeite in California was established by Yoder and Chesterman (1951) along Clear Creek within the serpentine. It seemed desirable to make a complete study of the jadeite since there has been considerable interest in this particular locality. The jadeite is found in small veins cutting albite-glaucophane-acmite schist and as larger lens-shaped pods within serpentine. A more

complete description of the occurrence is given in the section dealing with the petrology of the district. The vein jadeite is coarsely crystalline and almost pure white whereas jadeite from the pods is variegated with fractured green jadeite healed by anastomosing veins of white jadeite. Prehnite, hydrogarnet, thomsonite, and minor sphene are associated with jadeite pods, while vein jadeite is found with albite, analcite, natrolite, and thomsonite. The detailed study of the jadeite was carried out on the white vein material which is almost pure jadeite (Coleman, 1954). The analyzed material was very carefully purified by centrifuging in heavy liquids and the resultant concentrate is 99.5% pure with possibly a minute amount of analcite present as inclusions. Two additional analyses of jadeite collected by Yoder and Chesterman from Clear Creek were obtained from George Switzer. The analyses of the white jadeite accompanied by physical properties are presented in Table 10.

These two independent analyses of the white jadeite from Clear Creek definitely establish this material as an almost pure jadeite. Recalculations of these analyses on the basis of six oxygen to the unit cell show a close correspondence to the ideal formula for jadeite (Table 10). In analysis number 2, sodium appears to be somewhat low, although this may indicate differences in the two analytical methods. The high water, in number 2, may be accounted for by the presence of analcite as an impurity. Some of the aluminum in analysis number 1 proxies for Si, although according to Yoder (1950a) most of the aluminum must be in six-fold coordination to allow for the closer packing and thus higher

TABLE 10. CHEMICAL AND PHYSICAL PROPERTIES OF WHITE JADEITE FROM CLEAR CREEK.

	1		METAL ATOMS		2		METAL ATOMS	
SiO ₂	59.06	1.99	.01	} 2.00	59.38	2.00	} 2.00	
Al ₂ O ₃	24.62	.98			25.82	1.02		
TiO ₂	.08	.002	.97	} 1.00	.04	-	} 1.03	
Fe ₂ O ₃	.41	.018			.45	.01		
FeO	.18	.006			trace	-		
MnO	.03	-			-	-		
MgO	.17	.008	} 1.00	} 1.00	.12	.003	} 0.88	
CaO	.35	.012			.13	.005		
Na ₂ O	14.95	.983			13.40	.876		
K ₂ O	.01	-			.02	-		
H ₂ O+	.07	-			.16	-		
H ₂ O	.03	-			.22	-		
Cr ₂ O ₃	-	-			.01	-		
	<u>99.96</u>				<u>99.75</u>			

PHYSICAL PROPERTIES OF No. 2

ALPHA = 1.654 ± .002

BETA = 1.657

GAMMA = 1.666

DENSITY = 3.43 ± .005

(Berman Balance)

OPTIC ANGLE = 70°

EXTINCTION ANGLE = 34°

X = Y = Z COLORLESS

	NORM	
	#1	#2
jd	97%	98%
di	2%	1%
ac	1%	1%

1 - From Switzer (Analyst - E. H. Oslund, U. of M. Lab.)

2 - Analyst - W. H. Herdsman.

density of jadeite. The optical properties of the jadeite compare favorably with those of other published data (Table 11). A further comparison of the analyzed material from Clear Creek was made on the powder diffraction pattern with the published data of Yoder (1951). The indexing of the lines was kindly done for the author by Daphne Riska of the U. S. Geological Survey (see Table 12). The close agreement between these X-ray powder diffraction measurements indicates without a doubt that the Clear Creek material is one of the world's better localities for pure jadeite. Wolfe (1955) has described a second locality of jadeite from Cloverdale, California and his careful crystallographic study shows well developed crystals of jadeite (94% jadeite - 6% diopside) formed in two generations in small veins cutting glaucophane schist.

Optical determinations on the green jadeite associated with the white jadeite indicate that considerable Ca, Mg, and Fe^{3+} are admixed with this variety. A chemical analysis of the green material kindly put at the disposal of the writer by George Switzer, shows about 10% diopside and 14% aegirine.

Jadeite has also been found as a crystalloblastic constituent in one of the metamorphic rocks (RGC-77-51) forming a large tectonic inclusion within the serpentine about 3/4 of a mile north and east of the Clear Creek locality. Mielenz (1939) was the first to recognize that jadeite was present in the schists of this area.

In contrast to the jadeite from the metamorphic rocks, the calcium-magnesium end member, diopside, dominates in the calc-silicate metasomatic rocks. Diopside from these rocks, white to very faint pale green,

TABLE 11. COMPARISON OF OPTICAL DATA ON JADEITES.

	ALPHA	BETA	GAMMA	2 V	Z _{AC}
1.	1.654	1.657	1.666	70°	34°
2.	1.655	1.659	1.667	70°	34.5°
3.	1.640	1.645	1.652	67°	40°
4.	1.664	1.671	1.694	-	-

1. Clear Creek, Calif. 2- From H. S. Washington (1922).
 3- Cloverdale, Calif., from C. W. Wolfe (1955). 4- From Larsen
 and Berman (1934).

TABLE 12. COMPARISONS OF X-RAY POWDER DIFFRACTION MEASUREMENTS ON JADEITE

C_{2h}^6	JADEITE - CLEAR CREEK	JADEITE - BURMA*
hkl	d(Å)	d(Å)
110	6.2	6.19
020	4.27	4.29
021	3.24	3.25
220	3.10	3.11
221	3.06	2.92
310	2.82	2.82
221	2.41	2.42
400	2.25	2.24
312	2.21	2.19
330	2.07	2.069
041	1.96	1.971
241	1.88	1.892
441	1.57	1.577
440	1.55	1.553

* Data taken from Yoder (1950 a)

forms thin bladed elongated crystals. Two habitats have been noted: (1) as an early mineral within the actasomatic rocks associated with idocrase and chlorite, and (2) as a late mineral forming delicate crystals in cavities and vugs. Optical determinations on diopside from eight localities (Table 15) show little variation from essentially pure ($\text{CaMgSi}_2\text{O}_6$) with little or no substitution of iron or sodium. Occurrence of diopside in such rocks as these is particularly noteworthy since the diopside has formed contemporaneously with hydrous minerals, such as chlorite, and is commonly in juxtaposition with andradite and titanian andradite. Diopside is a common mineral in 'skarn' type metamorphic deposits, but at New Idria, diopside has formed during metasomatic replacement of serpentine by introduction of Ca, Al, Fe, and Ti.

Acmite is found within the syenite as a late deuteric mineral in veins associated with natrolite and analcite, and also may be observed as rims to barkevikite in the syenite near these late deuteric veins. An interesting but isolated occurrence of acmite (RGC-39-50) was found in the Franciscan formation near the contact on the eastern edge of the serpentine. Here veins of albite up to three inches across cut glaucophanic rocks and contain vuggy areas implanted with bladed crystals of deep green acmite (Table 15, RGC-39-50). Acmite is a common constituent in schists associated with jadeite veins. Other optical determinations were made for pyroxenes in metamorphic rocks (Table 15) of the Franciscan type, and most were found to belong to the acmite-aegirine-augite series.

TABLE 13. OPTICAL CONSTANTS OF PYROXENES FROM THE NEW IDRIA DISTRICT.

MINERAL	BETA <u>1/</u>	Z \wedge c	2V _Z	COLOR	X	Y	Z	
RGC-34-50	DIOPSIDE	1.672	38°	60°	WHITE	COLORLESS	COLORLESS	COLORLESS
RGC-34-50	DIOPSIDE	1.569	35°	62°	WHITE	COLORLESS	COLORLESS	COLORLESS
RGC-56-50	DIOPSIDE	1.670	37°	59°	WHITE	COLORLESS	COLORLESS	COLORLESS
RGC-109-52	DIOPSIDE	1.672	33.5°	58°	WHITE	COLORLESS	COLORLESS	COLORLESS
RGC-109-52	DIOPSIDE	1.676	43°	60°	WHITE	COLORLESS	COLORLESS	COLORLESS
RGC-67-51	DIOPSIDE	1.636	40°	61°	WHITE	COLORLESS	COLORLESS	COLORLESS
RGC-37-50	DIOPSIDE	1.682	40°	61°	WHITE	COLORLESS	COLORLESS	COLORLESS
RGC-92-52	DIOPSIDE	1.686	41°	60°	WHITE	COLORLESS	COLORLESS	COLORLESS
RGC-44-50	ACMITE	1.780	95°	LARGE	GREEN	GREEN	LIGHT YELLOW	YELLOW
RGC-32-50	ACMITE	1.782	95°	LARGE	GREEN	LIGHT GREEN	COLORLESS	LIGHT YELLOW
RGC-39-50	ACMITE	1.791	95°	110°	GREEN	BLUE-GREEN	LIGHT BLUE-GREEN	YELLOW
RGC-55-51	*	1.638	40°	60°	GREEN	GREEN	GREEN	YELLOW

* Optics similar to aegirine-augite. First eight pyroxenes from calc-silicate rocks, RGC-44-50 is from syenite, and the last three are from metamorphic rocks.

1/ Limits of accuracy \pm 0.002.

AMPHIBOLE GROUP

Several unusual amphiboles are found in the New Idria District and these were given a more detailed study. A dark brown to black amphibole is an essential constituent of the camptonite and syenite intrusives and makes up from 10 - 60% of the rock; shown to be barkevikite by optical and chemical study. It forms elongate prisms ranging in size from several millimeters to 24 cm in length. Barkevikite is extremely fine-grained in the camptonite whereas in the syenite the crystals become much larger and in some spots form large radiating clusters of prisms several feet across. Optical determinations on the amphibole from the different intrusive facies indicate an extremely consistent composition; however where changes in composition of the crystallizing magma had taken place, the barkevikite reflected this change. In the late deuteric stage, the barkevikite became rimmed by aegirinaugite or by glaucophane and crossite near the igneous-serpentine contact.

Complete analyses have been made of barkevikite (Table 14) and of unweathered White Creek syenite (RGC-48-50) from which the amphibole was separated (Table 23). Recalculation of analysis in Table 14 on the basis of 24 (O,OH,F) to the unit cell was made in order to determine if the results fit the standard formula for amphiboles as established by Warren (1930). Almost one quarter of the theoretical amount of silicon is proxied for by aluminum to bring the four coordinated metal atom positions up to eight. The remainder of the metal atoms fit approximately the accepted formula except for the low percentage of water, 1.06 (OH) instead of the theoretical 2.00. A separate determination was made for fluorine

TABLE 14. CHEMICAL AND PHYSICAL PROPERTIES OF BARKEVİKITE
(RCC-48-50).

	WT. %		METAL ATOMS		IDEAL
SiO ₂	38.74	5.97	2.03	8.00	8.00
Al ₂ O ₃	14.02	2.56			
TiO ₂	3.96	0.46	.53	5.46	5.00
FeO	16.27	2.09			
Fe ₂ O ₃	2.32	0.26			
MgO	9.26	2.12			
MnO	.33	0.05			
CaO	11.28	1.86			
Na ₂ O	1.16	0.34	}	2.41	2.00
K ₂ O	.89	0.16			
H ₂ O+	1.02	1.06	}	1.06	2.00
H ₂ O-	.20				
	99.45				

ANALYST - W. H. Herdsman

ALPHA = 1.701 ± .002

Y = LIGHT REDDISH-BROWN

BETA = 1.695

X = LIGHT YELLOW-BROWN

GAMMA = 1.679

Z = DARK REDDISH-BROWN

Z Δ c = 13°

2V = 60°

DENSITY = 3.40 ± .005 (pycnometer, 24°C)

Fluorine determination on a separate portion gives 0.02%.

and combined water was rechecked in order to establish definitely the low (OH) content of the amphibole. Comparison with other barkevikite analyses shows that low (OH) content is a common characteristic of these amphiboles and Sundius (1946) includes barkevikite with the oxyhornblendes stating: 'The barkevikite may conveniently be included in the same group (oxyhornblende). The members of the group have also been named oxyhornblende because of their high content of Fe_2O_3 being ascribed to a reduction of OH and a contemporaneous oxidation of Fe.' This may explain the low water content; however the Fe_2O_3 content is too low to compensate for the low combined water and therefore, the water determination is felt to be in error. The optical character of the New Idria material when compared with other published data on barkevikites shows good agreement.

The metamorphic rocks from the district are largely characterized by glaucophane or crossite as an essential mineral. These two amphiboles usually form as a result of low-grade metamorphism of the greywackes or basic igneous rocks of the Franciscan formation and do not form coarse crystals that can be distinguished in the hand specimen but impart a characteristic bluish cast to the rock. Extremely fine hair-like crystals of crossite were found in the vugy cavities of the natrolite vein at the Gem mine and here again the individual crystals could not be distinguished except under the microscope. Time did not permit a comprehensive study of these amphiboles and the optical properties of the crossites and glaucophanes are given in Tables 15 and 16. The optical constants of these blue amphiboles compare favorably with the published

TABLE 15. OPTICAL CONSTANTS OF GLAUCOPHANE FROM THE NEW IDRIA DISTRICT.

	RGC-80-51	RGC-80-51	RGC-54-51	RGC-60-51	RGC-107-52	RGC-73-51
BETA ^{1/}	1.644	1.634	1.655	1.632	1.638	1.645
EXTINCTION ANGLE	Z:c=7°	Z:c=5°	Z:c=8°	Z:c=5°	Z:c=9°	Z:c=8°
2V	10-20°	20°	30°	5-10°	30°	20°
SIGN	(-)	(-)	(-)	(-)	(-)	(-)
ORIENTATION	Y=b	Y=b	Y=b	Y=b	Y=b	Y=b
X	COLORLESS	COLORLESS	COLORLESS	LT. YELLOW	COLORLESS	LT. YELLOW
Y	LAVENDER	LAVENDER	VIOLET	BLUE	BLUE	SKY BLUE
Z	LIGHT BLUE	LIGHT BLUE	LIGHT BLUE	VIOLET	LAVENDER	VIOLET

^{1/} Limits of accuracy ± 0.002.

TABLE 16. OPTICAL CONSTANTS OF CROSSITE FROM THE NEW IDRIA DISTRICT.

	GEM MINE	RGC-32-50	RGC-51-50	RGC-50-50*	RGC-21-50*
BETA ^{1/}	1.662	1.662	1.663	1.665	1.669
EXTINCTION ANGLE	Y:c=17°	Y:c=35°	Y:c=15°	Y:c=5°	X:c=0°
2V	24°	SMALL	10°	20°	75°
SIGN	(-)	(-)	(-)	(+)	(+)
ORIENTATION	Z=b	Z=b	Z=b	Z=b	Z=b
X	COLORLESS	LIGHT YELLOW	LIGHT YELLOW	BLUE GREEN	DEEP BLUE
Y	BLUE GREEN	BLUE GREEN	SKY BLUE	LIGHT YELLOW	LAVENDER
Z	VIOLET	VIOLET	VIOLET	LIGHT GREEN	COLORLESS

* BLUE AMPHIBOLES SIMILAR TO CROSSITE.

^{1/}Limits of accuracy \pm 0.002.

data for crossite and glaucophane (Switzer, 1950), although the amphiboles from (RGC-50-50) and (RGC-21-50) show anomalous optic character that fits neither glaucophane nor crossite. Further chemical and optical study of these amphiboles is needed, since the present published data are not complete enough to characterize these species by optics alone.

MICA AND CLAY GROUP

The sheet structure minerals are quantitatively the most important group within the serpentine. Individual localities will not be listed except where analytical work was performed, since these minerals are so common. The mica and clay minerals of this district may be divided into two distinct groups, (1) those making up the serpentine, (2) those found within the metasomatic bodies that have formed at the expense of the serpentine. It is assumed, that antigorite and chrysotile making up the serpentine, crystallized during the change of the ultrabasic rocks to serpentine; whereas the chlorites included in the second group crystallized during the metasomatic replacement of the serpentine.

Antigorite is the most abundant mineral in the serpentine making up 80 to 95% of the rock. Antigorite produces a variety of textures within the serpentine, where it does not pseudomorph olivine; however, where pyroxenes are present, bastite assumes the form of the original pyroxene. Coarsely crystalline antigorite characteristically forms flaky fan-like aggregates whereas the finer-grained antigorite commonly shows felt-like aggregates composed of minute flakes (Pl. VIII, Fig. 3). Rarely large blade-like antigorite areas are found within the fine-grained facies. Shearing is commonly present in the antigorite masses and a distinct

fabric is formed with the schistosity parallel to the alignment of the antigorite. Identification of the antigorite is facilitated by its characteristic crystalline form and optical character which is distinct from chrysotile. Antigorite was not found in any of the metasomatic chlorite-rich bodies within the serpentine formed under static conditions.

Brindley (1951) points out that antigorite does not have a structure similar to chlorites but more closely resembles that of the kaolin group minerals. Since X-ray techniques were not used in the identification of these minerals, antigorite is included in Figure 4 with the other chlorites to compare their composition. No analytical work was completed on the antigorite (Table 17).

Chrysotile is included in this group although it cannot be considered a true chlorite-type mineral. Chrysotile is most commonly found as a product of the serpentinization of olivine, forming small veins in the fractures within olivine with a fibrous structure normal to the vein walls. Where olivine is completely replaced by chrysotile, it assumes a web-like structure roughly pseudomorphing olivine (Pl. VIII, Fig. 2). Chrysotile also commonly forms irregular veins, up to four inches in width, that cut the serpentine and in this case approaches an asbestos-form character. Identification of chrysotile was verified by its optical properties, and mean indices determined on several specimens are: alpha 1.562, and gamma 1.569.

The chlorites received a more intensive study, since they make up a large bulk of the interesting metasomatic bodies. Winchell's (1951) classification was used to chemically categorize the various chlorites, since it was possible to determine their chemical composition by their

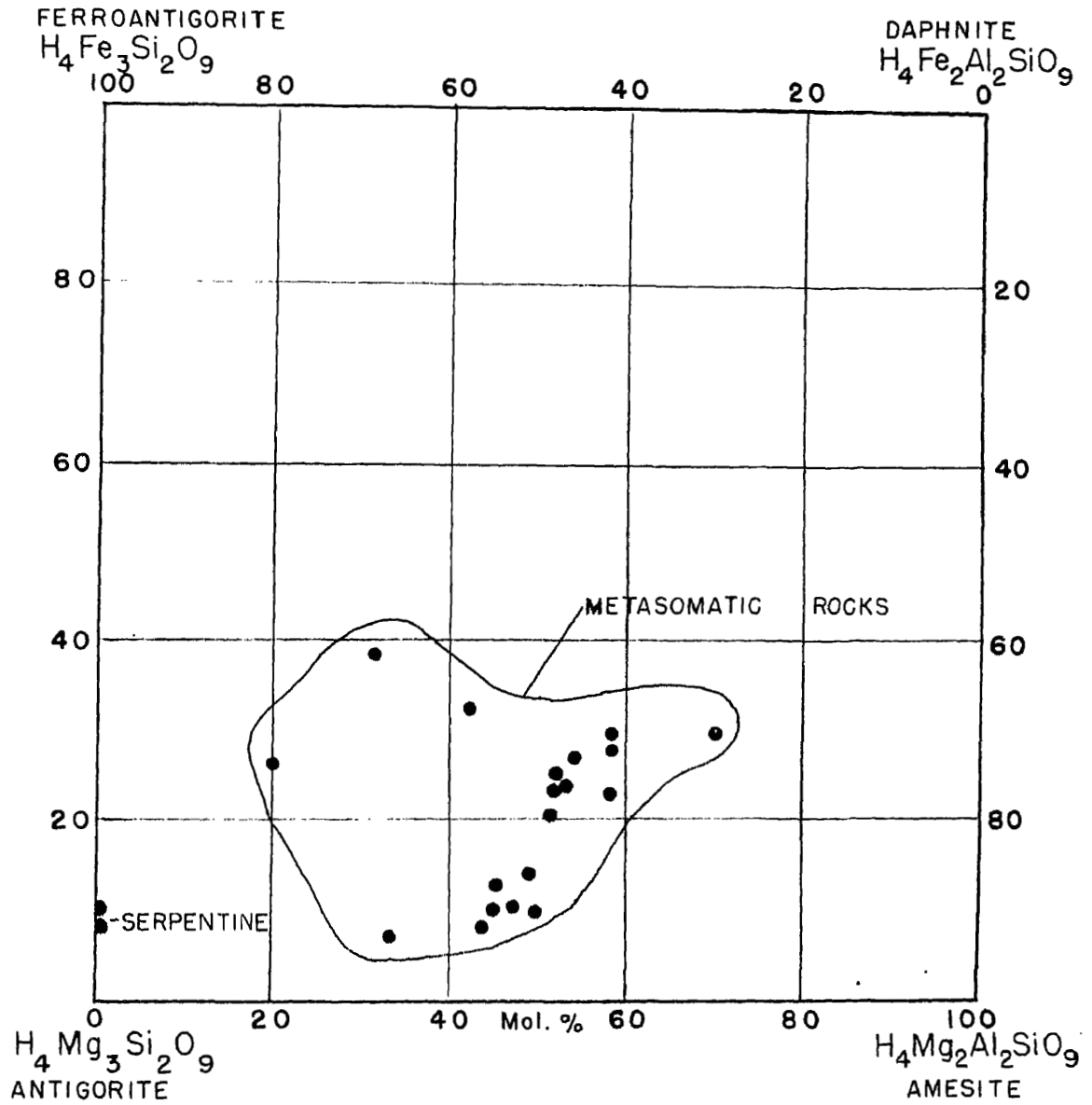


FIGURE 4. NEW IDRIA CHLORITES PLOTTED ON WINCHELL'S OPTICAL AND CHEMICAL CLASSIFICATION FOR CHLORITES. THE OPTICAL DATA FOR THESE CHLORITES IS GIVEN IN TABLE 17.

TABLE 17. OPTICAL CONSTANTS OF NEW IDRIA CHLORITES AND RELATED MINERALS.

MINERAL	BETA ^{1/}	2V	SIGN	BIREF.	DISP.	X	Y	Z	
RGC-79-51	CLINOCHLORE	1.584	10-20°	(+)	.002	V>R	CL.	CL.	P. GR.
RGC-79-51	CLINOCHLORE	1.584	10-20°	(+)	.003-.004	V>R	CL.	CL.	P. GR.
RGC-70-51	CLINOCHLORE	1.584	10-20°	(+)	.003	V>R	CL.	CL.	P. GR.
RGC-70-51	CLINOCHLORE	1.587	10-20°	(+)	.003	V>R	CL.	CL.	P. GR.
RGC-109-52	CLINOCHLORE	1.578	10°	(+)	.002	V>R	CL.	CL.	P. GR.
RGC-56-50	CLINOCHLORE	1.580	5-10°	(+)	.004	V>R	CL.	CL.	P. GR.
RGC-36-50	DELESSITE	1.604	5°	(-)	.001-.002	V>R	L. PK.	L. GR.	L. GR.
RGC-57-50	DELESSITE	1.608	7-5°	(-)	.004-.005	V>R	L. YL.	L. GR.	L. GR.
RGC-105-52	DELESSITE	1.590	5-10°	(-)	.003	V>R	L. YL.	L. GR.	L. GR.
RGC-83-51	RUMPFITE	1.594	2-5°	(+)	.002	V<R	L. GR.	L. GR.	YL. PK.
RGC-83-51	RUMPFITE	1.597	5-7°	(+)	.001-.002	V<R	L. GR.	L. GR.	YL. PK.
RGC-42-50	RUMPFITE	1.608	5-7°	(+)	.001-.002	V>R	L. GR.	L. GR.	YL. PK.
RGC-56-50	RUMPFITE	1.601	5-7°	(+)	.002	V<R	CL.	CL.	L. GR.
RGC-34-50	RUMPFITE	1.598	5-7°	(+)	.002	V<R	L. GR.	L. GR.	P. PK.
RGC-34-50	RUMPFITE	1.598	5-7°	(+)	.002	V<R	GR.	GR.	L. YL.
RGC-67-51	PENNINITE	1.581	5-7°	(+)	.002	V>R	GR.	GR.	P. YL.
RGC-37-50	FROCHLORITE	1.595	5-7°	(+)	.007-.008	V<R	CL.	CL.	CL.
RGC-13-50	ANTIGORITE	1.570	10-20°	(-)	.009	V<R	CL.	P. GR.	P. GR.
RGC-109-52	ANTIGORITE	1.560	10°	(-)	.009	V<R	CL.	P. GR.	P. GR.
RGC-50-50	KAMMERERITE	1.589	10°	(-)	.004	V<R	PK.	CL.	CL.
RGC-57-50	STILPNOMELANE	1.637	0	(-)	.034	-	G. YL.	DR. BR.	DR. BR.

CL. - colorless
P. GR. - pale green
L. PK. - light pink
PK. - pink

P. PK. - pale pink
GR. - green
P. YL. - pale yellow
G. YL. - golden yellow

L. GR. - light green
L. YL. - light yellow
YL. PK. - yellow pink
DR. BR. - dark brown

1/ Limits of accuracy ± 0.002.

optical properties. More recent work on chlorites by Hey (1954) has produced a better classification but chemical analyses are needed in order to utilize this system. However several semi-quantitative spectrographic analyses on these chlorites (Pl. IV) show that Winchell's system can be used with some degree of confidence to reflect the composition of the chlorites. Table 17 gives the recorded optical data on chlorites and related species, which in turn are plotted on Winchell's diagram (Figure 4). Picked samples were also used for X-ray diffraction study in order to establish a difference in their respective patterns, however no sharp differences could be detected. Brindley (1951) suggests that the difference in intensity of the basal spacings of the higher order (001) reflections might be used to distinguish the different chlorite species, although this approach did not produce conclusive results in this study.

The chlorites in the metasomatic bodies are well developed and they make up 80 - 90% of some specimens. Some bodies, viz., (RGC-79-51), (RGC-70-51), and (RGC-56-50) have well developed crystals of penninite or clinocllore, up to a centimeter in diameter, that form perched 'books' lining cavities. The texture of the chlorite-rich rocks is quite variable and grades from rocks showing a strong preferred orientation to others where the chlorite forms in a vuggy cavernous rock with well formed platelets of chlorite at random orientation.

Penninite and clinocllore, the only species found as well developed crystals, show twinning in all specimens examined and this is manifested

by the variable position of the optic axial plane in the various sectors of the basal plane. This twinning was found only in those crystals formed in open cavities whereas those chlorites found within the more dense rocks show no twinning but produce a marked schistosity with the (001) faces parallel to the direction of schistosity.

The chlorite-rich rocks are assumed to represent metasomatic replacement rocks within the serpentine, and therefore the chlorite composition should reflect, in part, the composition of the metasomatic fluids. The composition as determined from Winchell's diagram (Fig. 4) shows that from antigorite (essentially the composition of the original serpentine) to the chlorite in the metasomatic bodies, there has been an increase in both Al and Fe with a concomitant decrease in Si and Mg. Penninite and clinocllore are the common chlorites found in the least mineralized metasomatic rocks, followed by rumpfite and prochlorite as the intensity of the mineralization increases. Where iron is exceptionally high, delessite forms and sometimes it is accompanied by stilpnomelane (Pl. XI, Fig. 2). Optical data for this stilpnomelane corresponds with that of Hutton's (1938) ferrostilpnomelane (see Table 17). Spectrographic analyses (Pl. IV) of some of these chlorites show that Ni, Co, Cu, Cr, Pb, and Mn are commonly camouflaged in the structure of the New Idria chlorites.

The widespread occurrence in this district of the rare chromium chlorite, kammererite, associated with small local concentrations of chromite and uvarovite led to a complete study of this species. Kammererite was not found in any of the chlorite-rich rocks and it seems to be an alteration product of chromite, probably formed during serpentinization (Fig. 5). The mineral is easily identified in the field by its charac-

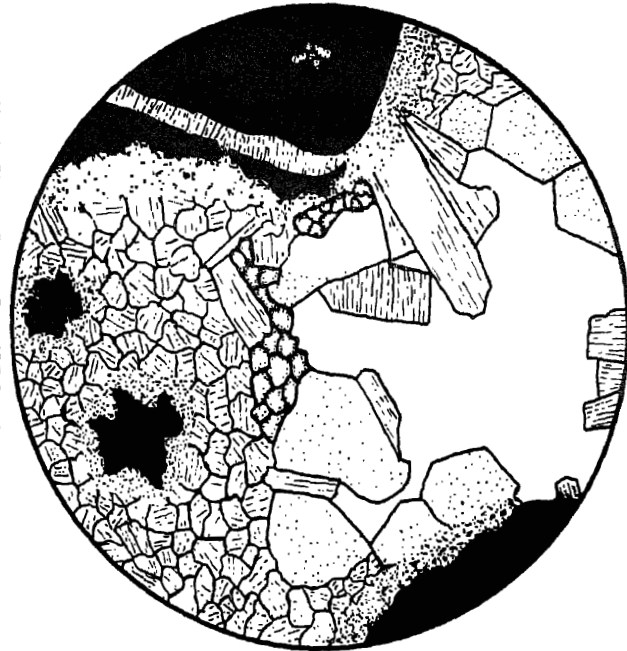


Figure 5. Camera lucida drawing of kammererite showing its formation from chromite. Note small patches of uvarovite within the kammererite. (X 40)

teristic pink to lavender color.

A chemical analysis of the kammererite and optical determinations are given in Table 18. The structural formula of the kammererite was calculated on the basis of 18 (O,OH,F) atoms to the unit cell and the analysis shows fair agreement with the ideal formula; the OH group is slightly low and the octahedral positions are above the theoretical value of 6.00. Substitution of Al for Si in the tetrahedral positions is necessary to completely fill the four Si positions assigned to the ideal formula. Cr substitutes for Al in the octahedral positions and the tabulated analyses of kammererite from the literature (Table 19) show a general decrease in Al with an increase in Cr. The optical properties of the tabulated kammererites do not show a distinct correlation with their Cr content.

NATROLITE

Natrolite is a common mineral in three distinct localities within the district and at all three it forms stubby equant crystals—a somewhat rare form, since natrolite is characterized by its acicular habit. The vein-material from the Gem mine is composed mostly of natrolite where it forms beautiful cockscomb coatings in the vugy parts of the vein. Almost perfect single crystals of natrolite are present in late deuteric veins within the syenite where they are associated with analcite and acmite. Jadeite veins contain well developed fan-shaped aggregates of natrolite associated with thomsonite, albite, and analcite. The natrolite crystals from the syenite were examined in detail and the physical properties are listed below. The crystals from the syenite and Gem mine show twinning

TABLE 18. CHEMICAL AND PHYSICAL PROPERTIES OF KAMMERERITE
(RGC-50-50).

	WT. %	METAL ATOMS		IDEAL
SiO ₂	32.12	3.10	} .90	4.00
Al ₂ O ₃	13.13	1.48		
Cr ₂ O ₃	5.96	.45	} .58	6.30
Fe ₂ O ₃	1.27	.09		
FeO	1.50	.12	}	6.00
M ₂ O	35.08	5.05		
CaO	.05	.01		
NiO	.04	-	}	7.16
H ₂ O+	11.12	7.16		
H ₂ O-	.04			8.00
	<u>100.27</u>			

ANALYST - R. G. Coleman

ALPHA = 1.585 ± .002

X = PINK

BETA = 1.589

Y = COLORLESS

GAMMA = 1.589

Z = COLORLESS

2V = 10°

OPTIC SIGN = (-)

DENSITY = 2.56 ± .01 (pycnometer 25.2°C)

TABLE 19. OPTICAL PROPERTIES OF KAMMERERITE COMPARED WITH Cr₂O₃ and Al₂O₃ CONTENT.

	1	2	3	4	5	6	7	8
Cr ₂ O ₃	13.46	7.88	7.49	5.96	4.16	3.90	1.70	0.85
Al ₂ O ₃	12.40	9.50	13.18	13.13	15.24	13.94	13.20	16.95
2V	SMALL	SMALL	3°	10°	SMALL	20°	0°	0-31°
SIGN	(+)	(-)	(+)	(-)	(+)	(+)	(+)	(+)
BETA	1.590	1.590	1.579	1.589	1.579	1.585	1.580	1.571
DENSITY	2.709	-	-	2.56	2.67	-	2.57	2.65

1-Sakok Ruopsak, Sweden, Du Rietz (1935)
 2-Deer Park, Wyoming, Shannon (1920)
 3-Kraubath, Kopetzky (1948)
 4-New Idria, California

5-Togo, French West Africa, Orcel (1925)
 6-Webster-Addie, North Carolina, Miller (1953)
 7-Piemonte, Italy, Sanero (1933)
 8-Togo, French West Africa, Orcel (1925)

which is unusual for natrolite. The gamma index for both the Gem mine and jadeite vein-material is 1.488 ± 0.002 , identical with the gamma index for the syenite natrolite. Qualitative spectrographic examination of these three natrolites shows no minor or trace elements which might produce this unusual crystal form.

Natrolite from syenite

Alpha - 1.476 ± 0.002	$2V = 56^\circ (+)$
Beta - 1.478	$Z = c$
Gamma - 1.488	Optic plane parallel (010)
Birefringence - 0.012	Twinning - Composition
$110 \wedge \bar{1}\bar{1}0 - 88^\circ 17'$	plane (110) with twin axis
$111 \wedge 110 - 63^\circ 10'$	\perp to the (110) plane.
Density - 2.23 to 2.25 (Berman Balance)	

IDOCRASE

Idocrase has been identified in four calc-silicate bodies within the New Idria District: (RGC-37-50), (RGC-56-51), (RGC-92-52), and (RGC-109-52). Two distinct types of idocrase are present, (1) pale green massive material intergrown with chlorite, calcite, and diopside; and (2) dark reddish-brown euhedral crystals present in open veins and vuggy areas of the calc-silicate rocks. The massive pale green material has normal optical constants and the X-ray pattern matches the standard for idocrase, although the reddish-brown material has higher refractive indices and is biaxial. Spectrographic determinations on three of these samples show varying amounts of Ti which can be correlated with the optical anomalies (Table 20).

TABLE 20. VARIATION IN THE OPTICAL CONSTANTS OF IDOCRASE
WITH T1 CONTENT.

	RGC-37-50	RGC-92-52	RGC-109-52
EPSILON	1.719	1.720	1.729
OMEGA	1.721	1.726	1.732
	UNIAXIAL	BIAXIAL	BIAXIAL
2V	0	2-5°	10°
T1 %	1	2	5

T1 determined spectrographically.

The powder X-ray patterns of the two biaxial idocrases show a slight shift in the lines which can be seen visually but the measurements fall within the limits of accuracy. This suggests that there is an expansion of the idocrase structure, similar to that found in the andradites, in order to accommodate the excess titanium. Further work needs to be completed to establish definite relationship between optics, unit cell, and titanium content.

NEW MINERAL

A new mineral species was discovered associated with benitoite and natrolite from the Gem mine. The X-ray pattern and optical character of this mineral does not match any of the described minerals in the literature. Unfortunately only a very small sample was found and insufficient material was available for a complete chemical analysis. The mineral is a shiny blue-black with a blue streak forming elongated crystals in small radiating clusters. The hardness of the mineral is 3-4 and density 4.15. Qualitative chemical tests indicate that Ti is a major constituent. The optical constants of the mineral are listed:

Alpha	- 1.830 ± 0.002	- colorless to light yellow
Beta	- 1.908	- reddish yellow
Gamma	- 1.927	- deep indigo blue
2V	- 63° (-)	Z > Y > X
Birefringence	- 0.097	Parallel extinction Z = c

This same mineral has been found in well cuttings from the Coalinga oil field by C. O. Hutton (personal communication), probably a detrital fragment derived from the Gem mine locality. Further searching of the

Gem mine was unsuccessful in producing additional material for study.

MINERAL LIST

The following lists tabulate all of the minerals identified in the various rock types, i.e., serpentines, metamorphic rocks (Franciscan type), syenite-camptonite, and metasomatic rocks. The formulas given for each species are taken from Hey's (1950) classification.

SERPENTINE

Magnetite	$8(\text{Fe}_3\text{O}_4)$
Chromite	$8(\text{FeCr}_2\text{O}_4)$
Picrochromite	$8(\text{MgCr}_2\text{O}_4)$
Calcite	$2(\text{CaCO}_3)$
Magnesite	$2(\text{MgCO}_3)$
Hydromagnesite	$2(\text{Mg}_5(\text{CO}_3)_4(\text{OH})_2 \cdot 4\text{H}_2\text{O})$
Olivine	$4(\text{Mg,Fe})_2\text{SiO}_4 - \text{Fe}_{80}\text{Fe}_{10} \text{ to } \text{Fe}_{20}\text{Fe}_{20}$
Antigorite	$16(\text{Mg}_3\text{Si}_2\text{O}_5(\text{OH})_4)$
Bastite	Near $(\text{Mg,Fe})\text{SiO}_3 \cdot 4-5\text{H}_2\text{O}$
Chrysotile	$2(\text{Mg}_3\text{Si}_2\text{O}_5(\text{OH})_4)$
Penninite	$2(\text{Mg,Fe}^{II},\text{Al})_{12}(\text{Si,Al})_8\text{O}_{22}(\text{OH})_{16}$
Kammererite	Near $\text{Mg}_{2.5}(\text{Al,Cr})\text{Si}_{1.5}\text{O}_5(\text{OH})_4$
Andradite	$8(\text{Ca}_3\text{Fe}^{III}_2\text{Si}_3\text{O}_{12})$
Uvarovite	$8(\text{Ca}_3\text{Cr}_2\text{Si}_3\text{O}_{12})$
Glaucophanes	$2(\text{Na}_2(\text{Mg,Fe}^{II})_3\text{Al}_2\text{Si}_8\text{O}_{22}(\text{OH})_2)$

METAMORPHIC ROCKS (FRANCISCAN TYPE)

Albite	$4(\text{NaAlSi}_3\text{O}_8)$ - up to An_{10} .
Quartz	$3(\text{SiO}_2)$
Pumpellyite	$\text{Ca}_4(\text{Al}, \text{Mg}, \text{Fe})_6\text{Si}_8\text{O}_{23}(\text{OH})_3 \cdot 2\text{H}_2\text{O}$
Pyrite	$4(\text{FeS}_2)$
Lawsonite	$4(\text{CaAl}_2\text{Si}_2\text{O}_6(\text{OH})_4)$
Glaucophane	$2(\text{Na}_2(\text{Mg}, \text{Fe}^{2+})_3\text{Al}_2\text{Si}_8\text{O}_{22}(\text{OH})_2)$
Crossite	$2(\text{Na}_2(\text{Mg}, \text{Fe}^{2+})_3(\text{Fe}^{3+}, \text{Al})_2\text{Si}_8\text{O}_{22}(\text{OH})_2)$
Actinolite	$2(\text{Ca}_2(\text{Mg}, \text{Fe})_5\text{Si}_8\text{O}_{22}(\text{OH})_2)$
Tremolite	$2(\text{Ca}_2\text{Mg}_5\text{Si}_8\text{O}_{22}(\text{OH})_2)$
Pigeonite	$8(\text{Mg}, \text{Fe}, \text{Ca})\text{SiO}_3$
Acmite	$4(\text{NaFe}^{3+}\text{Si}_2\text{O}_6)$
Jadeite	$4(\text{NaAlSi}_2\text{O}_6)$
Epidote	$2(\text{Ca}_2(\text{Al}, \text{Fe})_3\text{Si}_3\text{O}_{12}\text{OH})$
Zoisite	$4(\text{Ca}_2\text{Al}_3\text{Si}_3\text{O}_{12}\text{OH})$
Clinozoisite	$2(\text{Ca}_2\text{Al}_3\text{Si}_3\text{O}_{12}\text{OH})$
Prehnite	$2(\text{Ca}_2\text{Al}_2\text{Si}_3\text{O}_{10}(\text{OH})_2)$
Muscovite	$4(\text{KAl}_3\text{Si}_3\text{O}_{10}(\text{OH})_2)$ - includes sericite.
Chlorite	Species not identified.
Stilpnomelane	Near $\text{K}(\text{Fe}^{2+}, \text{Fe}^{3+}, \text{Al})_{10}\text{Si}_{12}\text{O}_{30}(\text{O}, \text{OH})_{12}$
Garnet	Species not identified.
Thomsonite	$4(\text{NaCa}_2\text{Al}_5\text{Si}_5\text{O}_{20} \cdot 6\text{H}_2\text{O})$
Natrolite	$8(\text{Na}_2\text{Al}_2\text{Si}_3\text{O}_{10} \cdot 2\text{H}_2\text{O})$
Analcite	$16(\text{NaAlSi}_2\text{O}_6 \cdot \text{H}_2\text{O})$
Hydrogarnet	$8(\text{Ca}_3\text{Al}_2\text{Si}_3\text{-xO}_{12\text{-4x}}(\text{OH})_{4x})$, x up to 3

Sphene	4(CaTiSiO ₄ (OH,F))
Apatite	2(Ca ₄ (PO ₄) ₃ F)
Calcite	2(CaCO ₃)

~~SYENITE~~ AND CAMPTONITE

Galena	4(PbS)
Chalcocite	96(Cu ₂ S)
Pyrite	4(FeS ₂)
Cinnabar	3(HgS)
Magnetite	8(Fe ₃ O ₄)
Calcite	2(CaCO ₃)
Apatite	2(Ca ₄ (PO ₄) ₃ F)
Sphene	4(CaTiSiO ₄ (OH,F))
Acmite	4(NaFe ^{''} Si ₂ O ₆)
Aegirine-augite	8(Na,Ca,Mg,Fe ^{''} ,Fe ^{'''} ,Al)(Si,Al,Fe ^{'''})O ₃)
Pigeonite	8((Mg,Fe,Ca)SiO ₃)
Barkovikite	2(Na Ca ₂ (Mg,Fe ^{''} ,Fe ^{'''} ,Al) ₅ (Si,Al) ₈ O ₂₂ (OH) ₂)
Glaucophane	2(Na ₂ (Mg,Fe ^{''}) ₃ Al ₂ Si ₈ O ₂₂ (OH) ₂)
Crossite	2(Na ₂ (Mg,Fe ^{''}) ₃ (Fe ^{'''} ,Al) ₂ Si ₈ O ₂₂ (OH) ₂)
Richterite	2((Na,K) ₂ (Mg,Mn,Ca) ₆ Si ₈ O ₂₂ (OH) ₂)
Olivine	4((Mg,Fe) ₂ SiO ₄) - Fe ₈₄ Fe ₁₆ to Fe ₇₈ Fe ₂₂
Spessartine	8(Mn ₃ Al ₂ Si ₃ O ₁₂)
Biotite	2(K ₂ (Mg,Fe ^{''} ,Al,Fe ^{'''}) ₄₋₆ (Si,Al) ₈ O ₂₀ (OH) ₄)
Muscovite	4(KAl ₃ Si ₃ O ₁₀ (OH) ₂)
Chlorite	Species not identified.

Plagioclase	An ₅ to An ₈₉
Analcite	16(NaAlSi ₃ Si ₃ O ₁₀ ·2H ₂ O)
Natrolite	8(Na ₂ Al ₂ Si ₃ O ₁₀ ·2H ₂ O)
Prehnite	2(Ca ₂ Al ₂ Si ₃ O ₁₀ (OH) ₂)
Zoisite	4(Ca ₂ Al ₃ Si ₃ O ₁₂ OH)
Clinozoisite	2(Ca ₂ Al ₃ Si ₃ O ₁₂ OH)

METASOMATIC ROCKS

Magnetite	8(Fe ₃ O ₄)
Ilmenite	2(FeTiO ₃)
Rutile	2(TiO ₂)
Perovskite	8(CaTiO ₃)
Calcite	2(CaCO ₃)
Dolomite	(CaMg(CO ₃) ₂)
Apatite	2(Ca ₅ (PO ₄) ₃ F)
Sphene	4(CaTiSiO ₄ (OH,F))
Benitoite	2(BaTiSi ₃ O ₉)
Neptunite	8((Na,K) ₂ (Fe ^{II} ,Mn)TiSi ₄ O ₁₂)
Joaquinite	4(NaBaTiSi ₄ O ₁₅)
Chevkinite	Near (Fe ^{II} ,Ca)(Ce,La) ₂ (Si,Ti) ₂ O ₈ ?
Zircon	4(ZrSiO ₄)
Titanian andradite	8(Ca ₃ (Fe ^{III} ,Ti) ₂ (Si,Ti) ₃ O ₁₂) TiO ₂ up to 14%
Andradite	8(Ca ₃ Fe ^{III} ₂ Si ₃ O ₁₂)
Idocrase	4(Ca ₁₀ (Mg,Fe ^{II} ,Fe ^{III}) ₂ Al ₄ Si ₈ O ₃₄ (OH) ₄) up to 5% Ti substituting in structure.
Diopside	4(MgCaSi ₂ O ₆)

Natrolite	$8(\text{Na}_2\text{Al}_2\text{Si}_3\text{O}_{10} \cdot 2\text{H}_2\text{O})$
Stilpnomelane	Near $\text{K}(\text{Fe}^{II}, \text{Fe}^{III}, \text{Al})_{10}\text{Si}_{12}\text{O}_{30}(\text{O}, \text{OH})_{12}$
Clinochlore	$2(\text{Mg}, \text{Al}, \text{Fe}^{II})_{12}(\text{Si}, \text{Al})_8\text{O}_{20}(\text{OH})_{16}$
Delessite	Near $(\text{Mg}, \text{Fe}^{II})_{3.5}\text{Al}_3\text{Si}_3\text{O}_{10}(\text{OH})_8$
Knapfite (Leuchtenbergite)	$2(\text{Mg}_{10}\text{Al}_2)(\text{Al}_2\text{Si}_6)\text{O}_{20}(\text{OH})_{16}$
Penninite	$2(\text{Mg}, \text{Fe}^{II}, \text{Al})_{12}(\text{Si}, \text{Al})_8\text{O}_{22}(\text{OH})_{16}$
Pyrochlorite (Ripidolite)	$2(\text{Mg}, \text{Fe}^{II})_9\text{Al}_6\text{Si}_5\text{O}_{20}(\text{OH})_{16}$

PETROLOGY

Franciscan type rocks

The New Idria District contains a heterogeneous group of rocks with lithologies similar to those of the Franciscan formation. From stratigraphic evidence, the oldest formation exposed in the district is probably Franciscan in age, although there is no direct fossil evidence to corroborate this assumption. The bulk of this formation is made up of sedimentary greywackes accompanied by minor amounts of greenstone, cherts, and schists containing glaucophane. They are found flanking the serpentine and show a universally faulted contact relationship. Many tectonic inclusions within the serpentine have lithologies similar to the peripheral Franciscan rocks; and therefore, have been included in this discussion of the Franciscan rocks.

The Franciscan type rocks have been divided into three categories for convenience of discussion, (1) rocks peripheral to the serpentine, (2) tectonic inclusions within the serpentine, and (3) jadeite bearing rocks within the serpentine in and near the tectonic inclusions.

Peripheral Franciscan rocks

The major rock type found in this category is a sedimentary greywacke characterized by a brown to gray cast and containing abundant secondary quartz veinlets. Many isolated lenses of thin-bedded chert are found interbedded with the greywacke. These chert beds may reach a thickness of 100 feet or more in this district. Taliaferro (1943) has pointed out that these cherts probably formed as a result of the volcanism attendant

during the Franciscan time of deposition.

Altered volcanic rocks are sparsely interbedded with the greywacke and are characterized by light green color and dense texture. Alteration of these rocks has produced a rock that may be best described as a spilitic greenstone.

Small isolated patches of schist are commonly found within the greywackes and these appear to be concentrated along the Franciscan-serpentine contact; however, no regular spatial relationship could be established between the schist zones and the local structure. These schists commonly contain glaucophane as a major mineral and are usually referred to as glaucophane schists. All of the Franciscan rocks within the New Idria District show evidence of low-grade dynamothermal metamorphism and it may be that these local schist zones are areas that have undergone a slightly more intense pulse of shearing and pressure. No field evidence was found in this district to support Taliaferro's (1943, p. 182) view that these schists have formed by pneumatolytic action resulting from the serpentines emplacement.

It is not the purpose of this paper to discuss the origin of the glaucophane schists, one of the unsolved problems in metamorphic petrology; however a brief petrographic description of the major rock types is given.

The peripheral Franciscan rock types are divided into five groups as follows:

Group I*

Greywacke (RGC-26-50)

do. (RGC-39-50)

*Sample numbers may be located in Plate I.

Group I (continued)

Greywacke (RGC-20-50)

do. (RGC-18-50)

do. (RGC-49-50)

do. (RGC-40-50)

Group II

Chert (RGC-21-50)

Group III

Greenstone (RGC-22-50)

do. (RGC-73-51)

do. (RGC-21-50)

Group IV - Schists

Glaucophane-chlorite-muscovite-sphene (RGC-60-51)

Glaucophane-chlorite-garnet-pyroxene (RGC-73-51)

Glaucophane-crossite-lawsonite (RGC-51-50)

Glaucophane-muscovite-lawsonite (RGC-80-51)

Group V - Schists

Calcite-glaucophane-stilpnomelane (RGC-21-50)

Quartz-stilpnomelane-lawsonite (RGC-29-50)

Albite-glaucophane-chlorite (RGC-80-51)

Tremolite (RGC-62-51)

Group I - The greywackes are brown to dark gray and tend to show a very crude schistosity or a platy direction of fracture. Secondary veins of white quartz commonly cut the bedding or may extend along the bedding planes. Angular to sub-angular quartz, the most abundant mineral, almost universally shows strong undulatory extinction and forms sheared augen

with mortar structure. The quartz in the secondary veins shows similar features. Plagioclase makes up 25% or more of the greywacke; it usually retains its original twinning, although determination of its former composition is difficult due to alteration. Saussuritization is typical of all the feldspars and dense aggregates of clinozoisite and epidote form within the crystals. Index determinations on the altered feldspar shows it to be albite (An_{5-10}). Lithic fragments of andesite and basalt are abundant and detrital chert fragments (RGC-20-50) may be locally abundant. The matrix of these rocks is 'pasty' and is molded around the larger detrital fragments. This matrix is a finely crystalloblastic, dense mass consisting mostly of clinozoisite, sericite, chlorite, sphene (leucoxene), and iron ores. Shear planes that have developed are manifested by semi-opaque dark brown bands containing iron ores, sphene, sericite, and occasionally wisps of glaucophane and stilpnomelane (RGC-26-50) and (RGC-39-50).

This cursory examination strongly indicates that the greywackes surrounding the serpentine have undergone a low-grade dynamothermal metamorphism, that is comparable to that in Hutton's (1940) Chlorite sub-zone Chl. 1.

Group II - The chert is thin-bedded, often rhythmically interbedded with shale, and it may be red or brown like jasper, but more often green, light gray, or blackish. It is composed of cryptocrystalline quartz and chalcedony with a fibrous structure. Many small euhedral platelets of chlorite are dispersed within the chert and also concentrated in thin sinuous lines with small magnetite grains. Many small secondary veins of coarser-grained quartz cut the fine-grained groundmass of these cherts. Radio-larian tests were not seen in the section studied, although Taliaferro

(1943, p. 147) reports that they are common in Franciscan cherts.

Group III - The greenstones are dense fine-grained rocks cut by white reticulated veins. Clinzoisite and albite form a dense crystallo-blastic groundmass and in some instances relict diabasic textures are discernable, with relict pyroxenes apparently unchanged. Minor sphene, chlorite, and quartz are also present. Foliation, lineation, or schistosity is not developed within these rocks. Preserved cavities reminiscent of original vesicular volcanic rocks are not uncommon. The reticulated veins contain quartz, calcite, and albite in that order. These rocks are probably altered fine-grained volcanic rocks similar to spilitic basalts.

Group IV - Most of the schist zones, less than 100 square yards in areal extent, are characterized by a light blue to gray color and exhibiting a fairly well developed schistosity. The dominant glaucophane (Pl. VI, Figs. 1 and 3) forms well developed crystals and produces a lepidoblastic texture in these rocks. Crossite commonly accompanies the glaucophane either as discrete crystals or zonally arranged on the glaucophane (RGC-51-50), whereas large, well crystallized plates of chlorite and muscovite (Pl. VI, Fig. 4) form the interstitial areas between the amphiboles. Porphyroblastic garnets (Pl. VI, Fig. 2) developed in (RGC-73-51) show some evidence of retrograde change to chlorite. Jadeitic pyroxene found rimming glaucophane in (RGC-73-51) appears to contradict the evidence of retrograde change in this rock; although it is not clear what P-T conditions are favorable to form jadeite. Lawsonite forms colorless square tabular crystals and anhedral aggregates (Pl. VI, Fig. 1) interstitial to the amphiboles, and it seems to have formed later

than the other constituents. Idioblastic crystals of sphene are universally present (Pl. VI, Fig. 2 and 4) and may make up 10% of the rock.

These metamorphic schists characterized by glaucophane-chlorite, contain no relict minerals or textures and appear to have been completely recrystallized by low-grade chlorite zone metamorphic processes.

Group V - This group contains diverse rock types showing individual characteristics. (RGC-60-51) was probably a quartz-albite-glaucophane rock that has been brecciated and subsequently replaced, in part, by calcite. Stilpnomelane has formed contemporaneously with the carbonate.

An albite-chlorite-glaucophane schist (RGC-80-51) is similar to Group IV rocks, except for abundant albite. The quartz-stilpnomelane-lawsonite schist (RGC-29-50) forms a small selvage in a large mass of slightly metamorphosed greywacke where it has completely recrystallized with a well developed schistosity.

The tremolite schist, the only monomineralic rock found, is coarsely crystalline with a lepidoblastic texture. A faint bluish tint is developed around the borders of the individual crystals, suggesting late introduction of Na.

Tectonic inclusions

Present within the serpentine are numerous foreign rock bodies of variable size and shape; the largest mass is about five acres in areal extent and the smaller bodies are less than 100 square yards. The distribution of these inclusions is entirely random and the observed attitude of their structural trends is also random; however, the larger bodies

PLATE VI. Photomicrographs of peripheral Franciscan schists.

- Figure 1. Glaucophane-crossite-lawsonite schist. Prismatic gray crystals are glaucophane with borders of crossite. Lawsonite fills the interstices. Plain light (X 80).
- Figure 2. Glaucophane-chlorite-garnet-pyroxene schist. Idioblastic garnet shows incipient alteration to chlorite. Large, high relief crystal diagonal to the field is sphene. Interlocking prisms of glaucophane are present in the upper part of the field. Plain light (X 80).
- Figure 3. Albite-glaucophane-chlorite-muscovite schist. Idioblastic grains of glaucophane associated with albite and muscovite. Plain light (X 80).
- Figure 4. Glaucophane-chlorite-muscovite-sphene schist. Large warped plate of chlorite containing grains of sphene. Plain light (X 80).



2



4



1



3

appear to roughly parallel the regional NW-SE structural trend (see Pl. I). The contacts between the serpentines and these inclusions are almost invariably sheared and faulted, and where contacts show no apparent shearing or faulting, microscopic examination reveals shearing, and reconstitution of the serpentine to chlorite and andradite. Antigorite develops along shear planes of the serpentine up to ten feet away from the contact. Careful field examination of these contacts revealed no evidence of contact metamorphism within these bodies that might have resulted from deep seated alteration by an ultrabasic magma. There is no mineralogical evidence to indicate magnesium metasomatism within the included rocks, although there appears to have been some movement of elements from the tectonic inclusions into the serpentines as there is local development of soda-rich pyroxenes near the contacts.

The nature of these foreign rock bodies suggests that they are tectonic inclusions, similar to Brother's (1954, p. 616) glaucophane schist bodies within the serpentine of the Berkeley Hills, California. The direction of movement of these tectonic inclusions within the serpentine is extremely hard to interpret. The general shape of the inclusions, usually elongate, tabular with vertical bedding or schistosity, suggests a downward movement and, therefore, it appears that these inclusions have foundered from the roof of the serpentine mass or have been dragged around into parallel position with the bounding thrusts yet immersed in a mass of semi-plastic serpentine. It is difficult to imagine under what conditions the present serpentine was emplaced in the country rock as it is evident that it was not a magma at that time. If the inclusions were brought up from depth, a higher grade of metamorphism should be present in them. The observed

relations of these inclusions, in the field, strongly suggest that they were floated or rafted into the ultrabasic rock during serpentinization, or after serpentinization during an intense tectonic movement of the Diablo Range.

It is assumed that the tectonic inclusions were derived from the Franciscan formation, on account of similarity of mineralogy and bulk composition. The grade of metamorphism is similar to that found in the peripheral Franciscan rocks, however the metamorphic minerals within the tectonic inclusions are much finer grained than those in the peripheral rocks (compare Pls. VI and VII). This suggests that the period of metamorphism was shorter lived on the tectonic inclusions than that exerted on the peripheral rocks.

The main rock types found within these tectonic inclusions are grouped below according to their similarity in mineralogy.

Group I

- pyroxene-pumpellyite (RGC-53-51)
- pyroxene-albite-chlorite (RGC-53-51)
- chlorite-pumpellyite-lawsonite-sphene (RGC-107-52)
- pyroxene-albite-chlorite (Gem mine)
- gabbro-saussuritized (Gem mine)

Group II

- quartz-albite-glaucophane-stilpnomelane (RGC-76-51)
- quartz-albite-sericite-chlorite (RGC-53-51)
- quartz-albite-zoisite-chlorite (RGC-98-52)
- quartz-albite-chlorite-actinolite (RGC-68-50)

Group II (continued)

quartz-albite-chlorite-sericite (RGC-77-51)
 quartz-albite-chlorite-zoisite (RGC-93-52)
 quartz-sericite-chlorite-albite (RGC-107-52)

Group III

albite-quartz-stilpnomelane-tremolite (RGC-103-52)
 albite-quartz-crossite-acmite (RGC-32-50)
 albite-quartz-glaucophane-stilpnomelane (RGC-76-51)

Group IV

albite-glaucophane-actinolite (RGC-81-52)
 albite-glaucophane-acmite (RGC-54-51)
 albite-glaucophane-acmite-stilpnomelane (RGC-32-50)
 albite-glaucophane-stilpnomelane (RGC-54-51)
 albite-glaucophane-epidote (RGC-54-51)
 albite-glaucophane-crossite (RGC-99-52)
 albite-glaucophane-epidote (RGC-106-52)
 albite-crossite-epidote (Gem mine)
 albite-crossite-glaucophane (RGC-50-50)

Group I--These rocks are characterized by a light to dark green color and relict igneous textures that reveal the original nature of the rock. The texture and mineral composition indicate that they were medium- to fine-grained rocks ranging from gabbro to augitites in composition. Relict pyroxenes are abundant and usually show little or no alteration. Optical and X-ray determinations on these pyroxenes establishes their composition as varying from aegirine-augite to pigeonite. Albite has

formed at the expense of the original calcic-feldspars. Pumpellyite and lawsonite also form at the expense of the calcic-feldspars and partial breakdown of the pyroxene. Sphene is abundant in several of these rocks and may be found as large wedge-shaped crystals. In the hand specimen, these rocks are extremely fine-grained, tough, greenish in color and are indistinguishable from the greenstones found in the peripheral Franciscan. Foliation, lineation, and schistosity are not found. These rocks are probably slightly metamorphosed spilitic basalts and gabbros, since their calculated compositions from their modes are similar to these basic rocks.

Group II--This group includes greywacke-type rocks that are gray to brown, medium-grained rocks having a crude foliation and schistosity. Thin quartz veins are abundant in most of these rocks. Quartz and plagioclase are the most abundant constituents accompanied by lesser amounts of altered lithic fragments and fine-grained chlorite, sericite, zoisite, and actinolite. A weak dynamothermal metamorphism has partially recrystallized the finer constituents, but the original character of the rocks is easily ascertained. The rocks are greywackes, for they are composed of clastic quartz and feldspar (25% or more) accompanied by lithic fragments and the intergranular cement is made up of a paste or titrated equivalents of the above mentioned minerals. The greywackes exhibit recrystallization along the shear planes and the pasty intergranular cement is crystalloblastic. Glaucophane (RGC-77-51) has formed fine needles in the shear zones and tufts around the periphery of the detrital pyroxenes in response to dynamothermal metamorphism. The greywackes within the tectonic inclusions are similar to those described by Hutton (1940) and could be classed in his Chlorite sub-zone Chl. 1. These rocks show slightly higher

metamorphism than the peripheral greywackes.

Group III--The rocks in this group are characterized by their bluish to grey coloration and by the moderately to well developed schistosity and foliation. The schists are fine-grained compact rocks and many contain late fractures filled by quartz, calcite, or prehnite. The quartz and albite in the schists are completely recrystallized and only rare porphyroclasts of quartz remain. Usually the quartz and feldspar separate into folia and the crossite, glaucophane, and stilpnomelane form along the shear planes that are still recognizable by the abundance of opaque material still uncombined with the recrystallized minerals. Actinolite is present as a stable relict mineral forming porphyroclasts that may or may not have 'whiskers' of glaucophane growing out from the surface (Pl. VIII, Figs. 1 and 2). It is difficult to determine the original nature of these rocks although they seem to be the metamorphic equivalents of the quartzo-feldspathic greywackes. These schists show a slightly higher rank metamorphism than that observed in the greywackes, but still in the Chlorite zone of metamorphism (Chlorite sub-zone Chl. 4, Hutton, 1940).

Group IV--The schists in this group are quite similar to those in Group III; fine-grained, bluish to grey, and moderately developed schistosity and foliation. Albite is the most abundant mineral forming crude segregation bands. Quartz is minor or lacking in these rocks and when present it has been completely recrystallized. Relict calcic-plagioclase was not found in this group. Glaucophane is the dominant dark mineral forming delicate needles along the shear planes, aggregates of fibrous bundles, or

as "whisker-like" mats around relict pyroxene grains (Pl. VII, Figs. 1 and 4). Crossite is commonly associated with glaucophane and in many instances a small needle-like crystal may have a core of glaucophane and a rim of crossite. Actinolite and pigeonite appear as detrital relicts and show only incipient recrystallization to glaucophane (Pl. VII, Figs. 1 and 2). Epidote forms equigranular aggregates along the shear planes and has apparently formed at the expense of calcic-feldspars and mafic minerals. These schists seem to be the metamorphosed equivalents of quartzo-feldspathic sediments that were unusually rich in feldspar and ferromagnesian minerals.

Jadeite bearing rocks

Jadeite was first reported from California by Mielenz (1939) as an essential constituent in a quartz-albite-jadeite schist from the Franciscan formation in San Benito County. Bolander (1950) reported jadeite boulders along Clear Creek in the northwestern part of the serpentine (see Plate I). Following the article by Bolander, considerable interest was aroused and in 1951 Yoder and Chesterman described the occurrence of jadeite-bearing rocks, in place, along the banks of Clear Creek near Bolander's original discovery.

Yoder and Chesterman (1951) reported eight large exposures of jadeite in the canyon of Clear Creek. Several more bodies near the original site and one large isolated mass near Santa Rita Peak (RGC-84-52) were discovered during this investigation.

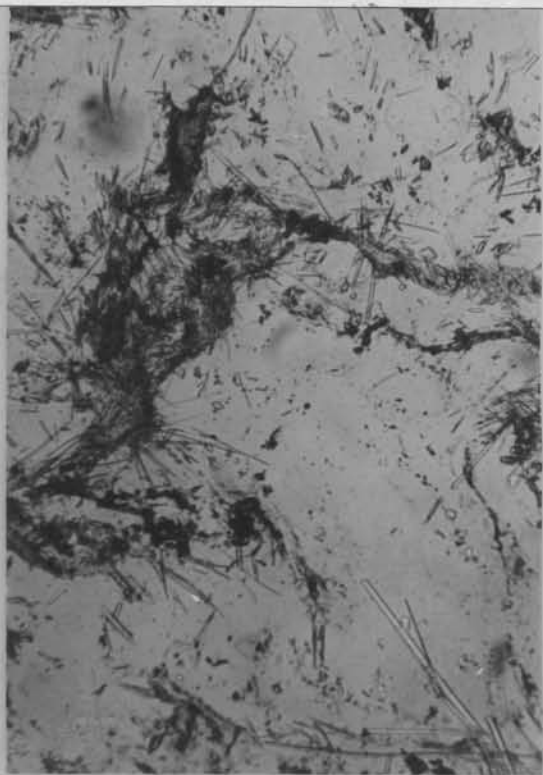
The jadeite is found in two distinct occurrences. (1) Lens-like bodies having an irregular vuggy surface and completely surrounded by sheared antigoritic serpentine. The central portion of these bodies contains

PLATE VII. Photomicrographs of schist from tectonic inclusions.

- Figure 1. Albite-glaucophane-pigeonite schist. Groundmass of colorless albite containing relict grains of pigeonite. Alteration by metamorphism has produced 'whiskers' of glaucophane around the pigeonite. Plain light (X 100).
- Figure 2. Albite-glaucophane-crossite schist. Groundmass of albite containing relict grains of pyroxene. Glaucophane and crossite 'whiskers' forming on the pyroxene in response to metamorphism. Plain light (X 100).
- Figure 3. Albite-glaucophane-epidote schist. Groundmass of albite containing 'bundles' of glaucophane. Irregular shear zones contain iron oxides and epidote. Plain light (X 100).
- Figure 4. Albite-glaucophane-actinolite schist. Groundmass of albite cut by sinuous shear zone where needles of glaucophane and actinolite are concentrated. Plain light (X 100).



2



4



1



3

an irregular 'eye' of crushed jadeite (Figure 6). (2) Veins of jadeite around the periphery and central portions of tectonic inclusions (Fig. 7).

The lens-like bodies (Figure 6) form bold resistant outcrops within the serpentine and have a very indistinct contact with the serpentine country rock; near the contact the serpentine is blackish and glassy containing antigorite surrounding blebs of chrysotile. The contact zone is composed of earthy weathered material that apparently has undergone extreme crushing and shearing. Andradite garnet is present within the serpentine near this contact zone. Yoder and Chesterman (1951) report a contact zone containing grossularite, lawsonite, pumpellyite, and a green amphibole. The outer zone of the lens is composed of a tough, greenish to brown, fine-grained rock composed essentially of fibrous prehnite, hydrogarnet, and sphene with minor amounts of biotite altering to chlorite. The sphene seems to be relict as it is in distinct bands reminiscent of an original metamorphic structure. The outer zone grades imperceptibly into a similar rock that is brownish with a cavernous weathered surface. The groundmass is composed of irregular grains of fully hydrated thomsonite containing inclusions of fibrous prehnite. Relict grains of sphene are present as residual crenulated, segregated bands again suggesting inherited metamorphic structure. Minor amounts of chlorite may be found in the interstitial areas of the rock.

The central portion of the lens-like body is composed of an 'eye' of greenish jadeite. The jadeite 'eye' is monomineralic except for extremely thin veinlets of biotite. Two generations of jadeite can be distinguished; (1) greenish jadeite that has been crushed and fractured, (2) white jadeite healing the fractured and crushed jadeite. The green jadeite is cloudy and

SKETCH OF LENS-LIKE JADEITE BODY

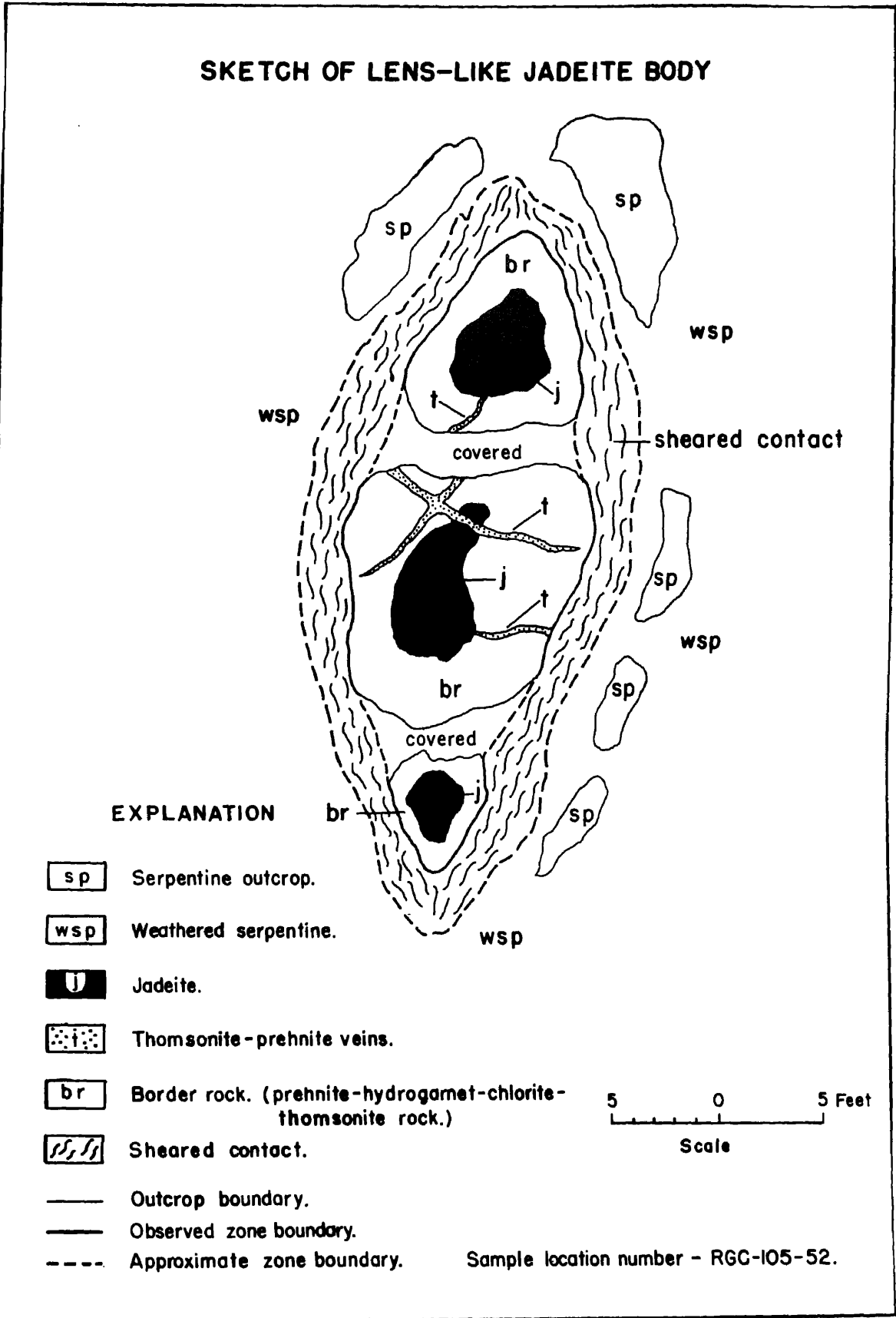


Figure 6

has abundant fine-grained opaque inclusions. In contrast, the white jadeite is clear, with very few inclusions. Optical determinations on the green jadeite reveal that it must contain some diopside and aegirine in solid solution.

Veins, up to two inches in width, containing thomsonite, prehnite, and minor hydrogarnet transect these various zones in the lens and are the latest stage of mineralization observed in the bodies. Natrolite and prehnite are present in veins from other lens-shaped bodies in the vicinity. The zoned hydrogarnet from these bodies is discussed under mineralogy.

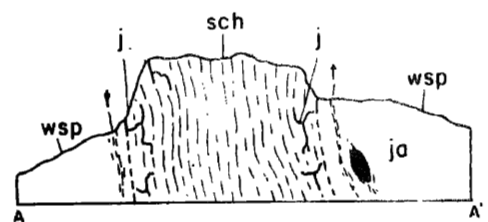
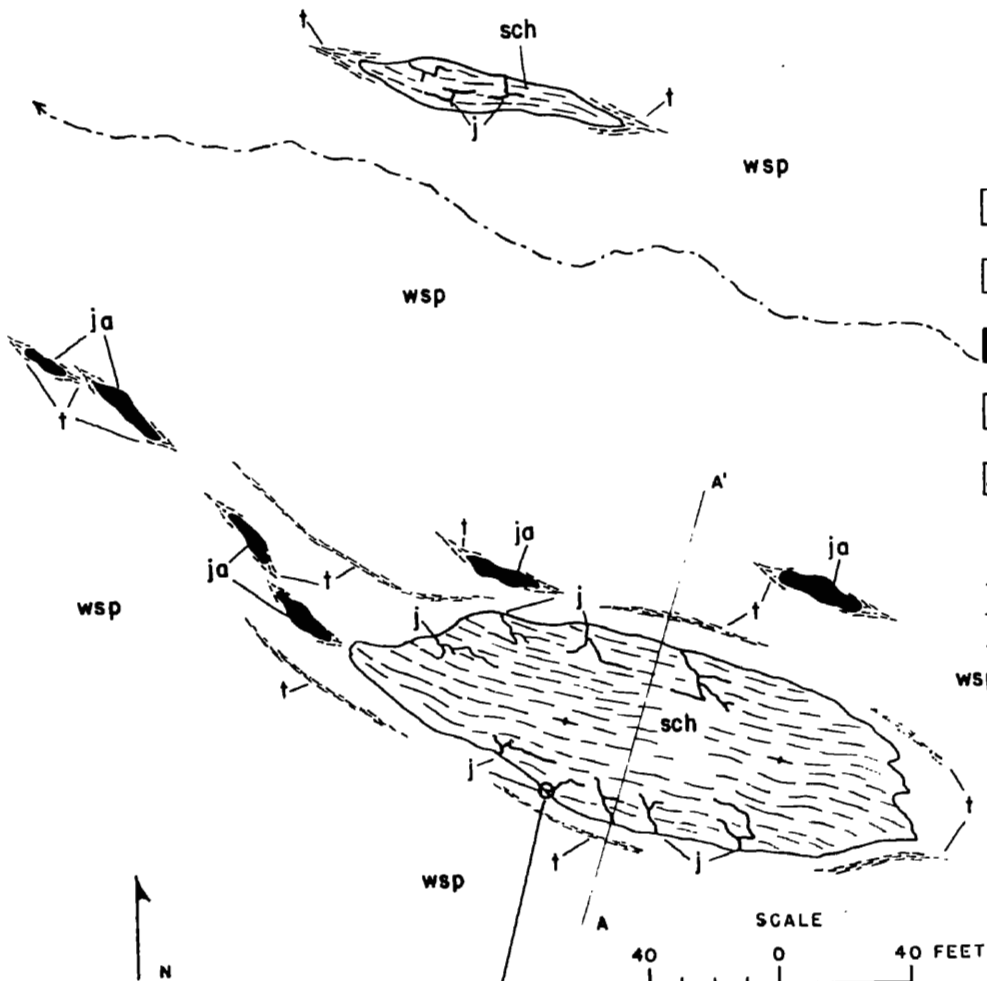
The banded character of these rocks and the relict stringers of sphene in the outer-zone rocks suggest that these lens-like bodies may have originally been metamorphic rocks similar to others found as tectonic inclusions within the serpentines. The mineralogy of the lens-like body described by Chesterman and Yoder is somewhat different than the one studied by the author, although the general characteristics are similar and cursory examination of other lens-like bodies shows a variable mineral composition.

Individual veins of jadeite were found in schist bodies along Clear Creek (Fig. 7). These veins are usually along the periphery of the schist and show cross cutting relationships to the enclosing schist (Fig. 8). The veins are quite variable in composition and color, and show irregular form. Most of these veins are less than one inch in width with local swellings up to eight inches. The larger veins contain two generations of jadeite, a dark green variety containing diopside and aegirine in solid solution cut by intersecting veinlets of white jadeite accompanied by minor analcite and low albite. These large veins pinch and swell, and

GEOLOGIC MAP
OF
TECTONIC INCLUSION
CONTAINING
JADEITE

EXPLANATION

- wsp Weathered serpentine.
- A J A Jadeite veins. (Contain white jadeite, albite, analcite, prehnite, and natrolite.)
- ja Pods containing jadeite and antigorite.
- t t Shear zones of tremolite.
- sch Schist - albite-glaucophane-stilpnomelane
albite-glaucophane-acmite
albite-glaucophane-epidote
albite-quartz-crossite
- Outcrop boundary.
- - - Approximate boundary.
- · - · - Intermittent stream.
- wsp ↗ Strike of vertical schistosity.



NE 1/4, SEC. 12, R 11E, T 18S.

Sample location numbers. RGC-32-50
RGC-54-51

Analyzed jadeite taken from this vein.

Geology by R.G. Coleman, 1951

Figure 7

BS

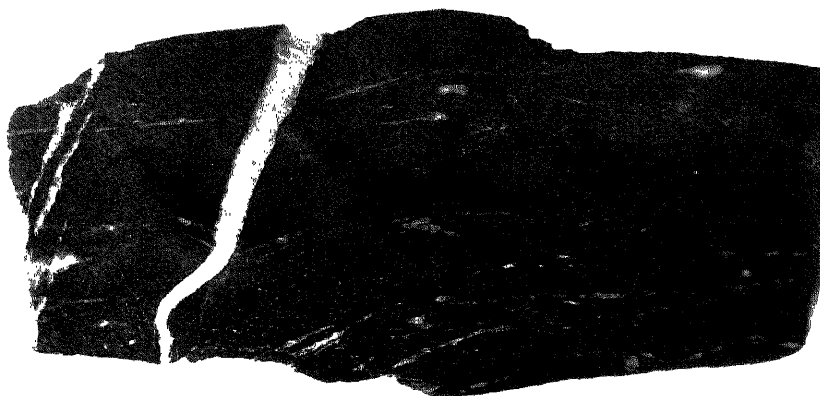


Figure 8. Polished slab of albite-glaucophane-actinolite schist cut by vein of white jadeite. Note folia of jadeite developed along planes of schistosity.

in many places are offset by minor cross faults. Smaller veins of almost pure white jadeite show very little fracturing or secondary veination. The detailed relationships between the smaller veins and the enclosing schist are shown in Figs. 8 and 9. The contact between the enclosing schist and the jadeite vein is always very sharp and is marked by a thin selvage of green jadeite about 5 mm in width. In places the jadeite penetrates the schist along the planes of schistosity, forming small discontinuous folia (Fig. 8). Microscopic study of these small jadeite veins shows that the jadeite forms normal to the vein walls and is grouped in semi-radiating clusters that are intimately interlocking. Albite and analcite are commonly present in the central portion of the veins. The albite (low albite from X-ray determinations) seems to have formed later than the jadeite followed by analcite which replaces both the jadeite and albite (Fig. 9). The albite in these veins is stable with respect to jadeite as it was not found replacing the jadeite. The distal ends of these veins may be completely lacking in jadeite and in its place are found albite, analcite, thomsonite, natrolite, and prehnite in variable amounts.

The large block of schist shown in Fig. 7 is composed mostly of albite-glaucophane-acmite with minor variations in composition. This block is similar to the tectonic inclusions which have been described earlier and exhibits a well developed foliation and schistosity accompanied by minor small-scale folding. The contact with the enclosing serpentine is highly sheared and tremolite is developed as very fine-grained crystals in this zone. Small elongate blebs of jadeite intergrown with antigorite are common near the schist body and appear to replace the serpentine.

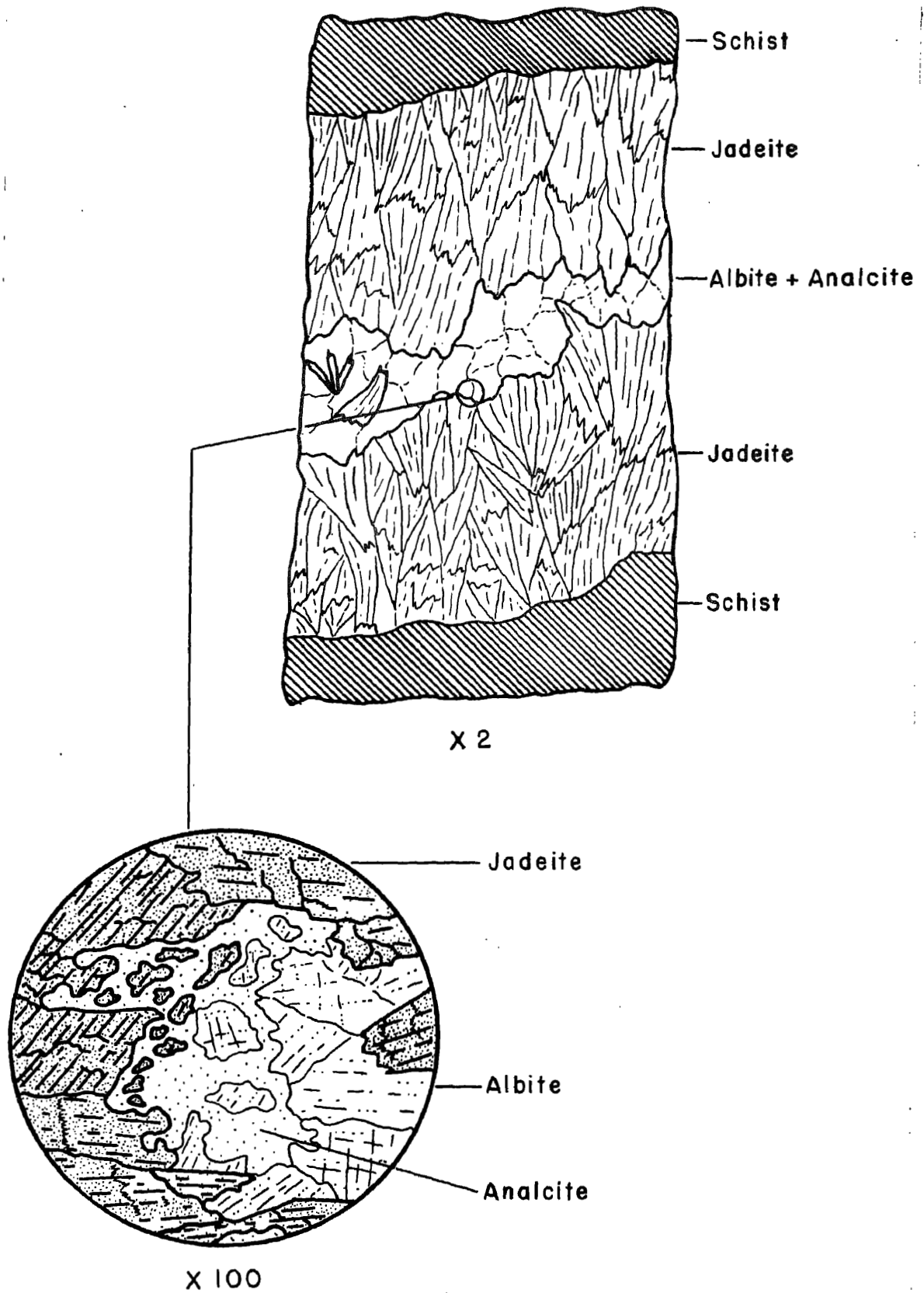


Figure 9. Sketch of jadeite vein showing relationship between jadeite, albite, and analcite. Camera lucida drawing exhibits replacement of jadeite and albite by analcite.

Origin of the jadeite

The mode of formation of jadeite in the New Idria district presents several problems, although the observed field and mineralogical data seem to verify some of the recent experimental work on the jadeite problem. Jadeite has been considered by many writers to be formed only at high pressures and temperatures because of its high density and its apparent association with eclogites. Yoder (1950a) has shown that analyzed jadeites fall into two distinct groups, (1) those high in Na and Al associated with albite and nepheline and (2) those lower in Na and Al associated with garnet, i.e., eclogite. The first group of jadeites are always found associated with serpentines, the Clear Creek jadeite falling in this group. Since there are no eclogite facies in the New Idria district or in other rocks containing Na-Al rich jadeites, it would seem that the formation of Na-Al rich jadeites is separate and distinct from the eclogite problem.

The jadeite veins in the schist are apparently formed in metamorphic rocks which belong to a low-grade metamorphic facies similar to the sub-zones of the Chlorite zone as described by Hutton (1940). The presence of stilpnomelane in some of the schists cut by jadeite veins and containing folia of jadeite suggests Chlorite zone metamorphism. Quartz-albite-epidote-stilpnomelane, therefore, are here considered as a mineral facies characteristic of the Chlorite zone. Thus it would seem that P-T conditions during the formation of the jadeite were similar to those characteristic of the Chlorite zone.

The presence of low albite and zeolites within the jadeite veins suggests that the pressures and temperatures following the formation of jadeite were not excessively high. Furthermore, the enclosing serpentine has not undergone any alteration which may have resulted from higher temperatures or pressures. Bowen and Tuttle (1949, p. 459) state that serpentine cannot be present in any layer of the earth's crust whose temperature is normally above the decomposition temperature of serpentine under the pressure prevailing. Bowen and Tuttle have also shown experimentally that serpentine inverts to forsterite and talc at a temperature above 500° C with pressure up to 45 kilobars having little effect. Thus from the following observations we have no positive evidence of extremely high pressures or temperatures involved in the formation of the jadeite from this locality, and it would appear from these observations that the P-T conditions during the formation of jadeite were similar to those characteristic of the Chlorite zone of metamorphism.

Jadeite has been synthesized by Griggs, Fyfe, and Kennedy (1955) using analcite powder at elevated temperatures and pressures. The jadeite-analcite boundary extends from the triple point (jadeite - nepheline + albite + vapor - analcite + vapor) at about 600° C and 12 kilobars to 300° C and 18 kilobars. Combining Yoder's (1950a) measurements on the nepheline + albite + water \rightarrow analcite equilibrium, and Adams' (1953) thermodynamic calculations on the formation of jadeite from nepheline and albite under anhydrous conditions, with that of Kennedy et al., a possible interpretation of the conditions during the formation of the Clear Creek jadeite can be made.

Jadeite is stable and can form from analcite at temperatures from 300 to 600° C and pressures from 18 to 12 kilobars, respectively (Griggs et al., 1955); however if an anhydrous system is assumed, following thermodynamic calculations of Adams (1953), it is found that jadeite is stable at temperatures below 240° C and at pressures below 2000 bars. The petrographic observations show that the jadeite in the veins could have formed in an anhydrous environment since there are no hydrated minerals formed at this stage. Replacement of jadeite and albite by later analcite suggests an introduction of water following the earlier formation of jadeite. If an anhydrous condition existed during the period of jadeite formation the thermodynamic calculations of Adams show that it would be stable at P-T conditions similar to those postulated for the Chlorite zone of metamorphism. The original reaction to form the jadeite is obscured; nepheline has not been found although albite is plentiful in these rocks.

Three possible sources for fluids responsible in the formation of the jadeite must be considered: (1) fluids from the syenite intrusion, (2) fluids residual from the process which gave rise to the serpentine, and (3) fluids produced by metamorphism of the tectonic inclusions.

The syenite intrusions are enriched in soda during the late stages of solidification and could have supplied fluids of the proper composition necessary for the formation of jadeite, however, the jadeite bodies are not closely associated with the intrusions. The apparent strong metamorphism accompanying the formation of jadeite is not manifest within the

syenite rocks, and it seems that the intrusives are younger than the formation of the jadeite.

During the serpentinization of the original ultrabasic rocks, fluids may have been enriched in sodium and alumina during the late stages and these fluids could have been concentrated in the lens-like bodies and along the contacts of the more resistant schists where the greatest fracturing and shearing would provide ample open spaces. The trace element study of the serpentines revealed that sodium was below the limit of sensitivity in all samples and it seems unlikely that serpentinization could produce a concentrated Na-Al rich fluid, unless it came from an outside source.

The close association of the jadeite with the tectonic inclusions strongly indicates that the soda-rich fluids may well have come from these rocks. The minerals formed by dynamothermal metamorphism of these rocks are in some cases soda-rich and analyses of most of the rocks of supposed Franciscan age are extremely soda-rich ranging from 5 to 6 percent Na_2O (Taliaferro, 1943, p. 136). It would appear most likely that the sodium-rich fluids have been produced during the metamorphism of these large tectonic inclusions. Higher confining pressures were probably developed in the tectonic inclusions than in the surrounding serpentine because of the resistant and brittle nature of the rock when compared to the plastic serpentine.

Jadeite was identified as a metamorphic mineral in a glaucophane-albite schist (RGC-77-51) and has also been reported as a metamorphic mineral in schist from this same region by Mielenz (1939). According to

de Roever (1955) jadeite has formed in quartz-albite schists from the Celebes associated with glaucophanic rocks. He has shown that the jadeite forms under metamorphic conditions characteristic of the glaucophane schist facies.

The production of larger veins and pods of jadeite may have resulted from mobilization by metamorphic differentiation. The metamorphism of these tectonic inclusions probably took place during the serpentinization of the ultrabasic rocks and these processes may have contributed, in part, to the peculiar set of conditions necessary in the formation of jadeite. The recent review of the jadeite problem by Yoder (1950a) has shown that jadeite (Na-Al rich) is not necessarily genetically associated with eclogites, but seems to be more closely related to serpentines. All of the jadeite localities, in place, described in the literature are in or near serpentine, and it would appear that the tectonic environments and rock types characteristic of the serpentine belts produce a situation favorable for the formation of jadeite.

SERPENTINES

The serpentine body is approximately thirteen miles long and four miles wide and at least 2,000 feet in thickness. Various interpretations have been given as to the structure of this body. Taliaferro (1945) suggests that it may be a large sill with laccolithic swelling in the thickest part of the sill, but Eckel and Myers (1946) conclude that it is a large plug. The contacts on all sides of the serpentine are fault contacts and nowhere can the original contact relations be observed (see Plate I). The bottom of the body is not exposed and the only basis for calling it a sill is its

somewhat concordant relations with the Franciscan formation along the southern border.

The serpentine occupies the center of an elongate asymmetric dome that forms a local bulge in the Coalinga anticline. Its emplacement and its form were controlled more by the tectonic development of the Coalinga anticline than by any other single factor. A diligent search of the entire serpentine contact demonstrates the fact, that this contact is faulted and sheared and evidence of an intrusive contact between the serpentine and enclosing rocks is completely lacking.

The serpentine mass must have been brought into its present position by tectonic movements even though it may have been an ultrabasic "magma" at greater depths. No field evidence can be found to substantiate the hypothesis that the serpentine was emplaced in its present position as an ultrabasic magma which had later been serpentinized in situ.

The serpentine in this district has been strongly weathered to produce a terrain of low rounded hills composed of flaky serpentine debris tens of feet thick. Scattered throughout the serpentine are many small and large areas which have not been completely weathered and these stand out as bold irregular outcrops. A comprehensive study of the structure and petrography was not possible because of these large deeply weathered areas.

Approximately 25 separate outcrops of unweathered serpentine were studied and the general petrography and mineralogy was established by thin section examination. One complete chemical analysis (Table 25) and seven semiquantitative spectrographic analyses (Pl. IV) were made to establish the composition of the serpentine.

The most important feature of the serpentine is the completeness of the serpentinization in the ultra-basic body. There is no marked difference between those specimens taken from the center and rocks taken from the edge of the body. This indicates that the serpentinization was not the result of local alterations produced by intrusives, a mechanism sometimes used for the serpentinization of ultrabasic rocks (Du Rietz, 1935). The serpentinization may well have taken place during the tectonic emplacement of the rock, a time which affords increasing temperatures and a plentiful supply of water from the enclosing sediments. This mechanism has been suggested by Bowen and Tuttle (1949) for the formation and emplacement of serpentine masses.

Antigorite and chrysotile are the two most abundant minerals within the serpentine. Antigorite predominates where the serpentine has undergone more pronounced shearing and typically forms sheaf or flame-like aggregates (Pl. VIII, Fig. 3). Antigorite-rich serpentines are found along the contacts between the tectonic inclusions and serpentine, also where serpentine is in contact with sediments around the periphery. Chrysotile commonly forms a structure which pseudomorphs the original texture of olivine. The overall texture produced is the typical mesh-type (Pl. VIII, Fig. 2). Chrysotile commonly forms larger cross-fiber veins within the serpentine measuring several inches across. A more detailed discussion of the antigorite and chrysotile is given in the mineralogy section.

Magnetite is a universal accessory in these serpentines and two distinct generations can be distinguished, (1) primary magnetite formed as

PLATE VIII. Photomicrographs of the serpentines.

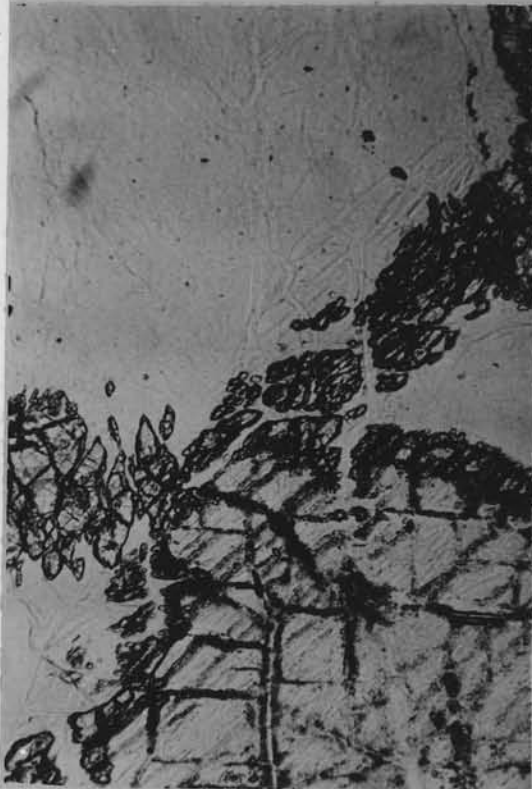
- Figure 1. Large bastite grain surrounded by andradite within antigoritic serpentine. Plain light (X 40).
- Figure 2. Relict olivine surrounded by chrysotile producing a typical serpentine mesh-texture. Large opaque grain of primary magnetite surrounded by a reaction rim of chlorite. Fine-grained opaque material within the chrysotile is exsolution magnetite. Plain light (X 40).
- Figure 3. Antigoritic serpentine illustrating typical sheaf- and flame-like aggregate forms. Crossed nicols (X 40).
- Figure 4. Andradite vein following a shear zone in antigoritic serpentine. Plain light (X 40).



2



4



1



3

an accessory mineral in the original ultra mafic rock, (2) exsolution magnetite formed during the serpentinization of the pyroxene and olivine (Pl. VIII, Fig. 2). The primary magnetite is characterized by much larger grains (up to 5 mm) and is usually surrounded by a halo of chlorite. The exsolution magnetite is extremely fine-grained (less than 0.2 mm) and follows the former outline of the olivine grains or may follow the cleavage lines in the pyroxene. Chlorite does not develop around the exsolution magnetite.

Chromite is erratically distributed within the serpentine as a minor accessory or as infrequent pod-like accumulations. The latter have been mined to some extent, although no single pod has produced more than several tons of ore. This chromite has been formed by segregation from the original ultrabasic magma as suggested by its tabular form and banded nature. Chromite from these pods has a density of 4.42 and an index of 2.043 matching very closely the density and index given for microchromite, $MgCr_2O_4$. The chromite segregations exhibit incipient alteration to uvarovite and kammererite (Figure 5) that may have resulted from the processes giving rise to serpentinization. A detailed description of the kammererite is given under mineralogy.

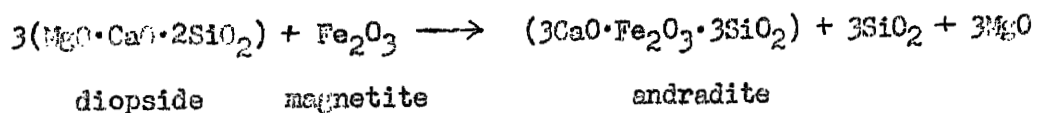
Olivine was detected in only three of the serpentines studied and in every case only a few relict grains were visible (Pl. VIII, Fig. 2). The average composition, determined by measuring the optic axial angle, is 17% Fe_2SiO_4 . Zoning was not detected in any of the olivines from the serpentines. The iron content of the serpentine, as determined spectrographically, ranges from 1 to 5% Fe and if the assumption is made that all of the iron was originally in olivine, this would give a very low amount

of fayalite, less than 10%, somewhat lower than that determined by optical measurements.

Several tabular and banded zones within the serpentine contained abundant relict pyroxene altered to bastite. The optical constants on the unaltered relict pyroxenes match those of enstatite. The bastite and relict pyroxene have retained their original criss-cross texture and the interstitial areas contain chrysotile pseudomorphing olivine. The pyroxene bands represent a partial differentiation of the ultrabasic magma, however, the volume of these rocks is small and probably does not represent more than 1% of the total. Many areas within the serpentine contained an isotropic serpentine mineral associated with chrysotile.

Andradite garnet is a prevalent mineral produced by the serpentinization process within the serpentine. Many of the more resistant knobs and ridges within the serpentine contain abundant small anastomosing veins of andradite. The crest of Santa Rita Peak, the highest point in the district, is composed of andradite-bearing serpentine and its survival as a prominent peak results from the garnet veination that produces a tough resistant rock. The garnet is always a late mineral and occurs in veins that follow, in part, the shear planes within the serpentine (Pl. VIII, Fig. 4); although in some instances the garnet is found intimately associated with bastite and in part pseudomorphs the original pyroxene (Pl. VIII, Fig. 1). The andradite is always found in antigoritic serpentines and its formation may depend upon the shearing conditions attendant in the crystallization of antigorite. Assuming that the garnet is formed by the breakdown of pyroxene (Ca-bearing) and magnetite, the following reaction shows

that it would take three molecules of diopside to make one of andradite.



The spectrographic analyses on the average serpentine show 0.01 to 0.05% Ca, whereas the andradite-bearing serpentines show 1 to 5% Ca, a hundred-fold increase. It would seem, from this data, that the formation of andradite within the serpentine must be accompanied by external source of Ca or an extremely efficient mechanism of mobilizing Ca from the pyroxenes within the serpentine.

The almost complete serpentinization precludes an exact determination of the original ultrabasic rock types. The textures observed in the unshered serpentine show that olivine greatly exceeded pyroxene; therefore it seems reasonable to assume that the bulk of the parent rock was dunitic in composition before alteration to serpentine. Locally where differentiation or accumulation is manifest by the presence of tabular bastite zones the original ultrabasic rocks were harzburgites and pyroxenites.

The spectrographic analyses of the serpentines, when compared to the data of Faust and Murata (1955), show that the elements characteristic of serpentines arising from a 'magmatic' source are also present in the New Idria serpentine in comparable amounts. This analogy produces further evidence that the ultimate source of these serpentines was magmatic; however, it does not imply that the emplacement of the serpentine in its present position was an ultrabasic intrusion.

Intrusive Rocks

Igneous rocks representing a restricted period of intrusive activity are present within the serpentine. Two small bodies crop out near the Gem mine, one in the NE 1/4 of sec. 26 and the other in the SW 1/4 of sec. 25. Along the southern border of the serpentine, a large exposure of igneous rock lies across the serpentine-Panoche shale contact near the headwaters of White Creek (see Plate 1).

The intrusive rock in section 26 is a small plug deeply weathered and covering about 25 square yards in areal extent. The weathered nature of the serpentine and igneous rock precludes any statement of the contact relationships. Specimens procured several feet below the surface show the rock to be a fine-grained, dark camptonite.

An elongate dike-like intrusion approximately 400 feet long and 60 feet wide crops out in section 25 (Fig. 10). The dike has been well exposed by differential erosion on the north flank of a ridge forming an irregular wall-like mass extending down the ridge. The contact between the serpentine and intrusion is obscured by talus and weathered serpentine. The dike rock is a coarse-grained, brownish barkevikite syenite. A thin selvage of albitite (6 inches to 1 foot) occurs sporadically along the contact.

The White Creek igneous mass covers several acres and is the most extensive exposure of this rock in the district. During the mapping of this exposure it became apparent that this mass has been displaced and was part of a large landslide that has ridden out over the upturned Panoche shales. Eckel and Myers (1946) show this igneous body in place intruding

both serpentine and Panoche shales. Detailed inspection of the contacts between the serpentine and intrusive shows a gouge zone made up of both serpentine and igneous rock. Several trenches dug along the serpentine-shale contact show a similar relationship. No hornfels or contact alteration of the shales could be found although several displaced fragments of baked serpentine were found in one of the trenches. The igneous rock in this exposure is extremely fresh in comparison to the other intrusive bodies. It is indeed unfortunate that this body has been dislocated so as to obscure the structural relations with the serpentine. It was decided, none the less, to use this rock for analytical and mineralogical study, keeping in mind that the relations with the other intrusive bodies would be somewhat obscured. The rock from this exposure is quite variable in texture, light brownish and made up of barkevikite syenite and minor camptonite.

These igneous rocks have been divided into three types on the basis of texture, mineralogy, and chemical composition.

- | | |
|----------------|--|
| I - Camptonite | fine-grained with dark brown to black color containing: barkevikite, olivine, pigeonite, and calcic-plagioclase. |
| II - Syenite | coarse to medium-grained with phenocrysts of barkevikite in light groundmass of feldspar and zeolites. |
| III - Albitite | vugy and coarse-grained containing: albite, analcite, natrolite, and acmite. |

Camptonite is found at two of the three exposures although its exact relationship is not clearly shown in the field. The exposure in section 26 is exclusively camptonite and is interpreted as an intrusive plug which has crystallized rapidly. Camptonite is found in the White Creek mass

only by digging along the southern border of the outcrop and here it is associated with baked serpentine; although no fragments were found which show a complete transition from baked serpentine through camptonite to syenite. The camptonite probably represents an early differentiated phase of the intrusion and has been preserved along the "chilled" margins of the intrusive.

The fresh camptonite is dark brown to black and has a distinct conchoidal fracture. It is extremely fine-grained and shows a rough banding along the face of the serpentine contact. The border zone or "chilled" contact has a groundmass consisting of a felted aggregate of calcic-plagioclase and needles of amphibole (Pl. IX, Fig. 2). Phenocrysts of olivine and barkevikite are "floating" in this extremely fine-grained groundmass. The groundmass feldspar is too fine-grained to determine exact composition but it probably is close to An_{60} . The amphiboles in the groundmass are variable in composition; richterite is found in cores rimmed by crossite and barkevikite crystals are rimmed by crossite and glaucophane. The formation of the blue $Na-Mg$ amphiboles in the "chilled" zone suggests contamination by Mg assimilated from the serpentine; although no partially assimilated inclusions of serpentine were found in the camptonite. The groundmass in parts of the "chilled" zone shows flow structure with a trachytic texture. The "chilled" zone is one to four inches in thickness and is followed by a thin selvage (about $\frac{1}{2}$ inch) rich in plagioclase. This plagioclase is lath-shaped and strongly zoned (An_{69} core to An_{40} rim) exerting strong euhedralism and forming a pilotaxitic texture (Pl. IX, Fig. 2).

Except for the chilled zone and plagioclase selvage the camptonite is uniform in composition and texture. The camptonite groundmass consists of plates of zoned plagioclase and small needles of barkevikite. Olivine with reaction borders of barkevikite and biotite form kelyphitic clots in the feldspar groundmass. Colorless pigeonite also forms cores in the barkevikite clots, although kelyphitic rims are not developed round the pyroxene.

The plagioclase has a strong continuous zoning and forms a groundmass of subhedral to euhedral plates. The cores of plagioclase are clear and fresh with an increasing cloudiness developing in the peripheral parts of the crystal, and rimming these crystals is a clouded and somewhat altered feldspar. The fresh cores of the plagioclase are An_{56-69} ranging outwards to the periphery by continuous zoning where a composition of An_{20} was determined. The "deuteric" rim surrounding the clear, zoned feldspar has an An content from 10 to 12 and contains fine-grained needles of prehnite. The plagioclase shows complex albite-ala twinning and less commonly simple albite twinning. Within the interstitial areas, minor natrolite and analcite replace, in part, the clouded albite rims.

The small euhedral crystals of brown barkevikite form small clots with olivine or augite as a central core, although it is more abundant as idiomorphic prisms in random orientation (Pl. IX, Fig. 4). The mineralogy of the barkevikite has been discussed earlier.

Olivine, as noted earlier, is always found with a kelyphitic rim which is composed of exsolution magnetite and fibrous pyroxene surrounded by barkevikite crystals. The olivine is strongly zoned and the $2V_x$ varies from 82° (edge) to 88° (core) giving Mg_2SiO_4 78% (edge) and 84% (core);

suggesting that the olivine has crystallized from a differentiated parent basic magma.

The colorless pyroxene within the barkevikite clots has a small $2V$ (ca. 30° to 40°), positive sign, and $Z \wedge c$ 37° ; probably pigeonitic in composition (Pl. IX, Fig. 4). Indistinct zoning was observed.

Elongated crystals of apatite are common in the groundmass, some attaining lengths up to 1 mm. Irregular blebs of sphene are associated with ilmenite and primary pyrite.

A modal point-count analysis is given in Table 21, the chemical analysis in Table 23 and the norm calculated from this analysis in Table 24.

Barkevikite Soda Syenite is the dominant rock type from the igneous mass at the White Creek locality and in the dike from section 25. The grain size and texture are quite variable ranging from fine-grained facies similar to the camptonite to a coarse-grained porphyritic facies with a granitoid groundmass and large prisms of barkevikite (up to 6 inches in length). The hornblende shows no preferred orientation although sharp changes in texture are quite common. Inclusions of foreign rock were not found within the syenite from either locality. Figure 10 shows the outcrop pattern of the syenite dike and such structural features as could be determined; no detailed map of the White Creek mass was made since it has been dislocated by landslide.

In the hand specimen, the syenite is mottled black and white with extremely well developed black prisms of barkevikite set in a white groundmass of feldspar. Where soda-pyroxenes dominate over barkevikite a greenish cast is developed in the syenite. The extreme variability in

TABLE 21. MODAL ANALYSIS OF CAMPTONITE (RGC-45-50).

MINERAL	PERCENT
PLAGIOCLASE (An 20-69)	40.0
BARKEVIKITE	39.5
OLIVINE (Fo ₈₀ -Fa ₂₀)	5.5
PYROXENE	1.3
APATITE	2.5
BIOTITE	4.2
SPHENE	.3
MAGNETITE	.6
PYRITE	4.8
PREHNITE	1.0
	<u>99.7</u>

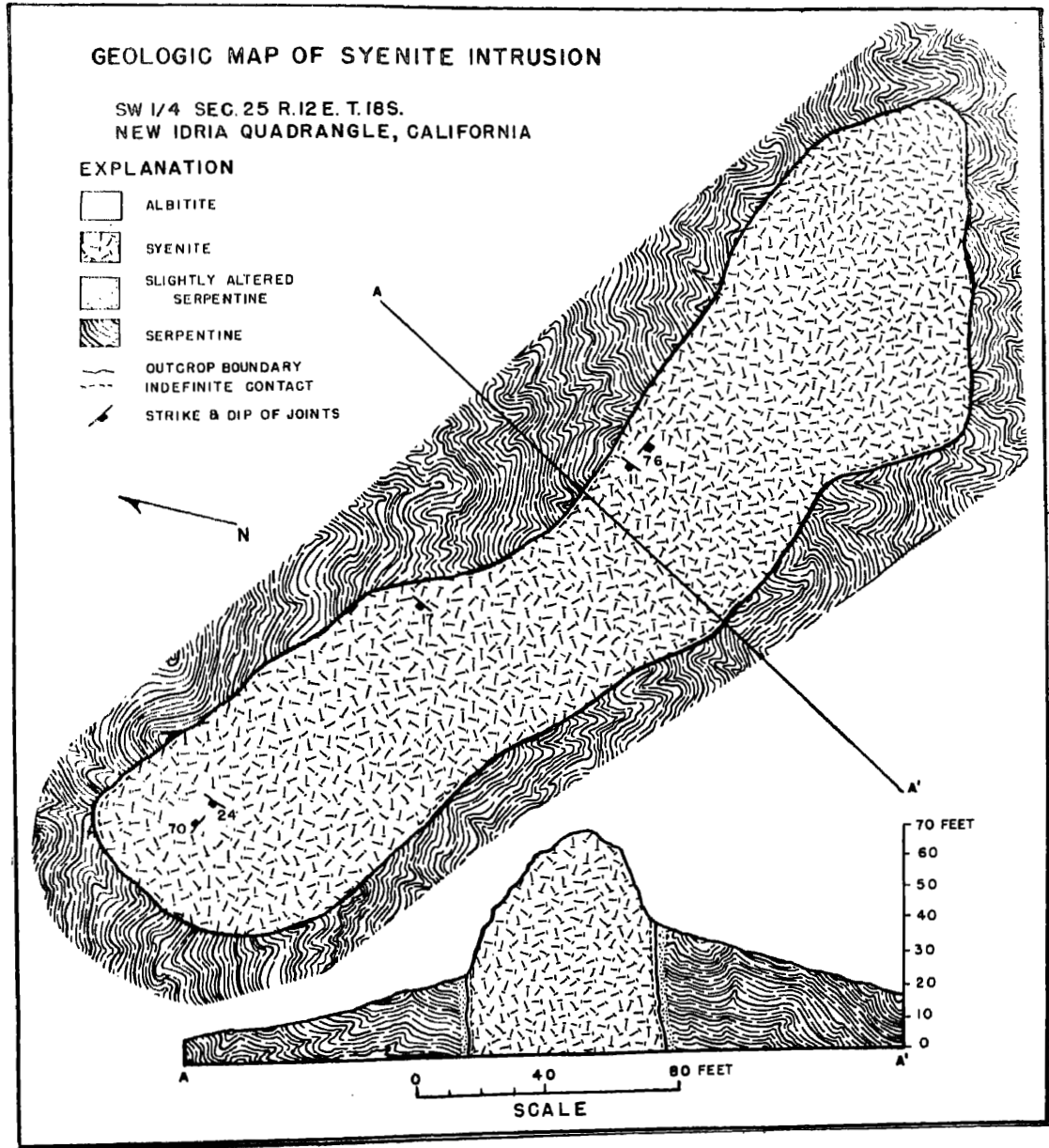


Figure 10

in size of the hornblende phenocrysts is the most striking feature of the various facies when contrasted to the groundmass which appears to remain medium to fine-grained.

The syenite has a panidiomorphic-granular texture and where the rock shows deuteric alteration the texture becomes porphyritic with a hypidiomorphic-granular groundmass. The feldspar forms almost equant tabular crystals which show strong zoning under crossed nicols. The inner portions of the crystals are usually clear except for incipient alteration; these cores grade out into rather thick rims of cloudy feldspar An_{5-10} which in turn may grade into natrolite and/or analcite (Pl. IX, Fig. 3). The composition of the fresh core is andesine (An_{45-55}) which grades out to the rim of the clear area in continuous zoning to a composition of An_{30} . Minor perthitic intergrowths were observed in several of the cloudy albite rims. The cloudy albite is the most abundant feldspar and in the syenite facies the calcic-plagioclase never exceeds 15% of the total feldspar. Calcic-plagioclase is completely lacking in some facies and in these rocks the feldspar is albite (An_{5-10}). The albite from the White Creek mass is always clouded and it seems to have formed by late deuteric or hydrothermal alteration. Under high magnification the clouding materials appear to be elongated fibers and short rods accompanied by opaque dust. Differential acid leaching of the clouded albite clears the albite and the inclusions that remain have optics similar to those of prehnite. The dissolved material is thought to be iron oxides and natrolite. MacGregor (1931) and Földerváart and Gilkey (1954) have shown that clouding in feldspars may be due to a deuteric or hydrothermal alteration.

TABLE 22. MODAL ANALYSES OF SYENITE.

MINERAL	RGC-1-50	RGC-48-50*
ALBITE (An ₅₋₁₀)	28.8	53
ANDESINE-LABRADORITE (An ₅₅₋₃₀)	-	.6
BARKEVIKITE	37.8	26.2
ANALCITE	-	2.3
NATROLITE	-	5.3
ZOISITE	10.3	-
MICA	12.2	4.9
CHLORITE	8.4	-
APATITE	.3	1.6
SPHENE	2.2	-
OPAQUES	.7	-
	<u>100.7</u>	<u>99.8</u>

* Same as analysed rock RGC-47-50.

In contrast to the syenite from White Creek, the syenite from the dike in section 25 contains abundant clear and fresh albite (An₅₋₁₀) which may have recrystallized during a late tectonic movement that the dislocated White Creek syenite has apparently escaped by landslide dislocation. The dike syenite does not contain any calcic-plagioclase and there is no zoning or twinning in the 'recrystallized' albite. The excess Ca has been taken up by prehnite and clinozoisite.

Analcite and natrolite in the syenite have formed by deuteric or hydrothermal alteration. Analcite seems to form first and is found enlarging cleavage traces of albite and as larger patches replacing albite. Large areas of analcite are found surrounding barkevikite and these commonly contain wormy biotite. Natrolite follows analcite and selectively replaces albite. Natrolite may completely replace feldspar preserving its original texture.

Barkevikite is the most abundant mafic mineral of the syenite and is characterized by well-developed euhedral habit and distinctive pleochroism (Pl. IX, Fig. 1). The physical properties of barkevikite are similar in all facies of the camptonite and syenite and it appears to be stable in both rocks except in the 'chilled' zone of the camptonite. The chemical and optical properties of barkevikite from the White Creek syenite are given in Table 14.

Accessory minerals from the syenites are similar to those found in camptonites with some minor variations. Apatite is abundant, forming elongate, light brown, prisms with weak pleochroism. A spectrographic analysis of the pure apatite from the White Creek syenite is given in Plate IV. Sphene is found both as a primary mineral and as an alteration

product of the barkevikite. Biotite is more abundant in the syenites than in the camptonites and is formed during late deuteric or hydrothermal alteration when it crystallized as wormy clots within the zeolites. Calcium released in the alteration of the calcic feldspar has produced prehnite, zoisite, and clinozoisite. Small amounts of muscovite are present in the syenite dike although it was not definitely identified in the White Creek syenite. Magnetite, ilmenite, and iron sulfides are scarce in all cases. Phenocrysts of a deep red garnet (up to 1 cm) are present in a syenite boulder in the White Creek syenite and optical and density determinations (N-1.800 and D-4.18) on these garnets are similar to those given for spessartite. Heavy mineral separations of the normal syenites also produced small quantities of this garnet. The chemical analyses of both the camptonite and syenite (Table 23) show that they are undersaturated rocks with respect to silica as nepheline is present in the calculated norms (Table 24); although nepheline was not found in any of the rocks. The absence of nepheline in these rocks could be explained by the fact that in a hydrous deuteric or hydrothermal stage, nepheline is unstable. Yoder (1950a) has shown that analcite forms in a hydrothermal system at temperatures below 575° C. and above this, albite and nepheline are stable. This experimental relationship becomes valuable in interpreting the presence of analcite and natrolite in the late stages of crystallization of the syenite intrusions. The presence of analcite and the absence of nepheline in an undersaturated rock, such as this, would seem to indicate that the final stage of intrusion was characterized by low temperatures and a hydrated condition. A modal analysis of the White Creek syenite and the syenite dike in section 25 are given in Table 22

TABLE 23. CHEMICAL ANALYSES OF CAMPTONITE AND SYENITE.

	1	2	3
SiO ₂	48.96	51.42	60.00
TiO ₂	2.01	2.20	.42
Al ₂ O ₃	15.72	16.58	16.88
FeO	9.65	7.62	3.02
Fe ₂ O ₃	.36	1.48	1.83
MnO	.17	.23	.12
CaO	7.76	6.77	3.16
MgO	6.52	3.68	1.40
K ₂ O	.75	1.06	.94
Na ₂ O	5.22	6.04	9.31
H ₂ O-	.42	.34	.43
H ₂ O+	2.29	1.41	1.53
ZrO	-	traces	.03
Cr ₂ O ₃	nil	-	-
BaO	.05	traces	.06
SrO	-	.08	.02
Li ₂ O	-	-	traces
P ₂ O ₅	-	.49	.14
CO ₂	-	.45	.59
S	-	-	traces
	99.88	99.85	99.88

1 - Camptonite (RCC-45-52), analyst - W. H. Herdsman.

2 - Syenite (RCC-47-52), analyst - W. H. Herdsman.

3 - Syenite from Arnold and Anderson (1910), analyst - W. F. Hillebrand.

TABLE 24. NORMS OF ANALYSED CAMPTONITE AND SYENITES.

	1*	2*	3*
ORTHOCLASE	4.19	6.12	5.56
ALBITE	30.92	43.73	73.56
ANORTHITE	17.24	15.29	1.44
NEPHELINE	8.10	3.83	2.72
DIOPSIDE	17.43	10.82	5.72
OLIVINE	15.96	9.75	2.99
MAGNETITE	.46	2.16	2.66
TILMANTITE	4.86	4.26	.98
APATITE	-	1.27	.34
CALCIUM CARBONATE	-	1.00	1.34
WATER	2.29	1.41	1.53

CIPW CLASSIFICATION

1 - Class III, salfemic
 Order 6, lendofelic
 Rang 3, alkali-calcic
 Subrang 5, persodic

2 and 3 - Class II, dosalic
 Order 5, perfelic
 Rang 2, domalkalic
 Subrang 5, persodic

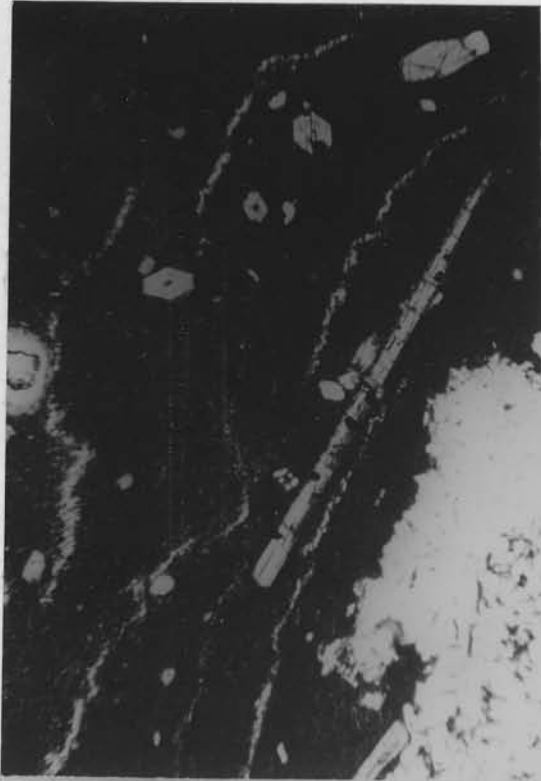
* See Table 23 for chemical analyses and identification.

and in Table 25 two independent analyses of the White Creek syenite are given.

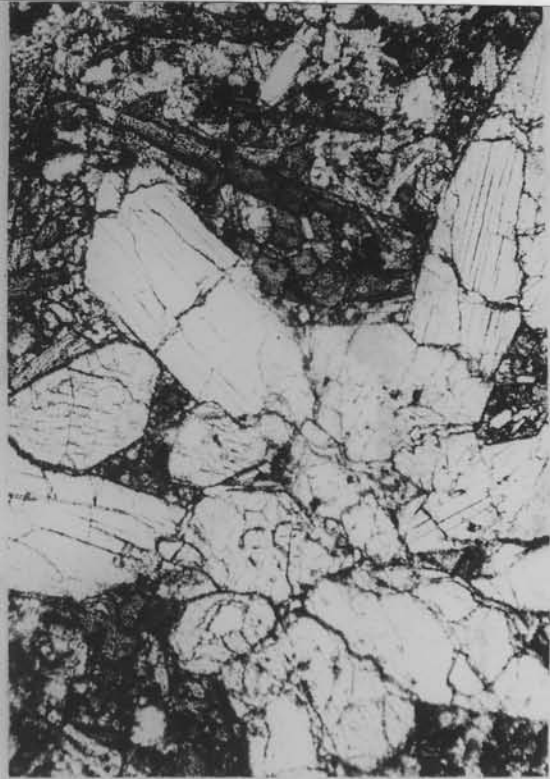
Albitite and Zeolite-Rich Rocks are found in minor amounts associated with the late stage hydrothermal or deuteric alteration of the intrusive. These rocks are characterized by a vuggy texture and almost pure white color. A small zone, up to one foot thick, of albitite is developed in the syenite dike along the contact between the intrusive-serpentine contact. The rock is made up almost entirely of clear albite (Ans-10) accompanied by clinzoisite that forms delicate needle-like druses in the numerous vugs. Clear sphene is a common accessory in the groundmass. Baskerville cores rimmed by aegirine-augite are present in subordinate amounts (1 to 5%) and the amphibole is the only mafic mineral observed. Isolated stringers and clots of albitite are found within the syenite but here it is a very minor facies. Numerous late, vuggy veins of zeolite are present in the White Creek syenite. These late veins vary in width from one to six inches and may extend to several yards in length. The minerals within the veins are particularly well developed and a fairly strong copper sulfide mineralization in many of these veins was observed. In addition, large irregular vugs (up to a foot across) are also present in the syenite and these contain the same well formed crystals that are found in the veins. Natrolite is the most abundant mineral in the veins and vugs, crystallizing as distinct prisms up to one inch in length and about 4 mm. in cross-section. The unusual morphology of this natrolite has been discussed earlier under mineralogy. Analcite, prominent in both vugs and veins, attains exceptional size in the larger isolated vugs where crystals up to one inch or more were found. The trapezohedral faces

PLATE IX. Photomicrographs of camptonite and syenite.

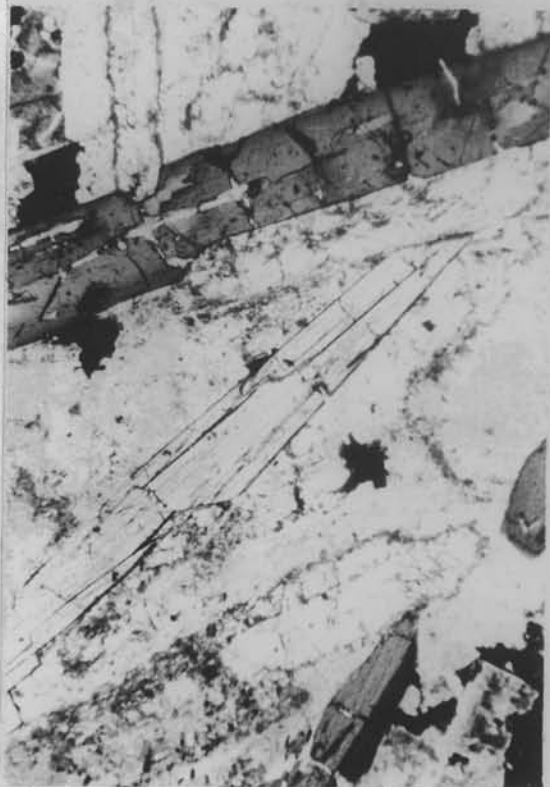
- Figure 1. Barkevikite soda syenite. Large prisms of barkevikite inclosed by plagioclase feldspar. Note grains of plagioclase with clear cores rimmed by cloudy albite. Interstitial areas contain zeolites and biotite. Plain light (X 25).
- Figure 2. Camptonite, 'chilled zone' showing a fine-grained groundmass with euhedral crystals of barkevikite and olivine which is surrounded by a kelyphitic rim. Note embayment of the 'chilled zone' by the plagioclase-rich selvage. Plain light (X 40).
- Figure 3. Alteration of calcic-plagioclase to albite. Note the fine inclusions within the albite contrasted to the clear calcic-plagioclase. Crossed nicols (X 100).
- Figure 4. Camptonite. Large clot of pigeonite surrounded by a fine-grained mat of barkevikite and calcic-plagioclase. Plain light (X 40).



2



4



1



3

are well developed on colorless to opaque white crystals containing numerous hair-like inclusions of acmite. The larger crystals have a very faint birefringence and a rather complicated twinning. Individual crystals of tabular, prismatic acmite are abundant in the vugs and veins intergrown and implanted on the natrolite and analcite. Occasional cores of barkevikite are found rimmed successively by acgirine-augite and acmite. The copper mineralization within the veins is present as small blebs of chalcocite accompanied by galena. Spectrographic analysis of this sulfide mixture shows 0.05-0.1% Hg and detailed inspection of the concentrate shows material similar to cinnabar.

Classification and Origin of the Igneous Rocks

Considerable difficulty is encountered in placing these rocks within present rock classifications, either on the basis of chemistry or mineralogy. The norms calculated in Table 24 certainly do not resemble the minerals reported in the modes (Tables 21 and 22). Nepheline was not found in any of the rocks, although all three calculated norms show nepheline; furthermore orthoclase is present in the norms and not in the modes. Diopside and olivine also are shown in all three norms but these mineral types have been identified only in the camptonites. Natrolite and analcite are present in all of the intrusive rocks and it seems that these minerals have proxied for nepheline. The stability relationships of nepheline-analcite as discussed earlier, suggest that in the late stages a hydrothermal low-temperature conditions may have removed any nepheline formed in the earlier intrusive stage. This, somewhat peculiar, situation has produced an under-saturated rock without the expected feldspathoids. The

high-sodium content contrasted to the paucity of potassium is another peculiarity of these rocks that poses a difficult problem in classification. The two rocks analyzed for this investigation have been classified according to both chemical and mineralogical methods; the results are tabulated below.

	<u>RGC-45-51</u>	<u>RGC-47-51</u>
Washington (1917)	III-6-3-5	II-5-2-5
Johannsen (1931)	Family 3216 camptonite	Family 2216 Nepheline-bearing diorite
Shand (1927)	DVM δ sub-basalt 'camptonite'	XUM δ essexite theralite
Niggli (1936)	soda gabbro magma Type 2 Mugearitisch	sommatische magma (sub-alkalic) Type Melarkitisch

The early facies of these intrusives, namely (RGC-45-51), is clearly shown to be a camptonite as it falls into the camptonite categories of Shand and Johannsen. The chemical classifications of Niggli and of Washington (CIPW) give erroneous placement as the normative minerals are grossly different from the modal minerals. The classification of the main intrusive rock (RGC-47-51) is still somewhat doubtful and it appears that the rock may be a hybrid. The rock was first described by E. S. Larsen for Arnold and Anderson (1910) as a soda syenite and has since been referred to as a soda syenite by Taliaferro (1943) and Eckel and Myers (1946). Following the definition of a syenite given by Johannsen (1931), it appears that this could not be called a syenite, since potash feldspar is an essential constituent in the later and the New Idria rocks contain less than 1% K_2O ; this is probably present in biotite. Following

Shand's classification this rock would be grouped with the theralites and Johannsen's classification shows it to be a nepheline-bearing diorite. The chemical classifications of Niggli and CIPW are of no value in determining a proper classification because of the unrealistic norms. A more descriptive petrographic name for the soda syenite would be barkevikite sodaclase diorite following Johannsen's nomenclature, but the original rock name given by Larsen is retained here to avoid confusion.

The rocks formed by late stage hydrothermal or deuteric action and containing albite and zeolites could be best called albitites with qualifying adjectives. Turner (1896) first described albitites as aplitic rocks composed entirely of coarse granular aggregates of albite.

The intrusives of the New Idria district seem to have arisen from a parent magma that was probably similar in composition to olivine basalt magmas. Marked zoning in feldspars and olivine of the camptonite indicates differentiation. The camptonite border facies seems to have crystallized from a mobile and somewhat high temperature magma, but the peculiar composition of the soda syenite cannot be readily explained by further differentiation of the camptonite. Several other factors may have influenced the course of crystallization and final composition; these are given below.

1. Contamination of the parent magma by soda-rich rocks.
2. Filter-pressing of residual liquor of a partially differentiated basaltic magma.
3. Selective migration of Ca, Mg, Fe, and Ti into the host serpentine during emplacement.

All these factors must be considered in any discussion on the origin and composition of the intrusive rocks. The genesis of the intrusive rocks bears important relationships to the origin of the metasomatic calc-silicate and chlorite rocks within the serpentine near the intrusives. A variation diagram of the available analyses shows that the rocks follow a differentiating trend with Ca, Mg, Fe, and Ti decreasing and Na and Al increasing with little change in K. This would indicate that the intrusive material differentiated after arriving at its point of emplacement within the serpentine. The lack of inclusions within the syenite indicate that little or no contamination has taken place, although this is based on negative evidence. Spectrographic analyses on the analyzed rocks has produced some very interesting data. The syenite and camptonite contain similar cobalt and nickel values with $Ni \approx Co$ (100-500) ppm. Nockolds and Allen (1954) have shown that in alkalic rocks during the early stages of differentiation $Ni > Co$ and as differentiation proceeds $Ni \approx Co$ with $Ni < Co$ in the later stages. The Ni-Co relationship suggests that these intrusives have arisen from a partially differentiated magma. The Ni, Co, and Cr content of these rocks is similar to the values given by Nockolds and Allen and it would seem that these elements would have been enriched had there been serpentine contamination of intrusive magma. Zr and Nb were not detected in these rocks whereas Nockolds and Allen consistently report these elements in alkalic rocks. Barium and strontium appear in normal quantities within these rocks although the low value of K has probably controlled, in part, the Rb and Ba content. The calc-silicate bodies near the intrusions generally have matching trace

elements, which suggests that there was a movement of metasomatic solutions from the intrusives into the serpentine. These metasomatic bodies show enrichment (Table 25) in Al, Ca, Fe, and Ti and it would appear logical to derive these elements from the intrusives since the late stages of the intrusive are depleted in these elements. This mechanism would result in a magma that was enriched in Na, probably with H₂O obtained from the enclosing serpentine.

Metasomatic Rocks

Within the serpentine are a number of small rock bodies formed by direct replacement of the serpentine and small veins and zones of metasomatism are also found in the tectonic inclusions. The fluids responsible for these replacements are in no way connected with the processes giving rise to the serpentine or schists; since these metasomatic rocks contain a suite of calc-silicate and titano-silicate minerals that could hardly have been produced by anything but emanations from an intrusive body.

The metasomatic rocks have been divided into three different types on the basis of their mineralogy. (1) Chlorite rocks characterized by dominant chlorite accompanied by minor amounts of garnet, perovskite, and titanium-bearing minerals. (2) Calc-silicate rocks characterized by diopside, idocrase, and chlorite. (3) Titano-silicates in soda-rich veins within tectonic inclusions. Each of these groups will be discussed separately and the mineralogy and geology of each separate occurrence will be described.

The lack of post-mineralization deformation is one feature that these metasomatic rocks have in common. This is important in a region where numerous structural movements through Tertiary time have deformed other rocks within the district. The apparent age of these metasomatic rocks must be fairly recent (late Tertiary), since they have formed vugy deposits within rocks that have undergone dynamothermal metamorphism during Tertiary time.

In the discussion to follow, melanite is used as a synonym for the titanian andradite described under mineralogy. The sequence of mineralization given for each described occurrence is based on the observed textural relationships and on other criteria normally used to establish a paragenetic sequence. The localities described may be located on the geologic map (Pl. I) by using the middle digits of the sample number.

Chlorite Rocks

(RGC-70-51) crops out along the serpentine-Panoche shale contact at the extreme southeastern edge of the serpentine mass, where it forms an elongate vein that strikes S 70° E in sheared serpentine. The vein is four to six feet wide and about 50 feet in length. It is a dense, compact, dark green rock with anastomosing veins of light brown garnet, a variegated texture and well developed foliation. Clinocllore is the most abundant mineral. The veins contain andradite with a brownish to reddish tint on outer surfaces. The tinting of the garnet is ascribed to late introduction of Ti. Isolated patches of garnet within the clinocllore groundmass contain idocrase cores. Small amounts of magnetite and

calcite form as late minerals in open cavities. Sphene formed as a further reaction with the andradite and was seen to replace it on the rims of several crystals. The sequence of mineralization is given below.

Chlorite	_____
Idocrase	_____
Garnet	_____
Sphene	_____
Magnetite	_____
Calcite	_____

(RGC-93-52) is found in several small outcrops (up to six feet long and one or two feet in width) trending in a north-south direction. The contact with the enclosing serpentine is marked by a distinct color change. The rock is gray to green, and dense, with a crude schistosity cut by anastomosing veins of light brown garnet. Clinocllore is the most abundant mineral and its preferred orientation produces the observed schistosity. Associated with chlorite as an early mineral, is a pyroxene of diopside composition, that makes up about 4 to 6% of the total rock. Small crystals of zircon and apatite are present in the chlorite ground-mass. Andradite veins cut the schistosity and are definitely later than chlorite and diopside. Small crystals of magnetite have formed on the open surfaces of the rock. The sequence of mineralization is given below.

Chlorite	_____
Diopside	_____
Apatite	_____
Zircon	_____
Garnet	_____
Magnetite	_____

(RGC-36-50) crops out as a small tabular vein striking N 30° E, about 20 feet long, and 4 to 5 feet wide. The rock is vugy with a crude schistosity parallel to the strike of the vein. The color is green to grayish-green, enhanced in the vugy areas where perfect crystals of garnet and chlorite produce brilliant reflections. The contact of the chlorite rock with serpentine is gradational showing alteration of serpentine to chlorite along shear planes. The rock is composed essentially of garnet and chlorite accompanied by minor amounts of sphene, pyroxene, and magnetite. Chlorite forms euhedral to subhedral platelets that have random orientation, and dark olive green color in hand specimen; under the microscope a strong pleochroism from green to light yellow is seen. The optics are similar to those of dalessite (Table 17). Garnet forms light yellow to olive-green euhedral crystals partly intergrown with the chlorite (Pl. XII, Fig. 4). The cores of the garnet may be hollow or mottled with a fine-grained mixture of sphene and pyroxene. Optical determinations are similar to those given for andradite. A light brownish zone around the periphery of the garnets is due to Ti introduced during late stages of formation. The mineralization sequence is given below.

Pyroxene _____
 Sphene _____
 Garnet _____
 Chlorite _____
 Magnetite _____

(RGC-57-51) forms a small bench on a smooth slope of weathered flaky serpentine, the largest outcrop of which is about 40 square feet and it rises only five feet above the surrounding terrain. The serpentine and chlorite rock are considerably broken up and altered by weathering processes obscuring the contact between the two rocks, but it is assumed that the chlorite rock has formed by replacement of the serpentine. The outcrop is very irregular and the only structural trend observed was a set of E-W joints dipping about 55° to the south. The rock is very irregular and vugy and shows no preferred orientation of the constituents. The weathered surface of the rock is rusty brown and on the fresh surfaces the true color is dark olive-green. Chlorite (possibly delessite), melanite, perovskite, and apatite are essential constituents accompanied by minor amounts of sphene and magnetite (Pl. XI, Fig. 2). The texture is porous and vugy, and magnetite and perovskite are the only euhedral minerals present in the cavities. The early stages of mineralization were richer in iron and many of the large fan-shaped aggregates of chlorite have cores of stilpnomelane that grade imperceptibly into delessite (Pl. X, Fig. 2). Melanite, the next most abundant mineral, forms irregular patches within the rock and does not exert its

normal tendency to form idiomorphic crystals. The irregular patches of melanite are commonly intergrown with sphene and perovskite (Pl. X, Fig. 2). Strong zoning of the melanite is not found at this locality and it seems that the garnet has formed late from Ti-rich fluids.

Perovskite is present in two forms, (1) perfect resinous yellow octahedra and (2) irregular granular aggregates. Pabst (1951) reported colorless and dark adamantine spinels from this locality, however, he did not report perovskite from this locality and it may be that the colorless spinel he described is the octahedral perovskite. Small elongate, colorless prisms of apatite are common within the groundmass. Magnetite forms euhedral octahedra and also irregular patches within the groundmass. Sphene is present within the cores of melanite and has formed in the early stages. The mineralization sequence is given below.

Stilpnomelane	_____
Delessite	_____
Magnetite	_____
Apatite	_____
Sphene	_____
Melanite	_____
Perovskite	_____

(RGC-83-51) is one of the larger areas of metasomatic rocks and six separate outcrops cover an area of about 300 square yards. The individual bodies are tabular in shape and show moderate contortions parallel to the shear planes in the serpentine. The contacts between the chlorite bodies

and the serpentine are gradational and are conformable with the local structure in the serpentine. The general strike of the bodies is E-W and their dip is almost vertical. The rock is dark, bluish-green with schistosity and elongate vugy areas parallel to the schistosity. Magnetite, ilmenite, and perovskite are common as euhedral crystals on open fractures and vugs. This body is the only one found that shows alteration of the earlier metasomatic mineral assemblage. The early phase of mineralization produced a garnet-chlorite rock containing little or no titanium. The garnet was probably andradite, but this is difficult to establish since there are very few relict grains of garnet. A late stage of mineralization, rich in CO₂, altered most of the garnet to calcite and chlorite. Many spots, where garnet was formerly present, are now pseudomorphed by a fine mixture of chlorite (delessite), calcite, and magnetite; and in other spots the area occupied by the garnet is now vacant (Pl. XII, Fig. 1). The rock is composed of chlorite (rumpfite and delessite), calcite, magnetite, and ilmenite. The chlorite assumes a crude schistosity and the magnetite forms anhedral clots within the calcite-chlorite replacements. Minor clots of chevkinite (?) were identified from the thin section and these small concentrations are characterized by pleochroic halos produced in the chlorite. Sodium fluoride bead tests on this mineral show it to contain uranium. Rutile was identified from the rock in one small isolated cluster of microscopic crystals.

A series of thin sections across the serpentine-chlorite rock contact indicates that metasomatism of the serpentine is accomplished by alteration of antigorite to rumpfite and delessite with little or no change in the original fabric of the serpentine, although within the center of these bodies a coarser crystallization obscures this original fabric. The large amounts of calcite produced in the late stages of mineralization obscure the replacement sequence, however, it is clear that the serpentine has been metasomatically replaced by fluids enriched in calcium, aluminum, iron, and titanium. The inferred mineralization sequence is given below.

Chlorite	_____
Andradite	_____
Magnetite	_____
Ilmenite	_____
Perovskite	_____
Calcite	_____
Chevkinite (?)	_____
Rutile	_____

(RGC-79-51) crops out 200 feet away from the contact between the serpentine and Franciscan formation. This body is irregular in shape and about forty feet long and fifteen feet wide. No general structural trend could be determined, although a crude schistosity within the rock conforms, in part, with the shear planes in the serpentine. The serpentine-chlorite rock contact is sharp and there is little interfingering. The surrounding serpentine is antigoritic and shows evidence of strong

shearing. The replacement rock is dense and compact with very few open fractures or vugs (Pl. X, Fig. 3). It is intensely veined with a yellowish-brown andradite. Clinocllore makes up most of the rock and forms a crude schistosity; in vugy areas beautiful well-developed crystals of clinocllore are associated with crystals of andradite, calcite, and magnetite. Small clots of colorless apatite are associated with the garnet and early sphene is present as cores within the garnets. The mineralization sequence is given below.

Clinocllore	_____
Andradite	_____
Sphene	_____
Apatite	_____
Calcite	_____
Magnetite	_____

(RGS-56-51) crops out as a small discontinuous body within a bold serpentine outcrop. This metasomatic zone is irregular in shape and about 40 feet long and 20 feet wide. The host serpentine is a dense rock which has been impregnated with thin veins of andradite. Serpentine has been strongly sheared and antigorite is the most abundant mineral in the rock. The chlorite rock is dense, grey-green and is cut by anastomosing veinlets containing melanite and perovskite (Pl. X, Fig. 1). The chlorite, similar to rumpfite in composition, exhibits a crude schistosity within the metasomatic rock. The veined perovskite and melanite are anhedral and show extremely irregular grain boundaries

with the chlorite. The melanite is also characterized by a zoning that grades from light colored cores to dark reddish-brown rims again manifesting the increased Ti substitution in the late stages. Apatite and sphene occur consistently, although sparingly, as early minerals within the chlorite groundmass. Several small crystals of zircon were noted. Along the veins within the metasomatic rock, there are many open fractures and vugs that are covered with a beautiful suite of crystalline material. All of the individual crystals exhibit almost perfect crystal forms, however, none of them are more than one centimeter in their longest dimension. Melanite is present as splendid black dodecahedrons producing drusy coatings on the vein walls. Yellow and metallic black perovskite has crystallized as cubes and octahedrons. A chemical analysis of the perovskite is given in Table 1. Red prisms of titaniferous idocrase are sparsely distributed on the drusy surfaces. White diopside has crystallized in delicate bladed crystals and forms small tufted clumps lining the vugy surfaces. This locality is well known to mineral collectors and has produced some of the finest mineral specimens from the district. The mineralization sequence is given below and it is considered that anhedral vein material formed during the same period as the drusy material.

Chlorite	_____
Apatite	_____
Sphene	_____
Melanite	_____
Perovskite	_____
Diopside	_____
Titaniferous idocrase	_____

(RGC-42-50) is a small body less than four square feet in size projecting out of weathered serpentine as a small knob. The relationships between the serpentine and the metasomatic rock are obscure and the author is not convinced that this rock is in place. It is coarse-grained with a porous, open texture, and the constituent minerals assume no preferred orientation. The rock is nearly bimineralic composed of black melanite and green chlorite (rumpfite) as shown in Pl. X, Fig. 4. Melanite shows a strong tendency to euhedralism with the dodecahedral form dominant. Zoning in the melanite is distinct and is manifested by a change in color from light brownish-red to a deep brownish-red. The analyzed garnet in Table 5 was taken from this body. Apatite is present as a minor constituent and has crystallized as small clear prisms. Minor amounts of magnetite, sphene, and perovskite are also present. The mineralization sequence is given below.

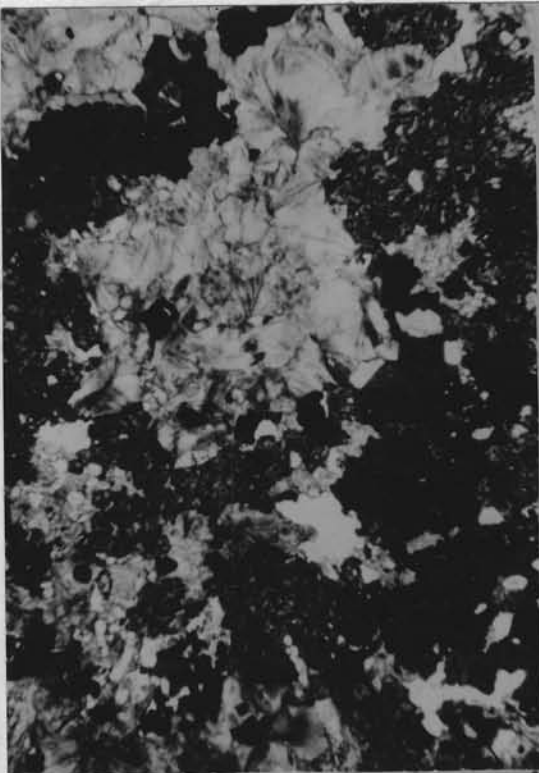
Magnetite	_____
Chlorite	_____
Sphene	_____
Apatite	_____
Melanite	_____
Perovskite	_____

PLATE X. Photomicrographs of metasomatic rocks.

- Figure 1. Chlorite rock. Groundmass of clinocllore and rumpfite cut by irregular veins of melanite garnet. Larger mass to the right of the field is perovskite. Plain light (X40).
- Figure 2. Chlorite rock composed of intergrowths of delessite and stilpnomelane in the light areas. Subhedral opaque grains of magnetite are associated with semi-opaque intergrowths of melanite garnet and perovskite, Plain light (X 40).
- Figure 3. Chlorite rock composed of clinocllore, light groundmass and irregular, distorted stringers of andradite garnet. Plain light (X 40).
- Figure 4. Chlorite rock containing anhedral grains of zoned melanite garnet intergrown with colorless rumpfite. Opaque areas are magnetite. Plain light (X 40).



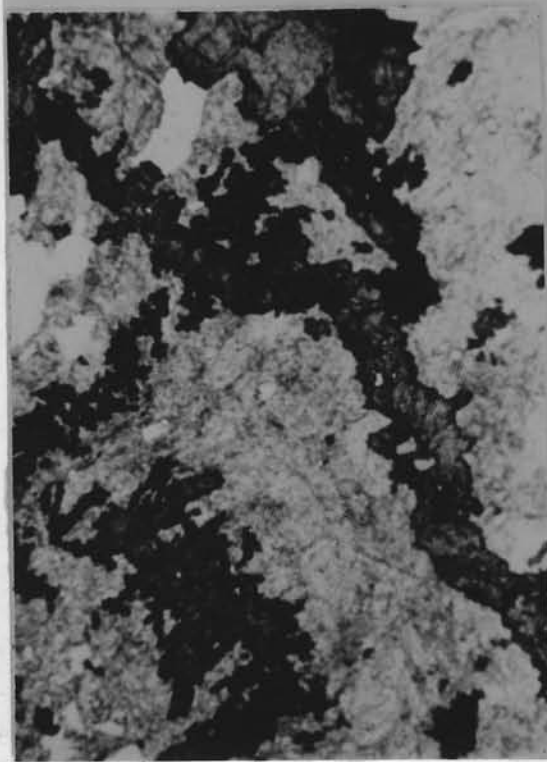
131



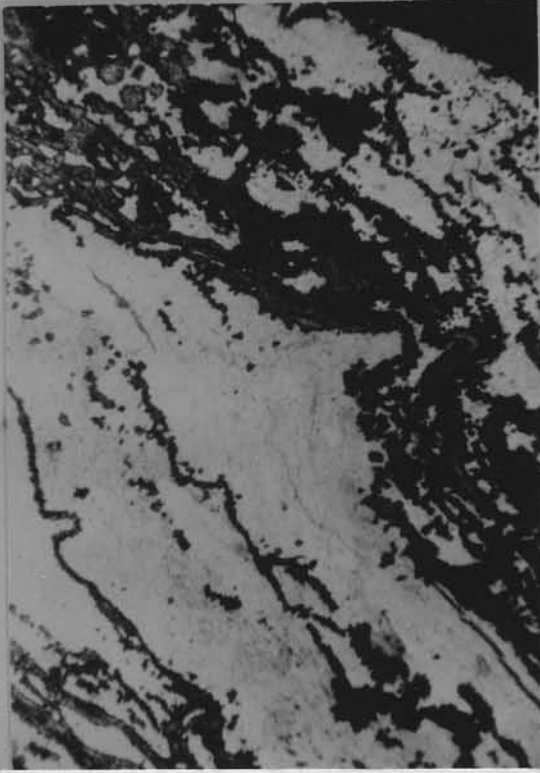
2



4



1



3

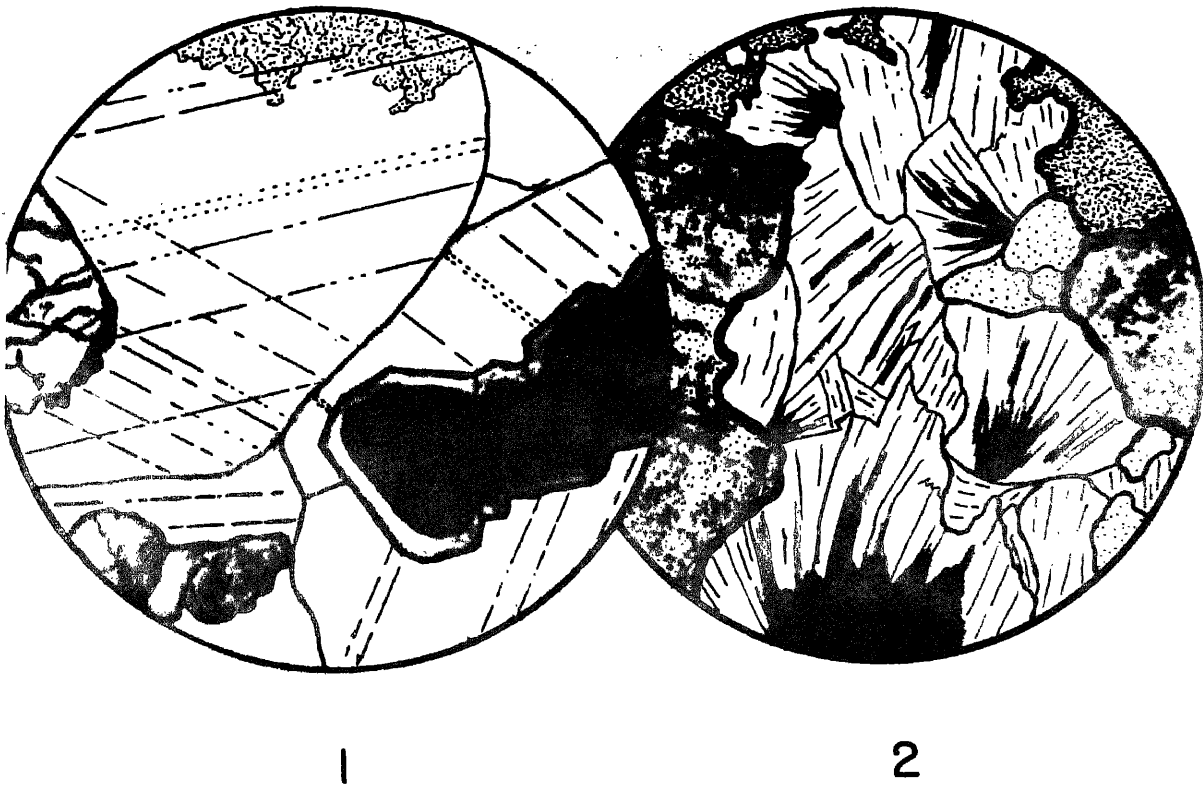


PLATE XI. Camera lucida drawings of metasomatic rocks.

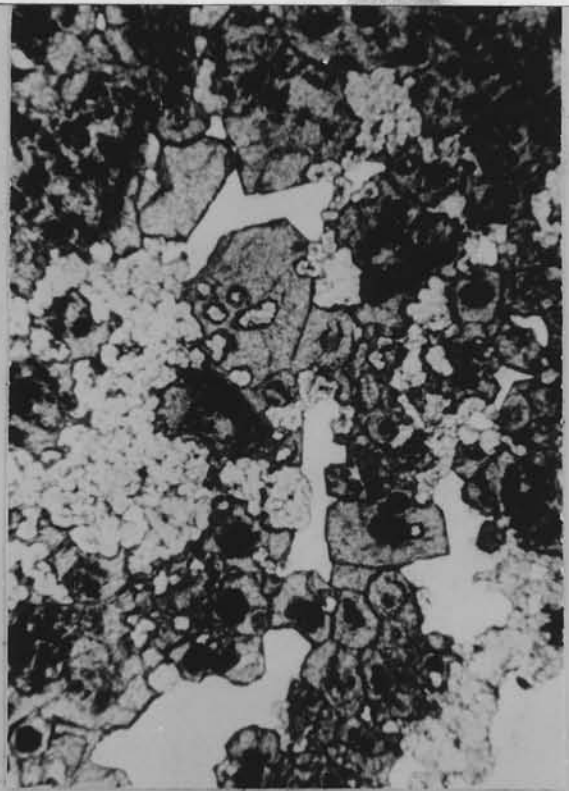
- Figure 1. Calc-silicate rock. Late calcite vein containing subhedral grains of melanite rimmed by idocrase accompanied by anhedral grains of idocrase and 'wormy' rumpfite. (X 40).
- Figure 2. Chlorite rock. Central area illustrates delessite-stilpnomelane intergrowths surrounded by melanite garnet, perovskite, and apatite. (X 60).

PLATE XII. Photomicrographs of metasomatic rocks.

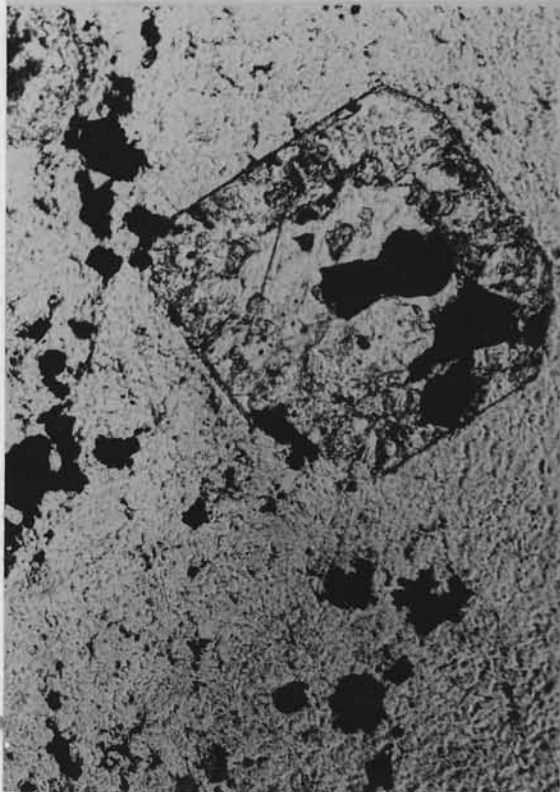
- Figure 1. Chlorite rock illustrating late stage alteration. Groundmass contains rumpfite and anhedral magnetite grains. Altered crystal of andradite replaced by rumpfite, calcite, and magnetite. Plain light (X 80).
- Figure 2. Calc-silicate rock composed of colorless diopside intergrown with melanite garnet. Late vein of titaniferous idocrase cuts the diopside and melanite. Plain light (X 40).
- Figure 3. Chlorite rock composed of clinocllore intergrown with andradite. Late vein of strongly zoned melanite garnet cuts the rock. Plain light (X 40).
- Figure 4. Chlorite rock composed of delessite intergrown with andradite garnet, note vugy openings. Fine-grained intergrowths of sphene and pyroxene produce dark cores in the garnet. Plain light (X 40).



2



4



1



3

Calc-silicate Rocks

(RGC-37-50) crops out as a small layered body about five feet long and three feet thick, tabular in form and dipping 55° S. 55° E. with an exposure so poor that the contact relation with the serpentine is obscured. Further the serpentine is flaky and weathered to a considerable depth, and digging was not helpful in determining the nature of the contact. However, it is assumed that this body was formed by metamorphism of serpentine.

The calc-silicate rock is banded and has crude schistosity and foliation, with vertical fractures normal to the schistosity healed by calcite. The light green bands are composed of chlorite and diopside and the darker green ones contain idocrase, diopside, and chlorite. In thin section, chlorite is almost colorless prochlorite with strong preferred orientation that is responsible for the schistosity. Diopside is also colorless and usually forms radiating clusters, whereas granular aggregates of idocrase cut pre-existing structures in the rock. The calcite is a late mineral that fills interstitial spaces within the granular aggregates and follows the planes of schistosity in the chlorite-rich bands. Sphene is present as a minor accessory and where it is in contact with chlorite, pleochroic halos are produced in the latter. The late calcite veins contain silicates that have been enriched in titanium. For instance, melanite is commonly found with cores of andradite or the melanite may be rimmed by idocrase (Pl. XI, Fig. 1). Small euhedral prisms of reddish-brown titaniferous idocrase are implanted in vugs

areas of the calcite veins. The observed mineralization sequence is given below.

Chlorite	_____	
Diopside	_____	
Idocrase	_____	<u>Ti-bearing</u>
Calcite	_____	
Melanite	_____	
Andradite	_____	
Sphene	_____	

(RGC-34-50) is the best exposed metasomatic body within the district and it was possible to work out some of the details of mineralization, that were obscured at the other metasomatic bodies. The geologic sketch map shown in Plate II presents the geologic situation. The rocks crop out in four individual knobs on the crest of a ridge composed of flaky weathered serpentine, and since these calc-silicate rocks are much more resistant to erosion than serpentine, they show remarkably good exposures as a result of differential weathering. Both the bottom and top contacts of the calc-silicate body are exposed. The body is tabular in shape with minor contortions that parallel the structure within the serpentine, and distinct layered sequence is made obvious by color changes. A columnar section through the calc-silicate body, shown in Plate II, gives the detailed relationships. The body marks a strong contrast with the dark green serpentine, since it is almost white in the upper portion and light green in the lower bands.

The serpentine-calc-silicate contact although gradational is marked by 'fingers' that replace the serpentine along shear planes. Diopside is the dominant mineral in the 'fingers' and in wavy areas light yellow andradite occurs. The sheared serpentine along the contact is composed of antigorite and relict chromite. Diopside directly replaces antigorite and where diopside contacts chromite it assumes a light green color probably as a result of addition of chromium to the pyroxene lattice. Andradite garnet also assimilates chromium and spectrographic analysis of andradite from this locality shows 1 to 5% Cr. The contact zone is about six inches wide and within this zone a gradual change from a diopside-antigorite rock to a diopside-chlorite rock takes place. The diopside-chlorite rock extends about one foot down from the top contact and is characterized by a well developed foliation and schistosity. This zone shows strong evidence of deformation during mineralization, as small folds, accompanied by vertical fractures, have developed. The fractures are, in part, healed by andradite and melanite, and in the fractures, garnet forms beautiful drusy surfaces together with radiating clusters of bladed prisms of white diopside. No evidence of post-mineralization movement can be shown, since these delicate drusy fractures have been perfectly preserved.

The transition from the upper diopside-rich zone to the underlying chlorite-rich zone is marked by a sharp color change from white to light green. The lower zone is composed dominantly of chlorite (rumpfite) containing folia of diopside. This zone exhibits schistosity and

foliation with small scale folding. Fractures developed within this zone are healed mostly by melanite which is strongly zoned with the periphery much darker than the core. The lower serpentine-calc-silicate contact is similar to the upper contact with diopside extending along the shear planes in the serpentine. Minor amounts of sphene and perovskite are present in both zones, with the sphene producing pleochroic halos in the chlorite.

The metasomatic replacement of serpentine at this locality was accompanied by deformation and fracturing, but the later stages of mineralization continued beyond the deformation and healed the fractures. The formation of titanium-rich melanite in the post-deformation stage seems to be the pattern for all the metasomatic bodies investigated. In order to gain some insight concerning replacement processes, quantitative chemical analyses of the host serpentine and the calc-silicate from this location were made (Table 25). The analyzed serpentine was taken one foot above the contact and a channel sample across the calc-silicate body, exclusive of the gradational contacts, was analyzed. The weight percents were recalculated into the standard rock cell following the method of Barth (1948) in order to determine the actual ion exchange (Table 25). It can be readily ascertained that the metasomatism of the serpentine was accomplished by solutions enriched in Ca, Fe, Al, and Ti; and a concomitant removal of Si, Mg, and H₂O. The mineralogical composition of the other calc-silicate bodies is similar to (RGC-34-50) and it would seem logical that the solutions responsible for their formation came from the same source. The observed mineralization sequence is given below.

TABLE 25. CALCULATION OF THE STANDARD ROCK CELL FOR SERPENTINE AND CALC-SILICATE

	SERPENTINE		CALC-SILICATE	
	WT. %	CATIONS	WT. %	CATIONS
SiO ₂	41.47	35.6	34.69	33.0
Al ₂ O ₃	1.35	1.4	10.72	12.0
FeO	5.57	4.0	9.76	7.7
Fe ₂ O ₃	2.62	1.7	4.52	3.2
TiO ₂	.04	-	1.90	1.4
MnO	.24	.1	.27	.2
CaO	nil	-	12.33	12.5
MgO	36.03	46.0	18.46	26.0
K ₂ O	nil	-	.05	-
Na ₂ O	nil	-	.08	.1
H ₂ O+	12.05	34.3	6.88	21.8
H ₂ O-	.76	-	.39	-
CO ₂	nil	-	nil	-
P ₂ O ₅	nil	-	traces	-
BaO	nil	-	nil	-
	<u>100.13</u>		<u>100.04</u>	

SERPENTINE ALTERS TO CALC-SILICATE

By adding

0.1 ions of Na
 12.5 ions of Ca
 0.1 ions of Mn
 1.4 ions of Ti
 5.2 ions of Fe
 10.6 ions of Al

29.9 cations

By subtracting

20.0 ions of Mg
 2.6 ions of Si
 25.0 ions of H

47.6 cations

Analyst - W. H. Kerdsmann

Chlorite	_____	
Diopside	_____	
Garnet	_____	<u>Ti-rich</u>
Sphene	_____	
Perovskite	_____	

(RGC-109-52) is a small roughly lenticular outcrop, 14 feet by 3 feet, that has been mutilated by enthusiastic collectors. The contact, when exposed, is extremely sharp and is marked by a change from dark green serpentine to an almost chalk-white chlorite rock. The surrounding serpentine shows little or no shearing and is composed mostly of chrysotile. Thin sections cut across the contact reveal an almost pencil line sharpness to the metasomatic replacement front in the serpentine. The chrysotile alters to clinocllore which retains the original structure of the serpentine. Small rosettes of diopside have developed within the serpentine about one inch away from the sharp contact zone.

The calc-silicate rock is fine-grained and made up of white needle-like crystals of diopside. Chlorite and andradite, commonly developed near the contacts, are lacking in the central portions of the body. Diopside has a crude lineation and is cut by late veins of melanite and titaniferous idocrase. Perovskite and sphene were not identified from this locality. Near the contact and implanted on the serpentine, are perfect crystals of cubic magnetite. Pabst (1951) was the first to report this rare occurrence of cubic magnetite and his X-ray work indicates that the pattern of the cubic magnetite does not differ from the normal magnetites of octahedral habit. The observed mineralization sequence is given.

Chlorite	_____	
Diopside	_____	
Garnet	_____	<u>Ti-rich</u>
Idocrase	_____	
Magnetite	_____	

(RGC-92-52) crops out as a long narrow vein-like body about two feet in width and about fifty feet long that pinches down to one or two inches in width. The contact between the serpentine and calc-silicate is obscured by flaky serpentine debris, but pieces of float that contain the contact show it to be gradational. Diopside and chlorite extend out along shear planes within the serpentine. Replacement of the serpentine by the calc-silicate rock was followed by fracturing and shearing with subsequent healing of fractures by idocrase and garnet.

This calc-silicate rock is dense, heavy with well developed foliation and lineation, is composed essentially of idocrase, diopside and chlorite (see Pl. XII, Fig. 2). Diopside forms colorless elongate, bladed crystals which produce a strong lineation, whereas colorless to green chlorite creates discontinuous folia within diopside. Idocrase is light green, forming anhedral grains cross-cutting the fabric of the rock. Andradite fills fractures and in vuggy areas produces drusy surface implanted with bladed diopside. The late fracture-filling garnets and idocrase are once again tinted a reddish-brown, due to late introduction of titanium. The observed mineralizing sequence is presented.

Chlorite	_____
Diopside	_____
Idocrase	_____
Andradite	_____ <u>Ti-rich</u>

Titano-Silicates and Sodium Silicate Rocks

The Gem mine is the best known mineral locality within the New Idria district and has long been famous as the only known occurrence of benitoite and joaquinite. Of this locality and its minerals, Louderback (1907, 1909) has given an excellent description that is much more complete than the one presented here, since he had the opportunity to study this deposit while it was being mined for benitoite. At the time of this investigation many of the original features had been obscured by slumping, and a dense brush cover precluded a detailed study. A plane table map of the area was completed and the principal rock types were plotted (Plate III). Surrounded by sheared serpentine, the Gem mine is situated within a tectonic inclusion that is more resistant than the inclosing serpentine and accordingly forms a small ridge which extends down to the headwaters of the San Benito River.

The tectonic inclusion contains three distinct rock types; (1) a dense, fine-grained greenstone composed essentially of pyroxene (near aegirine-augite), albite, and chlorite, (2) saussuritized gabbro, (3) albite-crossite-epidote schist. The relationships of these rock types may be seen in Plate III, and petrographic description was treated previously in the section on tectonic inclusions.

The zone of metasomatism is found wholly within the albite-crossite-epidote schist. This zone is elongate and consists of many irregular natrolite veins that parallel the elongation. The surrounding rock in the mineralized zone has been altered from the albite-crossite-epidote schist to a vuggy and porous rock impregnated with natrolite and fibrous crossite (Pl. XIII, Fig. 1). Replacement veins of natrolite form granular aggregates that project inward to produce cockscomb drusy surfaces. The center of these veins is usually open and vuggy, although many parts are completely filled with natrolite. Many of the open vugs are filled with very fine hair-like amphibole whose optics are similar to those of crossite, and these fibrous needles support small aggregates of natrolite. Implanted on the cockscomb drusy surfaces are euhedral crystals of blue, tabular, pyramids of benitoite (Pl. XIII, Fig. 2) and brilliant, black crystals of prismatic neptunite. Joaquinite is extremely rare and always is present as small, honey-yellow crystals not more than 2 mm. in size. Greenish clots on the surface of the natrolite are composed of a core of chalcocite surrounded by an alteration halo of chrysocolla. In this present investigation, a new mineral has been found in small bluish-black fibrous aggregates within small veins cutting natrolite. Preliminary work indicates that this may also be a titanium mineral, but insufficient material is at hand to complete the description.

The mineralized zone has several post-depositional faults accompanied by shearing, although extensive deformation is not apparent as many of the delicately implanted drusy surfaces have retained even the most

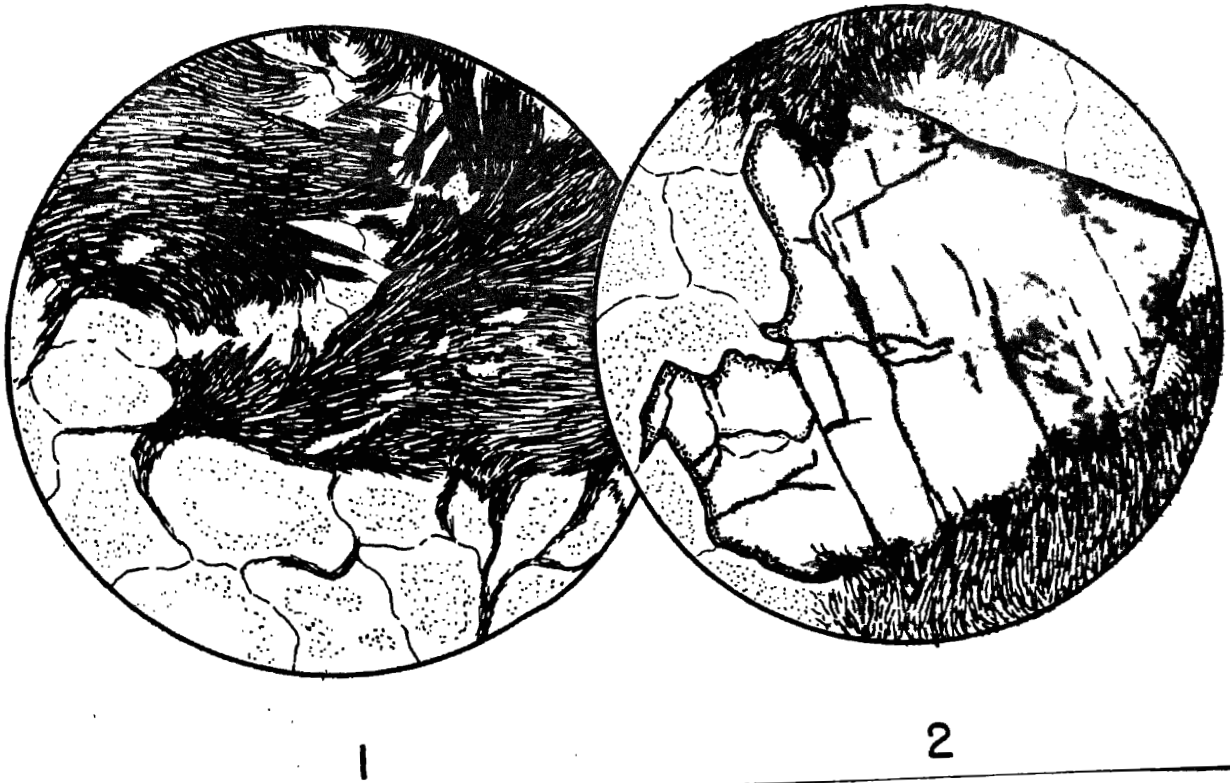


PLATE XIII. Camera lucida drawings of metamorphic rocks.

Figure 1. Crossite-natrolite rock from the Gem mine.
(X 40).

Figure 2. Benitoite crystal implanted in a crossite-
natrolite rock from the Gem mine. (X 40).

fragile crystals. As is typical, the contact between the tectonic inclusions and serpentine is strongly sheared. The observed mineralizing sequence is presented.

Natrolite	_____
Amphibole	_____
Benitoite	_____
Neptunite	_____
Joaquinite	_____
Chalcocite	_____

On the southeast flank of Santa Rita Peak is a small tectonic inclusion (RGC-81-52) that contains numerous natrolite veins with mineralogy quite similar to that found in the Gem mine. The natrolite veins are located within an albite-glaucophane-actinolite schist and follow an elongate trend similar to the Gem mine. Natrolite forms drusy surfaces of euhedral prisms and in the more vuggy spots, hair-like crossite is implanted on the natrolite. Natrolite impregnation of the host rock is not as extensive at this locality, although the metasomatism is similar to that found at the Gem mine. The only titanium mineral identified was joaquinite, but it occurs very sparingly. Chalcocite with chrysocolla alteration halos is quite common. This is the only other locality in the district which has a mineralization sequence similar to that found in the Gem mine and it would seem that the geologic conditions attendant on the formation of these rare barium-titanium silicates is indeed unique.

Origin of the Metasomatic Rocks

The peculiar replacement rocks within the serpentine and the tectonic inclusions present a difficult problem in genesis. A search of the geologic literature produced few descriptions of deposits similar to those found in the New Idria district; therefore genetic implications by analogy are not possible.

Turner (1933) has described lime-silicate masses in serpentines from New Zealand that contain antigorite, chlorite, talc, diopside, garnet, magnetite, and idocrase. These rocks, according to Turner, have been formed by alteration of the original pyroxenite by hydrothermal processes which took place under conditions of marked shearing stress. Grange (1927) has described grossularite-pyroxene rocks--rodingites of Marshall (1911)--from the peridotite belt of Nelson, New Zealand and they have been shown to be due to garnetization of a gabbroid rock, under the influence of 'Concentrated magmatic water' acting probably at high pressures. Tyrrell (1931, p. 29) and Arshinov and Merenkov (1930) have described and discussed dikes in the Ural Mountains that contain garnet-pyroxene, garnet-idocrase, and garnet-chlorite that invade serpentized harzburgites. They consider that these calc-silicate rocks are formed by garnetization of micro-diorites and alteration of pyroxenite schlieren by calcium-rich solutions liberated in the processes of serpentization.

All of the rocks from these different localities are somewhat similar to the chlorite and calc-silicate rocks from the New Idria district, but they have been related to alteration of pre-existing rock types within

the serpentines. The metasomatic rocks from this district, exclusive of the Gem mine material, have no relict minerals or structures that could be related to reconstituted rock types other than the serpentine itself. Furthermore, the existence of titanium minerals, zircon, apatite, and other minerals unusual in ultrabasic rocks, indicates that the fluids responsible for the metasomatism came from a source other than those processes related to formation of serpentine. Spectrographic analyses of the serpentines and metasomatic rocks, to be discussed later, show no affinities with each other.

All of these metasomatic bodies are clustered around the syenite-camptonite intrusions (Pl. I) and chemical study of these intrusives shows a progressive depletion of Ca, Mg, Fe, and Ti and in the late stages enrichment in Na. The calculation of the standard rock cell (Table 25) shows that metasomatism of serpentine was accomplished by fluids enriched in Ca, Fe, Al, and Ti. From these facts, it would seem reasonable to effect metasomatism of serpentine by fluids which had arisen from the intrusive during its emplacement.

Abundant evidence of deformation during metasomatism indicates tectonic activity during mineralization. The intrusions may well have been emplaced during a tectonic period and fluids arising from the magma probably migrated along shear zones selectively replacing the serpentine.

The titano-silicates from the Gem mine pose a special problem since the mineralogy here is quite different from that found in the calc-silicate and chlorite rocks. However, the high titanium and sodium content plus the copper mineralization favor the intrusive rocks as a source of the

mineralizing fluids. The intrusive shows an extremely strong Na enrichment during the late stages, accompanied by copper mineralization. The high barium content in several minerals produces an enigma since neither the intrusives nor serpentinite contain abnormal amounts of barium, and furthermore, barium minerals were not identified in any of the calc-silicate or chlorite bodies. Therefore, the intrusive rocks apparently did not supply barium for benitoite and the other Ba-rich minerals. The most likely source of the barium is from the host rocks that make up the tectonic inclusion. Barite is not uncommon in manganese concentrations within the Franciscan and there is evidence of considerable manganese within the Gem mine inclusion. The most plausible theory as to the origin of the Gem mine minerals is one which proposes a multiple source for the rare element assemblage, since this deposit has not resulted from a normal type of mineralization.

The author suggests that the unique deposit at the Gem mine has resulted from the fortuitous mixing of fluids from the intrusive rocks with barium-rich zones within the metamorphosed sediments, and this has resulted in the crystallization of the extremely rare mineral assemblage: benitoite, joaquinite, and neptunite.

MINOR AND TRACE ELEMENT STUDY OF THE ROCKS AND MINERALS

Introduction

A comprehensive study of the rocks and minerals involved in the formation of the metasomatic rocks within the serpentine by spectrographic methods has been very illuminating and helpful in the general problem of genesis.

Each rock type analyzed represented approximately a two pound sample. This material was ground to pass through an 80-mesh sieve and a representative split of ten milligrams was used for the analyses. The analyzed minerals were separated from the same rock specimen used for spectrographic determinations. Quantitative chemical analyses have been made on the same material used for the spectrographic determinations. Therefore, in the discussion on the distribution of the elements in rocks and their constituent minerals, the analyses have been on material from the same specimen eliminating the problem of variations due to poor sampling. The semi-quantitative spectrographic analyses followed the procedure of Waring and Annell (1955).

The results of the spectrographic analyses are presented in Plate IV, with the values obtained given in ranges. All of the elements detected are reported in the table, but not all of these elements are discussed, particularly the major elements. The sensitivity for each element is given at the bottom of the table and in the extreme left-hand column sample numbers are given. The location of each sample number may be determined by using the middle digits of these numbers which are plotted on the geologic map (Plate I).

Seven serpentine rock samples were taken and six of these from the immediate area of the metasomatic rocks whereas (RGC-101-52) comes from

the western part of the serpentine. The metasomatic rocks and minerals are divided into the calc-silicate and chlorite types defined earlier. The intrusive rocks were obtained from the White Creek body and this material is a split of that used for the quantitative chemical analyses.

These analyses were undertaken to determine, if possible, the source of the metasomatic fluids that formed these curious bodies within the serpentine and also to establish fundamental data on the partition of minor and trace elements in this type of mineralization.

The possible sources for fluids may be enumerated at this point in order to illustrate how the following observations fit the possibilities. Since the syenite-camptonite intrusions crop out in close proximity to these metasomatic bodies, fluids produced during the time of emplacement could have migrated up along the numerous shear zones within the serpentine and metasomatically replaced the serpentine and parts of the tectonic inclusions. If this had happened, we might expect to find minor and trace elements concentrated within the metasomatic bodies that are characteristic of an 'alkalic' magma. A second possible source are fluids that have formed by the processes that have given rise to the serpentine. The ultimate source of the serpentine was an ultrabasic 'magma' that had undergone crystallization and emplacement probably accompanied by serpentinization. The fluids responsible for the metasomatic bodies may have been the end product of these processes producing solutions enriched in Ca, Ti, and other elements characteristic of the replacement rocks. Again if this were the ultimate source the minor and trace elements within the bodies should reflect a suite of elements expectable from 'ultrabasic

magnas'. The third possibility would be a deep seated intrusive which was not apparent on the surface, but which may have produced emanations that were carried upward into the relatively previous serpentine and metasomatically replaced the serpentine and portions of the tectonic inclusions. The minor and trace element suite from such a source again would be distinct enough to eliminate the two previous alternatives. The following discussion is primarily aimed at a possible correlation between the observed minor and trace element suite with one of the three possibilities. Each element is discussed in turn except where two elements are similar in their geochemistry.

Boron

Boron shows above average concentrations in the serpentines. Rankama and Sahama (1950) give an average of 31 ppm (parts per million) for ultrabasics whereas these serpentines range from 100-500 ppm. The calc-silicate and chlorite rocks vary considerably in boron content but generally have a high content (up to 1000 ppm). The border rock from the jadeite pods (RGC-105-52) contains almost 1% boron. An extremely high content (1000-5000 ppm) was found in the ilmenite from the chlorite rock (RGC-85-51). Idocrase and chlorite from the metasomatic rocks show an enrichment in B when compared to the other minerals. The camptonite and syenite show 10 ppm B which is similar to that given for average igneous rocks by Goldschmidt (1954, p. 281). Boron was not detected in the minerals from the Gem mine. The high boron in selected rocks from this area indicates a possible outside source of boron. Goldschmidt (1954, p. 281) suggests that a high boron content in such rocks as these

may result, not from a magmatic source, but by contamination from marine sediments in juxtaposition with 'intrusive' rocks. The Franciscan formation, a marine sediment, is intimately associated with the serpentine and appears to be the logical source of the abnormal boron encountered here.

Vanadium

The serpentines contain 10-500 ppm without a positive correlation between Fe, Cr, or Ti as is commonly found in other rocks. The chlorite rocks show a slightly higher concentration of V (100-5000 ppm), again with no positive correlation between Fe, Cr, or Ti. Ilmenite from (RGC-83-51) contains no V, although the rock as a whole has 100-500 ppm V. This follows Rankama and Sahama (1949, p. 596) where they show that V does not enrich in ilmenite but prefers titanian magnetites. The calc-silicate rocks show 100-500 ppm V consistently and in these rocks vanadium is noticeably enriched in the chlorite as compared to the garnets, idocrase, and perovskite. The V^{5+} apparently substitutes in the chlorites for Al^{5+} in the octahedral positions. The intrusive rocks contain 100-500 ppm V; comparable to other rocks of this type (Higazy, 1954, p. 50).

Gallium

Gallium was not detected in the serpentine as would be expected since gallium is camouflaged in aluminum-bearing minerals; the serpentines all contain less than 1% Al. The calc-silicate and chlorite rocks averaged 10-50 ppm Ga. It is interesting to note that Ga is enriched in clinocllore

from RGC-109-52 when compared to idocrase from the same specimen even though the Al content of the idocrase is several times greater than that of the clinocllore. The garnets also appear to favor the substitution of Ga over idocrase. The intrusive rocks and minerals averaged 50-100 ppm with the exception of the late Cu-Pb sulfide from the veins within the syenite. The sulfide shows .1-.5% Ga showing an enrichment in Ga during the late stages of the syenite intrusion. Goldschmidt (1954, p. 329) has shown that sulfides of the 'tetrahedral' group commonly contain significant amounts of Ga.

Chromium

The serpentines with the highest Cr content, average 0.1-0.6% Cr, and it is probably contained within chromite, for the most part. Since all the other rocks analyzed are replacing, included in, or intrusive into the serpentine their high Cr content probably reflects contamination. The chlorite rocks show 100-1000 ppm with some tendency for the Cr to concentrate in the chlorites, and ilmenite that has crystallized late in RGC-83-51 shows extremely high Cr (0.1-0.5%). The calc-silicate rocks have the same range in Cr as the chlorite rocks, i.e., 100-1000 ppm., although andradite near the borders of the replacement bodies contains 1-5% Cr. The intrusive rocks contain above normal Cr; camptonite 100-500 ppm and syenite 10-50 ppm, indicating some serpentine contamination.

Titanium

The serpentines contain 10-100 ppm Ti which is generally low for ultrabasic rocks, Faust and Murata (1955) find an average of 140 ppm Ti

for seven serpentines and Higazy (1954, p. 53) on several ultrabasic rocks shows almost 1% Ti. This low Ti content summarily excludes the serpentine as a source of the high Ti in the metasomatic rocks within the serpentine since there is a hundred-fold increase from the serpentine to the metasomatic rocks. The chlorite rocks are extremely variable with respect to Ti; a high of 5% to a low of .05%. The titanium is concentrated within the minerals perovskite, melanite, and ilmenite and these minerals may make up a large part of the rock. The calc-silicate rocks are lower in Ti but more consistent than the chlorite rocks with an average content of .1-1% Ti. In these rocks Ti preferentially enters garnets, idocrase, and chlorite in that order. The camptonite and syenite contain 100-500 ppm which is considerably below the average for igneous rocks (0.61%); however, within the syenite barkovikite contains 1-5% Ti. The ultimate source of the Ti in the metasomatic rocks is obscured as both the serpentine and intrusive rocks are below average in Ti when compared to rocks of a similar type; possibly the late stages of the intrusions produced fluids enriched in Ti since there were no discrete titanium minerals formed in the early stages of crystallization.

Niobium

Niobium was not detected in any of the rock splits (sensitivity .001%); however, in the purified mineral separates from the rocks several minerals contained significant amounts of Nb. Perovskite shows 100-500 ppm, melanite 10-50 ppm, and benitoite from the Gem mine 100-500 ppm. Niobium is commonly found in perovskite, although this, so far as the

author knows, is the first known occurrence of significant amounts of Nb in garnet. Benitoite might be expected to carry Nb, but neptunite does not show Nb although it is rich in Ti. It is curious that Nb was not detected in the ilmenite from the chlorite rocks, in view of the fact Goldschmidt (1954, p. 503) reports several percent of Nb in ilmenite from granitic pegmatites. The close association of Nb with rocks of the later stages of magmatic evolution (granites and syenites) strongly suggests that the Nb found in the minerals from the metasomatic rocks has been derived from fluids produced by the syenite intrusion.

Nickel and Cobalt

In the serpentine, Co and Ni show a constant relationship with $Ni > Co$ (Co- .01-.1%, Ni- .1-.5%) and following the work of Faust and Murata (1955) this relationship is typical for serpentines derived from ultrabasic rocks of 'magmatic' origin, or from any igneous rock high in Mg^{2+} since Ni^{2+} follows Mg^{2+} (Wager and Mitchell, 1952). The chlorite rocks show less nickel and cobalt with $Ni \approx Co$ (Ni- .01-.05%) (Co- .01-.05%). In the chlorite rocks Co and Ni show preferential substitution in the various minerals. Perovskite contains 10-50 ppm Co, but Ni was not detected. Melanite shows $Ni > Co$ by a factor of ten. The calc-silicate rocks have a variable relationship with $Ni > Co$ in some bodies and $Ni \approx Co$ in others. The andradites from the calc-silicate rocks contain 100-500 ppm Ni; and Co was not detected. Clinocllore shows strong enrichment in Ni (1000-5000 ppm) and idocrase consistently has more nickel than Co. The syenite and camptonite are similar in nickel- and cobalt-content

with Ni Co (.01-.05%). Nockolds and Allen (1954) in their study of alkalic rocks show Ni Co in the early stages of differentiation with a trend during the magmatic descent for those elements to become equal and in the final stages Co is greater than Ni. Following this data, it might be said that the Ni-Co ratio in the syenite suggests that it has been intruded from a partially differentiated magma. Furthermore, the similarity of the Ni-Co ratio in the metasomatic bodies when compared to the intrusive rocks indicates a closer kinship to the intrusive rocks than to the serpentines.

Scandium

Although not detected in the serpentines, Faust and Murata (1955) report scandium in 7 out of 9 serpentines analyzed. Scandium was found in both the chlorite and calc-silicate rocks (10-50 ppm) and it shows concentration only within ilmenite (100-500 ppm). The low-iron chlorites did not contain detectable amounts of Sc, but the other mineral phases within the metasomatic bodies show 10-100 ppm Sc. Camptonite and syenite contain 10-50 ppm Sc with some concentration noted in the barkevikite and apatite.

Zirconium

Zirconium may be used in this investigation as a key trace element to establish, in part, the genesis of the metasomatic rocks. Zr was not detected in the serpentine nor in any of the other rock splits (sensitivity-.0002%); however, in the mineral separates from the calc-silicate and chlorite rocks Zr was found in ilmenite (50-100 ppm), melanite (100-500 ppm), perovskite (50-100 ppm), and idocrase (100-500 ppm).

In the intrusive rocks Zr was found in albite (10-100 ppm), barkevikite (100-500 ppm) and apatite (50-100 ppm). Benitoite from the Gem mine shows 10-50 ppm Zr. The partition of Zr in these rocks shows a strong genetic relationship between the metasomatic and intrusive rocks. Hevesy and Würstlin (1934) give 60 ppm Zr as the average for peridotites, eclogites, and dunitites; and Faust and Murata (1955) find that only two of 20 magmatic and metamorphic serpentines contain 60 ppm Zr. Therefore it would seem difficult for these metasomatic rocks within the serpentine to obtain such a high Zr content from other than solutions arising from the intrusive rocks. Elaborate separation on about 50 pounds of rock from the syenite were made in order to concentrate zircon for age determination; however, no zircon was recovered. It is assumed that the Zr present in the magma entered other silicate structures rather than forming zircon and in part may have been removed by emanations which led to the formation of the metasomatic bodies.

Rare Earths

Rare earths were not detected in any of the serpentines or serpentine minerals and this agrees with the work of Faust and Murata (1955) who report no rare earths from 20 spectrographic analyses of serpentines. The chlorite rocks show variable amounts of rare earths with $Y > Yb \approx La$. Perovskite from these rocks concentrates significant amounts of rare earths with $Ce \approx La > Y \approx Nd > Yb$, and melanite from the same rocks shows $Y > La$. The calc-silicate rock splits all show rare earths with

Y³⁺La Yb. Idocrase from these rocks shows a range of rare earth content with Y detected in all specimens and Ce and La present in (RGC-109-52). Camptonite contains La as the only detectable rare earth whereas the syenite shows Y > Yb. Barkevikite from the syenite contains 10-50 ppm Y. The apatite from the syenite contains an interesting suite of rare earths with Ce > La > Nd > Y > Dy > Er > Yb. Goldschmidt (1954) has shown that rare earths within a magma may concentrate within the apatite and, therefore, the rare earths present within the apatite from the syenite should show what rare earths may have been present in magmatic emanations available during the emplacement of the syenite. The marked similarity between the rare earths in the metasomatic rocks when compared to those present in the apatite suggest a strong genetic kinship.

Barium and Strontium

Barium presents a unique problem in distribution within the New Idria district, since benitoite, a rare barium titanate-silicate (36% BaO), is restricted to the metasomatic rocks of the Gem mine. Barium is not found as an essential constituent in other metasomatic rocks within the district, therefore, the source of the barium is important in the genesis of benitoite. The serpentines contain up to 50 ppm Ba and Sr is not present in detectable amounts (sensitivity 10 ppm). Faust and Murata (1955) show barium up to 7 ppm in 'magmatic' serpentines and do not report Sr from these rocks. The chlorite rocks contain 10-1000 ppm Ba and Sr with the Ba-Sr ratios variable from one

rock to the next. In the chlorite rocks Ba is concentrated in the late minerals, viz. ilmenite (1000-5000 ppm) and perovskite (100-500 ppm) and Sr is concentrated in melanite (100-500 ppm) and perovskite (500-1000 ppm). In the calc-silicate rocks, the Sr-Ba ratio is consistent with $Sr > Ba$ except for (RGC-105-52) where the ratio is reversed. Barium shows some tendency to concentrate in the chlorite (10-50 ppm) and strontium is enriched in idocrase (500-1000 ppm). The rock with the highest Ba concentration is the border rock (RGC-105-52) associated with the jadeite pods and here Ba is 1000-5000 ppm. The camptonite and syenite show $Sr \approx Ba$ (500-1000 ppm) and the separated minerals from these rocks have the same ratio and concentration. Ba exceeds Sr by a factor of 1000 in benitoite and neptunite. The intrusive rocks are extremely low in barium when compared to similar rock types; however, this is to be expected, since these rocks are extremely low in potassium; and Ba in igneous rocks is to a large extent camouflaged in potassium-bearing minerals. The ultimate source of the barium in the Gem mine seems to be related to the host rock as both the serpentine and intrusive rocks are extremely low in Ba. The barium minerals are restricted to metasomatic zones within the tectonic inclusions. As proposed earlier, the barium has probably been assimilated from Ba-rich zones within the metamorphosed sediments present in the tectonic inclusion.

Silver

Silver was detected in many of the rocks and minerals as the sensitivity of this element by spectrographic methods is extremely high

(0.1 ppm). Ag is present in all of the serpentines (0.1-10 ppm); however, Faust and Murata (1955) have not reported silver in such an environment. The chlorite and calc-silicate rocks contain 0.1-10 ppm with some tendency for the Ag to concentrate in the chlorites. The camptonite and syenite contain 1-10 ppm somewhat above Goldschmidt's (1954) average for igneous rocks (0.02 ppm). The late Cu-Pb sulfide within veins cutting the syenite contains significant amounts of Ag (500-1000 ppm).

Lead

Pb was detected in two serpentines (RGC-25-50) and (RGC-101-50), but it was not detected in the chlorite rocks, although melanite from these rocks has 100-500 ppm and perovskite shows 10-50 ppm. Three out of five calc-silicate rocks show 10-50 ppm Pb with prochlorite containing 500-1000 ppm and andradite 10-50 ppm. The camptonite and syenite contain 10-50 ppm with a marked concentration in the barkevikite (100-500 ppm).

Copper

Copper was detected in every rock and mineral analyzed and this affords a good opportunity to examine the behavior of Cu in relationship to substitution or camouflage in silicate minerals within a small province. The serpentines show a rather high background in Cu and consistently contain 10-100 ppm. The chlorite rocks have the same range as the serpentines (10-100 ppm) and the minerals from these rocks show the following partition of Cu: chlorite (50-100 ppm), melanite (100-500 ppm), perovskite (5-50 ppm) and ilmenite (50-100 ppm). The calc-

silicate rocks show 10-500 ppm and the minerals therein show the following partition of Cu: chlorite (10-50 ppm), andradite (10-50 ppm), and idocrase (1-100 ppm). The camptonite and syenite show a very high Cu content (100-1000 ppm) and albite and barkevikite therein show 10-50 ppm Cu. The late sulfide in the syenite is mostly chalcocite (Cu_2S) and there seems to be an enrichment of copper in the late stages of the intrusive rocks. In general, the district has a fairly high background in Cu and the source for Cu in the metasomatic bodies may be multiple.

Other Elements

Tin is absent in the serpentine and is below the sensitivity in most of the metasomatic rocks, however, tin was detected in the ilmenite (50-100 ppm) and in idocrase (100-500 ppm) from the metasomatic rocks. (RGC-36-50) a chlorite rock located fairly close to the small camptonite 'plug' shows 50-100 ppm Sn. The camptonite shows 10-50 ppm Sn while the syenite contains no detectable amounts. Here again, there seems to be strong kinship between the intrusive rocks and the metasomatic bodies.

Molybdenum was not detected in the serpentines; however, it was found to be present very sporadically in the other rocks and minerals. Mo is present in the chlorite rock (RGC-36-50) (10-50 ppm), prochlorite from (RGC-37-50) (10-50 ppm), andradite from (RGC-34-50) (10-50 ppm), calc-silicate (RGC-109-52) (10-50 ppm), and significantly in barkevikite from the syenite (10-50 ppm).

The late Cu-Pb sulfide from veins within the syenite contains significant amounts of metals; 500-1000 ppm Hg, 10-50 ppm Au, 100-500 ppm Cd, 1-5% Zn and 1000-5000 ppm Bi. The presence of mercury in this sulfide concentration is significant, since the New Idria district contains many mercury deposits and it may be that these intrusives produced those fluids responsible for the cinnabar deposits.

Summary

The minor and trace element content of the serpentine is similar to those serpentines studied by Faust and Murata (1955) and known to have formed from ultrabasic rocks of magmatic origin. There is no evidence that the peculiar suite of elements found in the metasomatic rocks originated from processes which have given rise to the serpentine. The nickel, cobalt, and chromium present within the metasomatic rocks and intrusives may well have been introduced by contamination from the serpentine. Boron and barium seem to have been introduced from the sediments in juxtaposition or incorporated within the serpentine. The striking similarity between the trace elements from the metasomatic rocks as compared to those from intrusive rocks indicates a very strong consanguineous relationship. The indicator elements within the metasomatic rocks that point to the intrusive rocks as their only apparent source are Nb, Zr, rare earths, Sn and Mo. Had the metasomatic rocks formed directly from the serpentine without introduction of material, it is quite improbable that the indicator elements listed could have been mobilized from the serpentine, even though large volumes of rock

were involved. There is no indication that a deep-seated igneous mass has contributed to the formation of these rocks, unless the exceptionally high boron content is construed as coming from a granitic magma.

The sparse data from the jadeite facies indicates that these rocks are a separate and distinct period of mineralization and may very well be related to the metamorphism of the tectonic inclusions either during serpentinization or in a later period of tectonic activity. The high boron and barium content combined with their close proximity to the large masses of metamorphosed sediments implies a very close association between the metamorphism of the sediments and serpentinization. This association and the unique P-T environment probably are responsible for the rare concentrations of jadeite.

It is concluded from this study of the minor and trace elements, that the peculiar metasomatic bodies within the serpentine have been produced by emanations arising from the emplacement of the syenite and camptonite.

LITERATURE CITED

- Adams, L. H., 1953, A note on the stability of jadeite: Amer. Jour. Sci., V. 251, p. 299-308.
- Anderson, R. and Pack, R. W., 1915, Geology and oil resources of the west border of the San Joaquin Valley north of Coalinga, California: U. S. Geol. Survey Bull. 603, 220 pages.
- Arnold, R., 1908, Notes on the occurrence of the recently described gem mineral, benitoite: Science, new ser., V. 27, p. 312-314.
- Arnold, R. and Anderson, R., 1910, Geology and oil resources of the Coalinga district, California: U. S. Geol. Survey Bull. 398, 354 pages.
- Arshinov, V. and Merenkov, B., 1930, Petrology of the chrysotile asbestos deposits of the Krasnouralsky asbestos mine in the Ural Mountains: Trans. Inst. Econ. Mineral., U.S.S.R., no. 45.
- Barth, T. W. F., 1952, Theoretical petrology: N. Y. John Wiley and Sons, 387 pages.
- Becker, G. F., 1888, Geology of the quicksilver deposits of the Pacific slope: U. S. Geol. Survey Monograph 13, p. 301-309, 379-381.
- Bolander, L. Ph., 1950a, New California mineral-perovskite: The Mineralogist, V. 18, p. 65.
- _____, 1950b, First jadeite discovery in America: The Mineralogist, V. 18, p. 186 and 188.
- Bowen, N. L. and Tuttle, O. F., 1949, The system MgO-SiO₂-H₂O: Geol. Soc. America Bull., V. 60, p. 439-460.
- Bowman, H. L., 1908, On the structure of perovskite from the Burguner Alp, Pfitschthal, Tyrol: Min. Mag., V. 15, p. 156-176.
- Brindley, G. W. (editor), 1951, X-ray identification and crystal structures of clay minerals: Monograph, Clay Minerals Group, Mineralogical Society, London.
- Brothers, R. N., 1954, Glaucophane schists from the North Berkeley Hills, California: Amer. Jour. Sci., V. 252, p. 614-626.
- Buttgenbach, H., 1937-38, Sur un cristal de neptunite: soc. géol. Belgique Annales 61, p. 324-325.

- Coleman, R. G., 1954, Optical and chemical study of jadeite from California: Geol. Soc. America Bull., V. 65, p. 1241. Abst.
- De Roever, W. R., 1955, Genesis of jadeite by low-grade metamorphism: Amer. Jour. Sci., V. 253, p. 283-298.
- Du Rietz, T., 1935, Peridotites, serpentines, and soapstones of Northern Sweden: Geol. Foren., Stockholm, Band 57, p. 134-260.
- Eckel, E. B. and Myers, W. B., 1946, Quicksilver deposits of the New Idria district, San Benito and Fresno Counties, California: California Jour. of Mines and Geol., V. 42, pt. 2, p. 81-124.
- Faust, G. and Murata, J., 1955, Unpublished data on trace elements in serpentine minerals, U. S. Geological Survey.
- Ford, W. E., 1909, Neptunite crystals from San Benito, California: Am. Jour. Sci., 4th ser., V. 27, p. 235-240.
- Goldschmidt, V. M., 1954, Geochemistry: London, Oxford Univ. Press, 730 pages.
- Gossner, B. and Mussgnug, F., 1928A, Cent. Min., p. 274.
- Grange, L. I., 1927, On the rodingite of Nelson: Trans. and Proc. New Zealand Inst., V. 58, p. 160-166.
- Griggs, D. T., Fyfe, W. S., and Kennedy, G. C., 1955, Jadeite, analcite, and nepheline-albite equilibrium: Geol. Soc. America Bull. V. 60, p. 1569, Abst.
- Hevesy, G. V. and Wirstlin, K., 1934, Die Häufigkeit des Zirkoniums: Zeits. anorg. allgem. Chem., V. 216, p. 305.
- Hoy, M. H., 1950, An index of mineral species and varieties arranged chemically: British Museum (Natural History), London.
- _____, 1954, A new review of the chlorites: Min. Mag., V. 30, p. 277.
- Higazy, R. A., 1954, Trace elements of volcanic ultrabasic potassic rocks of southwestern Uganda and adjoining part of the Belgian Congo: Geol. Soc. America Bull., V. 65, p. 39-70.
- Hillebrand, W. F. and Lundell, G. E. F., 1929, Applied Inorganic Analysis: N. Y., John Wiley and Sons.

- Hutton, C. O., 1938, The stilpnomelane group of minerals: *Min. Mag.*, V. 25, no. 163, p. 172-206.
- _____, 1940, Metamorphism in the Lake Wakatipu region, Western Otago, New Zealand: *New Zealand Dept. Sci. and Indus. Res., Geol. Mem. no. 5*, 90 pages.
- _____, 1943, Hydrogrossular, a new mineral of the garnet-hydrogarnet series: *Royal Soc. New Zealand Trans.* V. 73, p. 174-180.
- Johannsen, A., 1949, A descriptive petrography of the igneous rocks: Chicago, Univ. Chicago Press, V. 1, 318 pages and V. 4, 523 pages.
- Kopetaky, I., 1948, Chromhaltiger Chlorit (Kammererite) von Kraubath: *Tscher. Min. Petr. Mitt.*, ser. 3, V. 1, p. 69-70.
- Kranck, S. H., 1928, On turgite and the ijolite stem of Turga, Kola: *Fennia. Bull. Soc. Geogr. Finlande*, V. 51, no. 5, 104 pages.
- Lake, M. C., 1929, Geologic maps of the New Idria mine with brief description of the geology: Unpublished report, New Idria Quicksilver Mining Co.
- Larsen, E. S. and Berman, H., 1934, The microscopic determination of nonopaque minerals: *U. S. Geol. Survey Bull.* 679, 294 pages.
- Larson, E. S., 1942, Alkalic rocks of Iron Hill, Gunnison County, Colorado: *U. S. Geol. Survey Prof. Paper* 197-A, 64 pages.
- Louderback, G. D., 1907, Benitoite, a new California gem mineral: *Univ. California, Dept. Geol. Sci. Bull.*, V. 5, p. 149-153.
- _____, 1909, Benitoite, its paragenesis and mode of occurrence: *Univ. California, Dept. Geol. Sci. Bull.*, V. 5, p. 331-380.
- MacGregor, A. G., 1931, Clouded feldspars and thermal metamorphism: *Min. Mag.*, V. 22, p. 524-538.
- Mackowsky, M. T., 1939, Über die chemisch-physikalischen Zusammenhänge in den Granatsystemen von Grossular-Melanit und Melanit-titanmelanit unter dem Einfluss des Eisens bzw. Titans: *Chem. Erde.*, V. 12, p. 123-157.
- Marshall, P., 1911, The geology of the Dun Mountain Subdivision Nelson: *N. Zealand Geol. Surv. Bull.*, no. 12, p. 31-35.

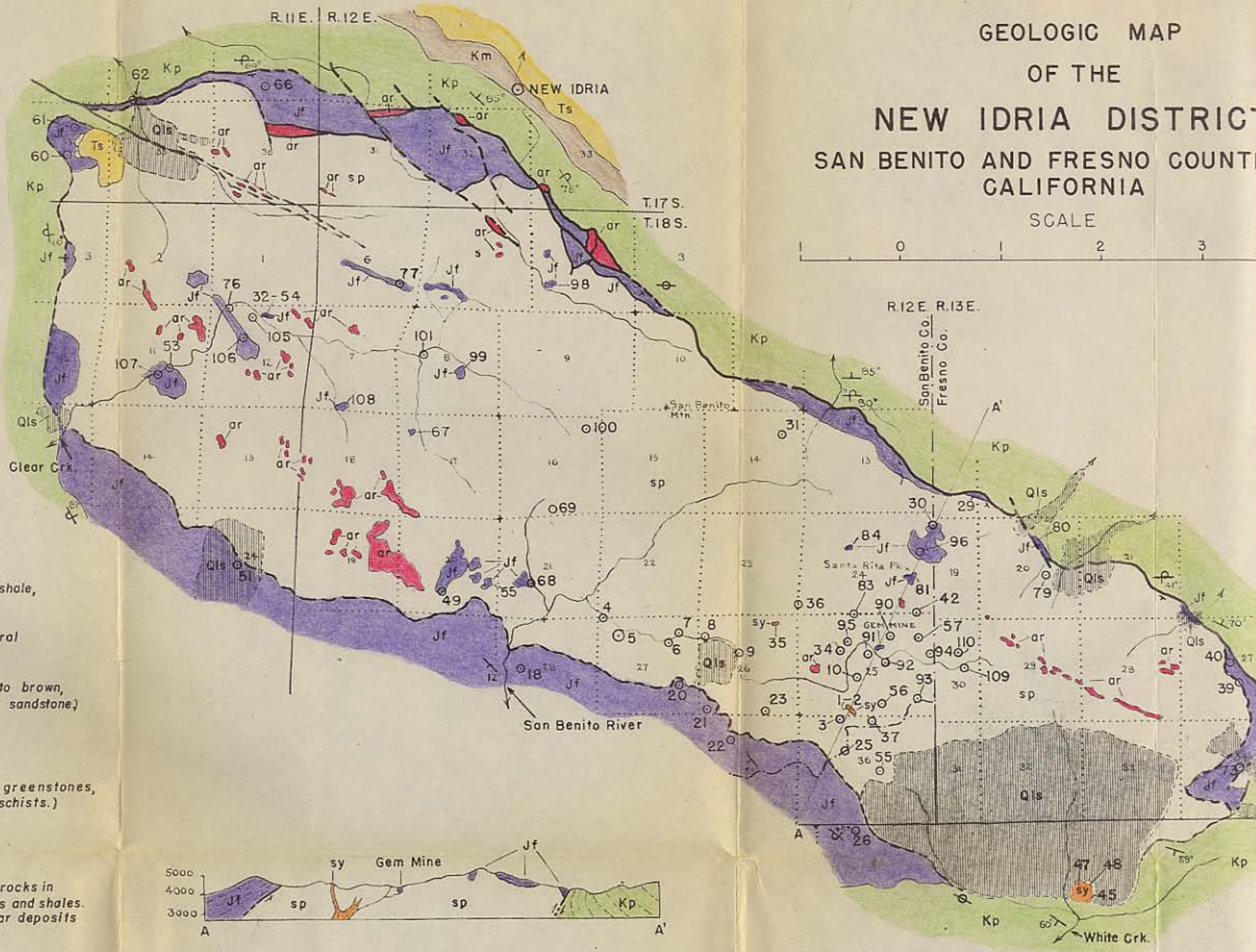
- Megaw, H. D., 1946, Crystal structure of double oxides of the perovskite type: Proc. Physical Soc. London, V. 58, p. 133-152.
- Mielenz, R. C., 1959, The geology of the southwestern part of San Benito County, California: unpublished thesis, Univ. Calif., 295 pages.
- Miller, R., 1953, The Webster-Addie ultramafic ring, Jackson County, North Carolina, and secondary alteration of its chromite: Am. Mineral., V. 38, p. 1134-1147.
- Murdoch, J., 1951, Perovskite: Am. Mineral., V. 36, p. 573-580.
- Niggli, P., 1936, Die Magmentypen: Schweiz. Min. and Pet. Mitt., V. 16, p. 375.
- Nockolds, S. R. and Allen, R., 1954, The geochemistry of some igneous rock series, Part II: Geochimica et Cosmochimica Acta, V. 5., p. 245-285.
- Orcel, J., 1925, Sur deux clinochlores chromiferes du Togo: Compt. Rend. Acad. Sci. Paris, V. 180, p. 836-838.
- Pabst, A., 1951, Minerals of the serpentinite area in San Benito County, California: Rocks and Minerals, V. 26, p. 478-485.
- Palache, C. and Foshag, W. F., 1932, The chemical nature of joaquinite: Am. Mineral. V. 17, p. 308-312.
- Palache, C., Berman, H., and Frondel, C., 1944, Dana's system of Mineralogy: 7th. ed., V. 1, N. Y., John Wiley and Sons, 834 pages.
- Pauling, L., 1930, The structure of the micas and related minerals: Proc. Nat. Acad. Sci., V. 16, pp. 123-129.
- Phillips, R. M., 1939, The general geology of a part of San Benito County, California: Univ. California, unpublished thesis, 76 pages.
- Poldervaart, A. and Gilkey, A. K., 1954, On clouded plagioclase: Am. Mineral., V. 39, pp. 75-91.
- Rankama, K. and Sahama, Th. G., 1950, Geochemistry: Chicago, Univ. Chicago Press, 912 pages.
- Reed, R. D., 1953, Geology of California: Am. Assoc. Petroleum Geologists, 355 pages.

- Reed, R. D. and Bailey, J. P., 1927, Subsurface correlation by means of heavy minerals: Amer. Assoc. Petroleum Geologists Bull., V. 11, p. 359-372.
- Sanero, E., 1933, Sulla presenza della kammererite nella lerzolite di Locana (Piemonte): Periodica Min. Roma, V. 4, p. 473-484.
- Schaller, W. T., 1911, Krystallographische Notizen ueber Albit, Phenakit, und Neptunit: Z. Krist., Band 48, p. 550-558.
- Schutte, C. W., 1931, Occurrence of quicksilver orebodies: Trans. Amer. Inst. Min. Engrs., Tech. Pub. 335, 87 pages.
- Shand, S. J., 1927, Eruptive rocks: N. Y., John Wiley and Sons, 488 pages.
- Shannon, E., 1920, Analyses and optical properties of amesite and corundophilite from Chester, Mass. and of chromium bearing chlorites from California and Wyoming: Proc. U. S. Nat. Mus., V. 58, p. 371-379.
- Sundius, N., 1946, The classification of the hornblendes and the solid solution relations in the amphibole group: Sver. Geol. Und. Årsb., V. 40, no. 4, p. 1-36.
- Switzer, G., 1950, Mineralogy of the California glaucophane schists: California Div. Mines Bull. 161, p. 51-70.
- Taliaferro, N. L., 1943, Franciscan-Knoxville problem: Bull. Amer. Assoc. Petrol. Geol., V. 27, no. 2, p. 109-219.
- Turner, F. J., 1933, The metamorphic and intrusive rocks of southern Westland: Trans. and Proc. New Zealand Inst., V. 63, p. 178-284.
- _____, 1947, Determination of plagioclase with the four-axis universal stage: Am. Mineral., V. 32, p. 389-410.
- Turner, H. W., 1896, Notice of some syenitic rocks from California: Amer. Geol. V. 17, p. 380.
- Tyrrell, G. W., Recent advances in Science-Geology: Science Progress, V. 26, no. 101, p. 26-34.
- Wager, L. R. and Mitchell, R. L., 1950, The distribution of Cr, V, Ni, Co during the fractional crystallization of a basic magma, Int. Geol. Congr. Rept. 18th Sess. 1948, Pt. 2, p. 140-150.

- Waring, C. T. and Anelli, C.S., 1953, Semiquantitative spectrographic method for analysis of minerals, rocks, and ores: Anal. Chem., V. 25, p. 1174-1179.
- Warren, R. E., 1930, The crystal structure and chemical composition of the monoclinic amphiboles: Z. Krist., V. 72, p. 493-517.
- Washington, H. S., 1917, Chemical analyses of igneous rocks: U. S. Geol. Survey Prof. Paper 99, p. 1157-1164.
- _____, 1922, The jades of middle America: Nat. Acad. Sci. Proc., V. 8, p. 319-326.
- Winchell, W. W., 1951, Elements of optical mineralogy, Part II, descriptions of minerals: New York, John Wiley and Sons, 551 pages.
- Wolfe, C. W., 1955, Crystallography of jadeite crystals from near Cloverdale, California: Amer. Mineral., V. 40, p. 248-260.
- Yates, R. G. and Hilpert, I. S., 1945, Quicksilver deposits of central San Benito and northwestern Fresno Counties, California: California Div. Mines Report 41, p. 11-35.
- Yoder, H. S., 1950a, The jadeite problem, Part I and II: Amer. Jour. Sci., V. 248, p. 225-248, 312-334.
- _____, 1950b, Stability relations of grossularite: Jour. Geol., V. 58, p. 221-253.
- Yoder, H. S. and Chesterman, C. W., 1951, Jadeite of San Benito County, California: California Div. Mines Special Report 10-c, 3 pages.
- Zachariasen, W. H., 1930, The crystal structure of benitoite, $BaTiSi_3O_9$: Z. Krist., Band 74, p. 139-146.
- Zedlitz, O., 1933, Über titanreichen Kalkeisengranat: Centr. Mineral. Geol., Abt. A, p. 225-239.
- _____, 1935, Über titanhaltige Kalkeisengranate II: Centr. Mineral. Geol., Abt. A, p. 69-78.
- _____, 1939, Der Perowskit mineralogische and rontgenographische Untersuchungen an Perowskit, Uhligit, Dysanalyt, sowie an deren synthetischen Produkten: Neues Jb. Mineral., Geol. Palaontl., V. 75, p. 245-296.

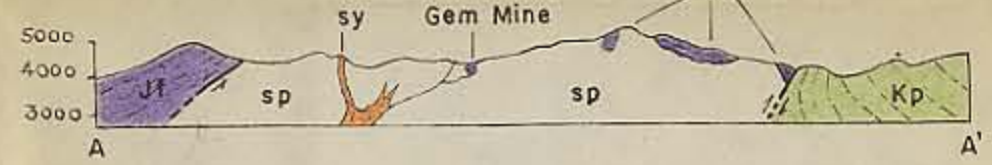
GEOLOGIC MAP OF THE NEW IDRIA DISTRICT SAN BENITO AND FRESNO COUNTIES CALIFORNIA

SCALE



EXPLANATION

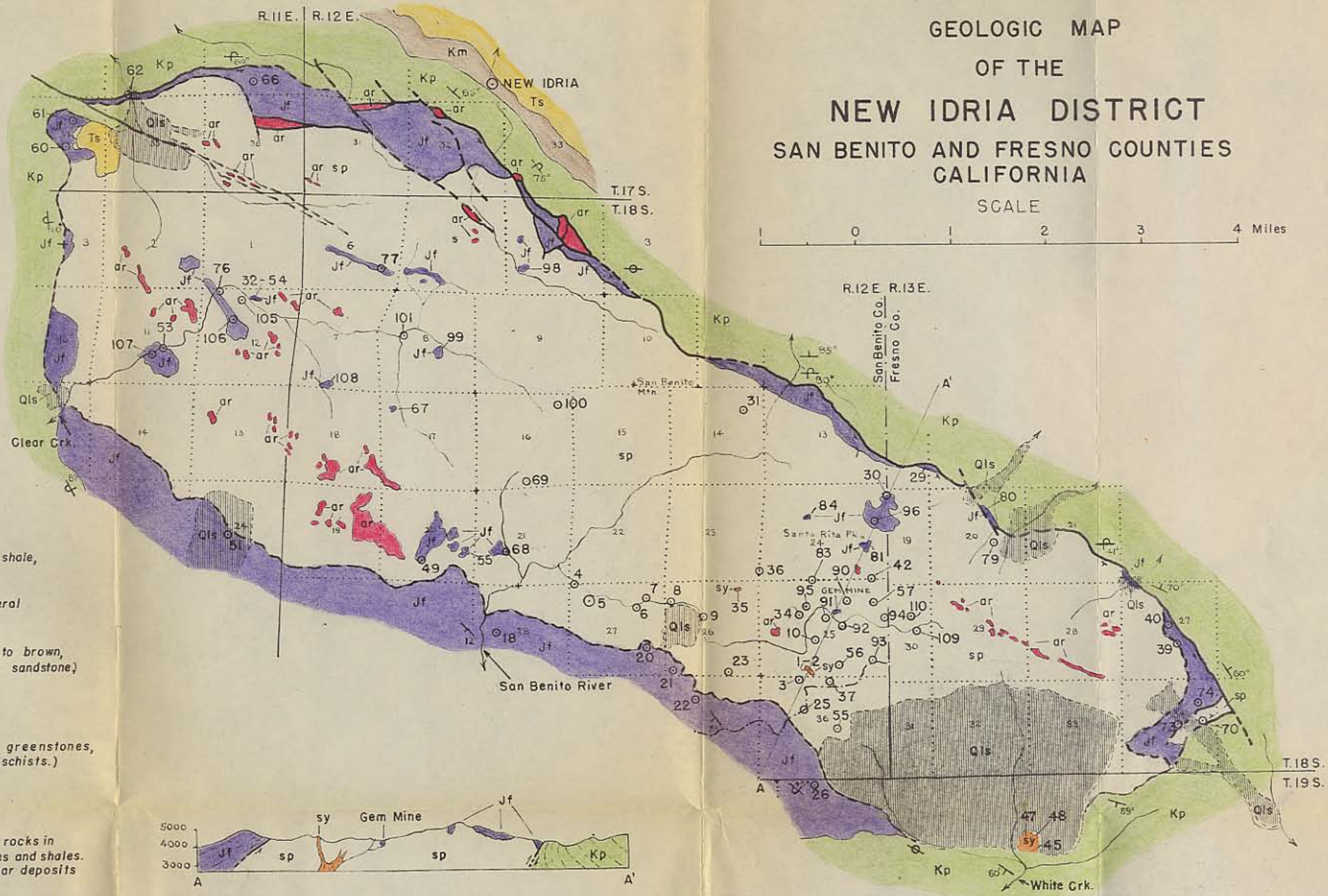
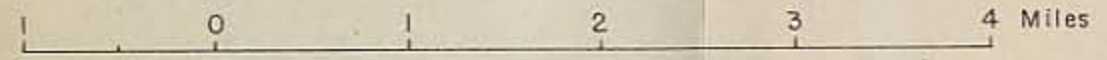
- | | | |
|------------|--|--|
| Quaternary | | Landslide. (Mostly serpentine debris.) |
| | | Sediments, undivided. (Slightly consolidated shale, sandstone, and conglomerate.) |
| Tertiary | | Moreno formation. (Organic shale with several lenses of sandstone.) |
| | | Panoche formation. (Gray shale and gray to brown, massive, concretionary sandstone.) |
| Cretaceous | | Serpentine. |
| | | Franciscan formation. (Greywackes, chert, greenstones, and glaucophane schists.) |
| Jurassic | | Syenite. (Small intrusions.) |
| | | Altered rocks. (Includes silica-carbonate rocks in serpentine and altered sandstones and shales. These rocks contain the cinnabar deposits of the district.) |
-
- | | | | | |
|----------|--|-----------------------------------|--|--|
| Contacts | | Known position. | | Strike and dip of beds. |
| | | Approximate or inferred location. | | Overturned beds. |
| | | Hidden. | | Vertical beds. |
| | | Probably faulted. | | Sample locations, numbers same as cited in text. |
-
- | | | |
|--------|--|---|
| Faults | | Known location. ∇ = upthrust side. |
| | | Approximate or inferred location. |



Base from Idria quadrangle, U.S.G.S. survey 1940.

GEOLOGIC MAP
OF THE
NEW IDRIA DISTRICT
SAN BENITO AND FRESNO COUNTIES
CALIFORNIA

SCALE



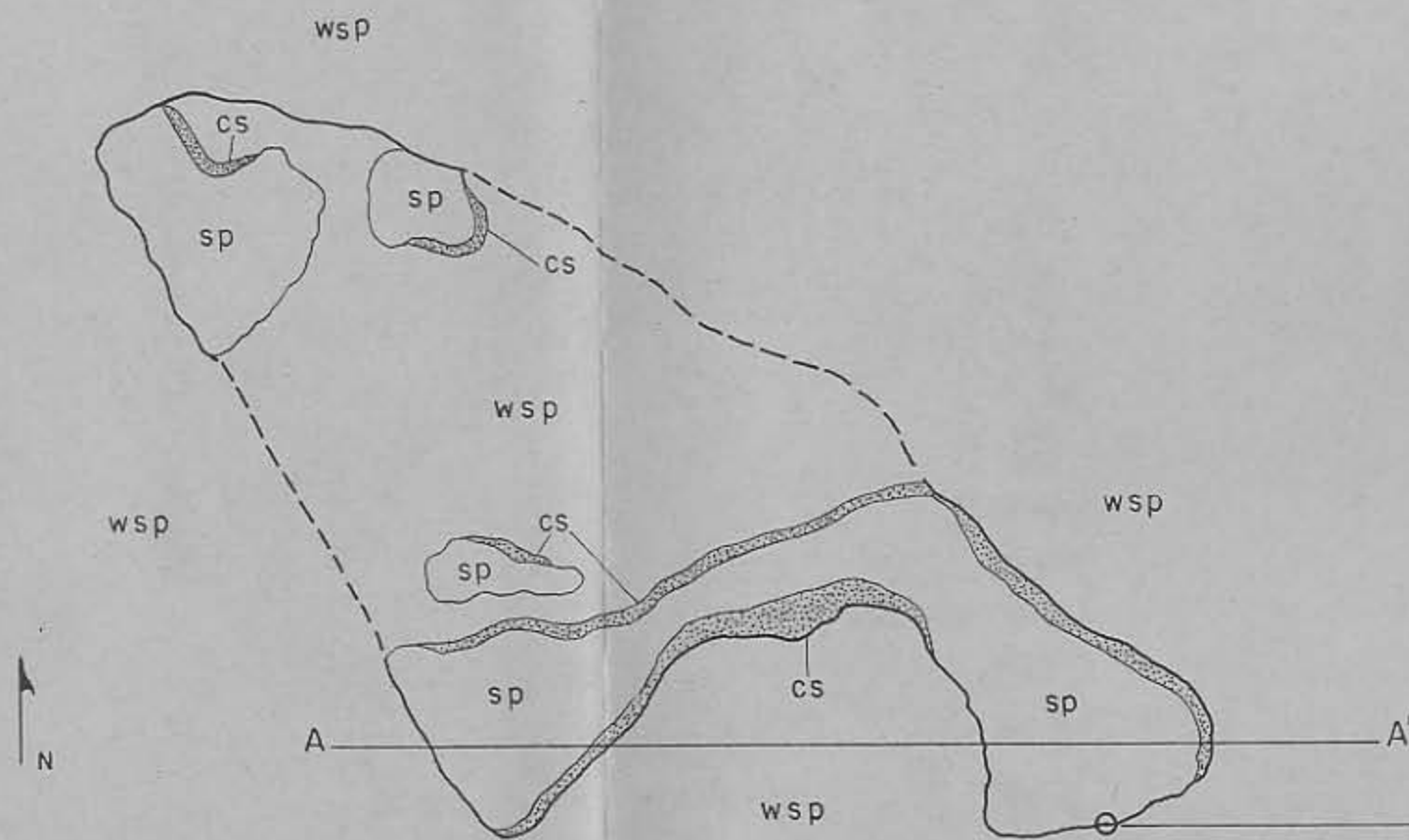
EXPLANATION

- le. (Mostly serpentine debris.)
- nts, undivided. (Slightly consolidated shale, sandstone, and conglomerate.)
- formation. (Organic shale with several lenses of sandstone.)
- e formation. (Gray shale and gray to brown, massive, concretionary sandstone.)
- tine.
- can formation. (Greywackes, chert, greenstones, and glaucophane schists.)
- e. (Small intrusions.)
- d rocks. (Includes silica-carbonate rocks in serpentine and altered sandstones and shales. These rocks contain the cinnabar deposits of the district.)
- osition.
- imate or inferred location.
- r faulted.
- ocation. ∇ = upthrust side.
- imate or inferred location.

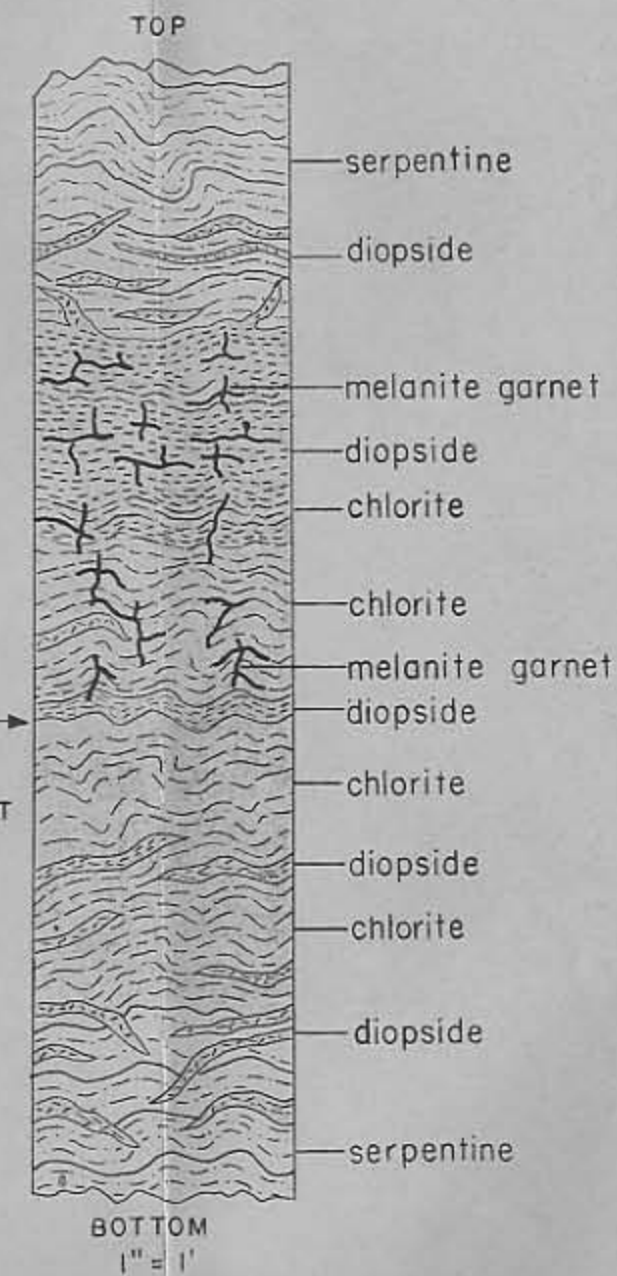
- $\angle 30^\circ$ Strike and dip of beds.
- $\angle 80^\circ$ Overturned beds.
- \perp Vertical beds.
- \odot Sample locations, numbers same as cited in text.

Base from Idria quadrangle, U.S.G.S. survey 1940.

GEOLOGIC MAP
OF
CALC-SILICATE BODY



Vertical Section
across
Calc-Silicate Body



EXPLANATION

wsp Weathered serpentine.

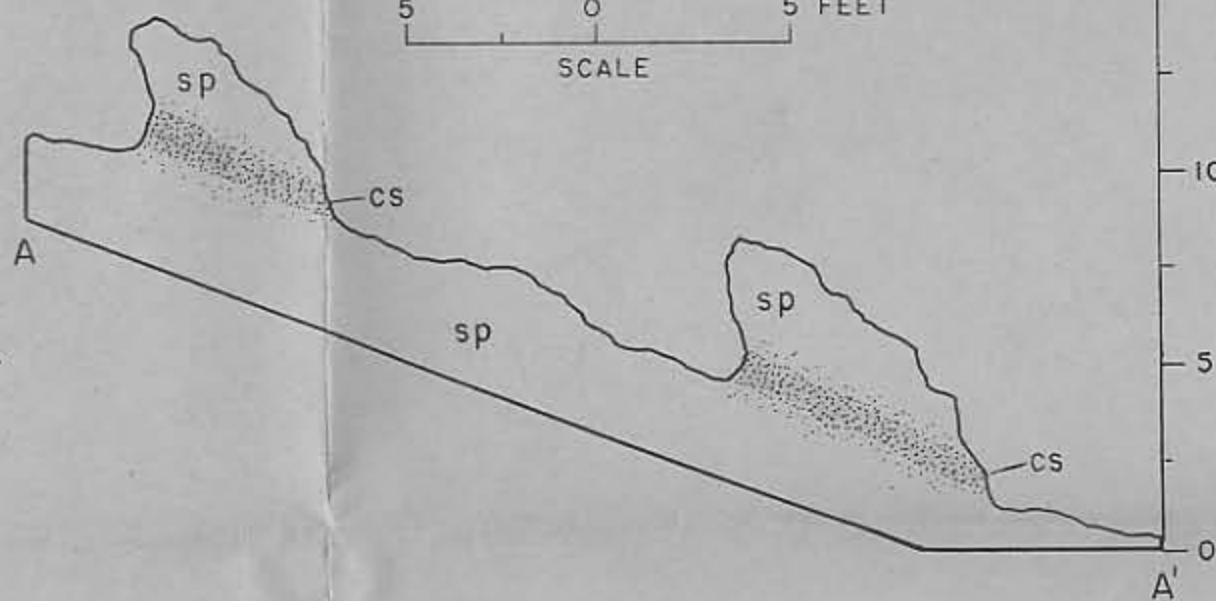
sp Serpentine.

cs Calc-silicate rock.

— Boundary of metasomatism.

- - - Approximate boundary.

— Outcrop boundary.



Sample location number - RGC-34-50

NE 1/4, SEC. 25, R. 12E., T. 18S.

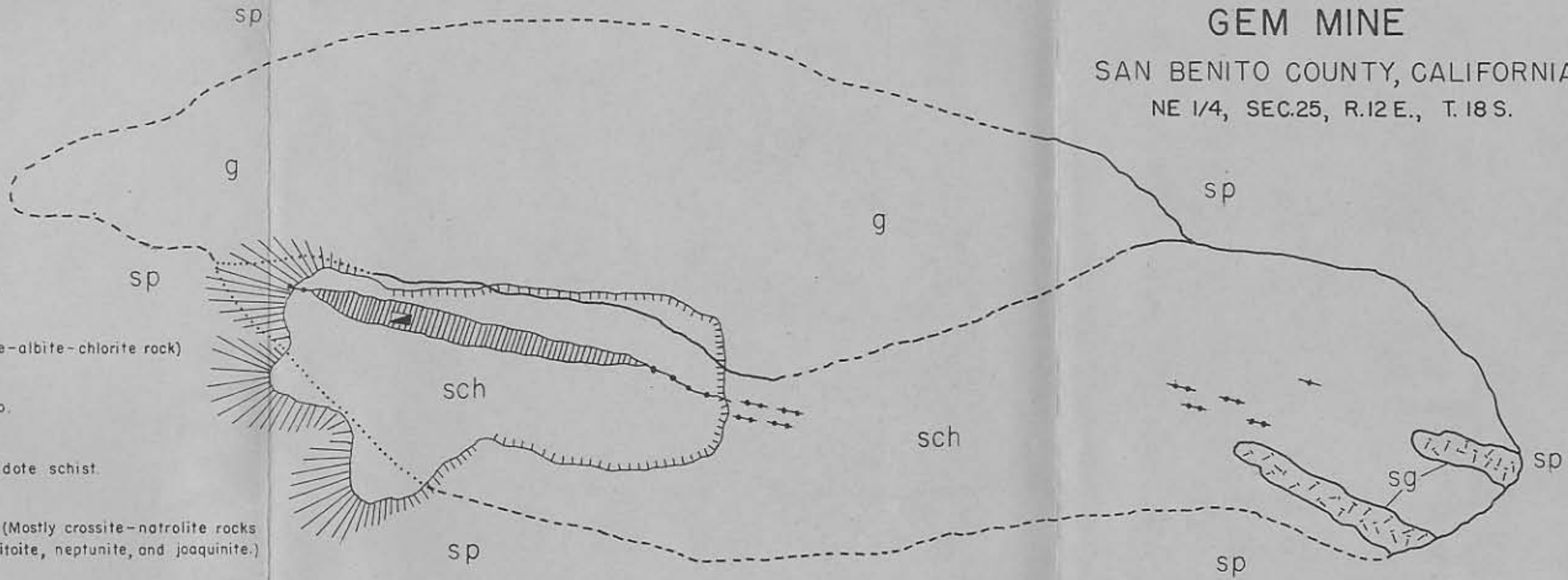
Geology by R.G. Coleman, 1951

GEOLOGIC MAP
OF THE
GEM MINE

SAN BENITO COUNTY, CALIFORNIA
NE 1/4, SEC.25, R.12 E., T.18 S.

EXPLANATION

- sp Serpentine.
- g Greenstone. (pyroxene-albite-chlorite rock)
- sg Saussuritized gabbro.
- sch Albite-crossite-epidote schist.
- ▨ Metasomatic zone. (Mostly crossite-natrolite rocks containing benitoite, neptunite, and joaquinite.)
-  Natrolite veins.
-  Open pit.
-  Dump.
-  Shaft.
-  Strike of schistosity.
-  Known position.
-  Approximate location.
-  Hidden.



Geology by R.G. Coleman, 1951

SPECTROGRAPHIC ANALYSIS OF R FROM SERPENTINE COMPLEX, NEW IDRIA DIS

		B	Si	Al	Ga	Cr	V	Fe	Ti	Nb	Co	Ni	Mn	Mg	Sc	Zr	Ca
SERPENTINE	RGC-25-50	-0X	XX.	+0X	-	-X	-0X	-X.	-00X	-	-0X	-X	-0X	+X.	-	-	-X
"	RGC-90-52	-0X	XX.	-X	-	-X	-0X	-X.	-00X	-	-0X	-X	+0X	+X.	-	-	-0X
"	RGC-35-50	-0X	+X.	+0X	-	+X.	+00X	-X.	-00X	-	+0X	-X	+0X	XX.	-	-	-0X
"	RGC-91-52	-	XX.	+X	-	+X.	-00X	-X.	-00X	-	-0X	-X	+0X	XX.	-	-	-0X
"	RGC-56A-51	+00X	XX.	-X	-	-X	-00X	-X.	-00X	-	-0X	-X	+0X	XX.	-	-	-X.
"	RGC-3-50	-0X	XX.	-X	-	-X	-00X	-X.	-00X	-	-0X	-X	+0X	+X.	-	-	-0X
"	RGC-101-52	-0X	XX.	-X	-	-X	-00X	-X.	+00X	-	-0X	-X	+0X	+X.	-	-	-0X
KÄMMERERITE	RGC-50-51	-0X	XX	+X.	-	XX.	-0X	-X.	-00X	-	+00X	-X	+00X	XX.	-	-	+X.
CHLORITE ROCK	RGC-83-51	-0X	-X.	-X.	-	+0X	-0X	XX.	-X	-	-0X	+0X	+0X	+X.	-00X	-	-X.
DELESSITE	"	-0X	XX.	+X.	-	+0X	-0X	-X.	+00X	-	-0X	+0X	-X	+X.	-	-	+X
ILMENITE	"	-X	-X	+0X	-	-X	-	XX.	XX.	-	+00X	-0X	-X	-X	-0X	+00X	+0X
CHLORITE ROCK	RGC-42-50	-	XX.	-X.	-	-0X	-0X	+X.	-X.	-	-0X	-0X	+0X	+X.	-00X	-	+X.
MELANITE	"	+00X	XX.	-X.	-00X	-0X	+00X	-X.	+X	-00X	-00X	-0X	-X	-X.	-00X	-0X	XX.
CHLORITE ROCK	RGC-79-51	-	XX.	-X.	-00X	+0X	-0X	-X.	+0X	-	-0X	-0X	-X	XX.	-00X	-	-X.
CHLORITE ROCK	RGC-56B-51	-	XX.	-X.	-00X	-0X	-0X	+X.	-X.	-	-0X	-0X	-X	+X.	-00X	-	XX.
PEROVSKITE	"	-	+0X	-0X	-	-00X	-	-X	XX.	-0X	-00X	-	-0X	-X	-00X	+00X	XX
MELANITE	"	-	XX.	-X.	-00X	-0X	-0X	-X.	+X.	-00X	-00X	-0X	-X	-X.	+00X	-0X	XX.
CHLORITE ROCK	RGC-36-50	-0X	XX.	+X.	-	+0X	-X	XX.	+X	-	-0X	+0X	+0X	+X.	-00X	-	XX.
CHLORITE ROCK	RGC-57-51	-	XX.	-X.	-00X	+00X	-0X	XX.	-X.	-	-0X	-0X	-X	-X.	-00X	-	+X.
DELESSITE	RGC-57-51	-0X	XX.	+X.	-00X	+00X	-0X	+X.	+00X	-	-0X	-0X	-X	+X.	-00X	-	+X.
PEROVSKITE	"	-	-X	-0X	-	-00X	-00X	-X	XX.	-0X	-00X	-	-X	-0X	-00X	-0X	XX.
CALC-SILICATE	RGC-37-50	+0X	XX.	XX.	-	-0X	-0X	-X.	-X	-	+00X	-0X	-X	+X.	-00X	-	XX.
PROCHLORITE	"	+00X	XX.	+X	-00X	-0X	-0X	-X.	+00X	-	-0X	-0X	+0X	+X.	-	-	+X.
VESUVIANITE	"	+0X	XX.	XX.	-00X	-0X	-00X	-X.	-X.	-	-00X	-0X	-X	-X.	-00X	-0X	XX.
CALC-SILICATE	RGC-34-50	-0X	XX.	+X	-	+0X	-0X	-X.	+X	-	-0X	-0X	-X	+X.	-00X	-	XX.
ANDRADITE	"	-	XX.	-X.	-00X	-X.	-00X	XX.	-X	-	-	-0X	-0X	+X	-	-0X	XX.
CALC-SILICATE	RGC-109-52	-0X	XX.	-X.	-	+0X	-0X	-X.	+X	-	-0X	+0X	+0X	+X.	-00X	-	XX.
CLINOCHLORE	"	-0X	XX.	+X.	-0X	+0X	-0X	-X.	+00X	-	+0X	-X	+0X	XX.	-	-	-X.
VESUVIANITE	"	-0X	XX.	XX.	-	-0X	-00X	-X.	-X.	-	-00X	+0X	-X	+X.	-00X	-0X	XX.
CALC-SILICATE	RGC-92-52	-0X	XX.	XX.	-00X	-0X	-0X	-X.	+X	-	-0X	-0X	-X	+X.	-00X	-	XX.
VESUVIANITE	"	-0X	XX.	XX.	-00X	+00X	-00X	-X.	-X.	-	-00X	-0X	+0X	-X.	-00X	-0X	XX.
JADEITE FACIES	RGC-105-52	+X	XX.	+X.	-00X	+00X	-0X	-X.	-X	-	+00X	-0X	+0X	-X.	-00X	-	XX.
ALBITE	RGC-54-50	-	XX.	XX.	-00X	-00X	-	+X	-0X	-	-	-	-00X	-0X	-	-	-X
CAMPTONITE	RGC-45-50	+00X	XX.	XX.	+00X	-0X	-0X	-X.	+X	-	-0X	-0X	+0X	-X.	-00X	-	-X.
SYENITE	RGC-47-50	+00X	XX.	XX.	+00X	-00X	-0X	+X.	+X	-	-0X	-0X	+0X	-X.	-00X	-	-X.
ALBITE	"	-0X	XX.	XX.	+00X	-00X	-	+X	-0X	-	-	-	-0X	-X	-	+00X	+X
BARKEVIKITE	"	-	XX.	XX.	+00X	-00X	-00X	+X	-X.	-	-00X	-	-X	+X.	-00X	-0X	-X.
APATITE	"	-	-X	-X	-	-	-	-X	-0X	-	-	-	-0X	-X	-00X	-00X	XX.
Cu-Pb SULFIDE	"	-	+X	-X	-X	-	-	-X	-	-	-	-	-	-	-00X	-	-
ALBITE	RGC-1-50	-	XX.	XX.	-00X	-00X	-	+X	+00X	-	-	-	-0X	+0X	-	-00X	-X.
BENITOITE	GEM MINE	-	XX.	-X	-	-	-00X	-0X	XX.	-0X	-	-	-	-00X	-	-00X	-X.
NEPTUNITE	"	-	XX.	+0X	-	+0X	-	+X.	XX.	-	-0X	-0X	+X	-X.	-	-	-X.
SENSITIVITY		.005	.005	.0001	.004	.0006	.001	.0008	.0005	.001	.008	.005	.0007	.00003	.001	.0008	.01

MELANITE = TITANIAN ANDRADITE
VESUVIANITE = IDOGRASE

Over 10% = XX., 5-10% = +X., 1-5% = -X., .5-1% = +X., .1-.5% = -X., .05-.1% = +0X.,
.005-.01% = +00X., .001-.005% = -00X., .0005-.001% = +000X., .0001-.0005% = -000X.,

ANALYSIS OF ROCKS & MINERALS

FROM

LEX, NEW IDRIA DISTRICT, CALIFORNIA

Ni	Mn	Mg	Sc	Zr	Ca	Y	Yb	Ce	La	Nd	Na	K	Ba	Sr	Ag	Pb	Cu	Sn	Mo	OTHER ELEMENTS
-.X	-.0X	+X.	-	-	-.X	-	-	-	-	-	-	-	-.00X	-	.000X	.00X	+00X	-	-	
-.X	+0X	+X.	-	-	-.0X	-	-	-	-	-	-	-	-	-	.000X	-	+00X	-	-	
-.X	+0X	XX.	-	-	-.0X	-	-	-	-	-	-	-	-	-	.000X	-	+00X	-	-	
-.X	+0X	XX.	-	-	-.0X	-	-	-	-	-	-	-	-.00X	-	.0000X	-	+00X	-	-	
-.X	+0X	XX.	-	-	-.X.	-	-	-	-	-	-	-	-.00X	-	.0000X	-	-.00X	-	-	
-.X	+0X	+X.	-	-	-.0X	-	-	-	-	-	-	-	-.00X	-	.0000X	-	+00X	-	-	
-.X	+0X	+X.	-	-	-.0X	-	-	-	-	-	-	-	-.00X	-	.0000X	-.00X	+00X	-	-	
-.X	+00X	XX.	-	-	+X	-	-	-	-	-	-.0X	-	+0000X	-	+0000X	-	-.00X	-	-	
+0X	+0X	+X.	-.00X	-	-.X.	-.00X	-.000X	-	-	-	-	-	+00X	-.00X	-	-	+00X	-	-	
+0X	-.X	+X.	-	-	+X	-	-	-	-	-	-	-	-.00X	-	-	-	+00X	-	-	
-.0X	-.X	-.X	-.0X	+00X	+0X	-	-	-	-	-	-.0X	-	-.X	-	-	-	+0000X	+00X	-	
-.0X	+0X	+X.	-.00X	-	+X.	-	-	-	-	-	-	-	-.00X	+00X	-.0000X	-	-.00X	-	-	
-.0X	-.X	-.X.	-.00X	-.0X	XX.	+00X	-	-	-.00X	-	-	-	-.00X	-.0X	-	-.0X	-.0X	-	-	
-.0X	-.X	XX.	-.00X	-	-.X.	-	-	-	-	-	-	-	-.00X	-.00X	-.0000X	-	+00X	-	-	
-.0X	-.X	+X.	-.00X	-	XX.	-.0X	-.00X	-	-.00X	-	-	-	-.00X	-.0X	-.0000X	-	+00X	-	-	
-	-.0X	-.X	-.00X	+00X	XX	-.0X	-.00X	-.X	-.X	-.0X	-.0X	-	-.0X	+0X	-	-.00X	-.00X	-	-	
-.0X	-.X	-.X.	+00X	-.0X	XX.	-.0X	-	-	-.0X	-	-	-	+00X	-.0X	-	-	-.0X	-	-	
+0X	+0X	+X.	-.00X	-	XX.	-.00X	+000X	-	-	-	-	-	+0X	-.0X	-.0000X	-	+00X	+00X	-.00X	
-.0X	-.X	-.X.	-.00X	-	+X.	-.00X	-.000X	-	-	-	-	-	-.00X	+0X	-.0000X	-	-.00X	-	-	
-.0X	-.X	+X.	-.00X	-	+X	-	-	-	-	-	-	-	-.00X	-	-.0000X	-	-.0X	-	-	
-	-.X	-.0X	-.00X	-.0X	XX	-.00X	-	-.X	-.X	+0X	-	-	-.0X	+0X	-	-.00X	+000X	-	-	
-.0X	-.X	+X.	-.00X	-	XX	-.00X	-.000X	-	-	-	-.0X	-	-.00X	+0X	-.0000X	-.00X	+00X	-	-	
-.0X	+0X	+X.	-	-	+X	-	-	-	-	-	-	-	-.00X	-.00X	+0000X	+0X	-.00X	-	-.00X	
-.0X	-.X	-.X.	-.00X	-.0X	XX	-.00X	-	-	-	-	-	-	-.00X	+0X	-	-	-.00X	-	-	
-.0X	-.X	+X.	-.00X	-	XX	-.00X	-.000X	-	-	-	-	-	-.00X	+0X	-.0000X	-.00X	-.0X	-	-	
-.0X	+0X	-.X.	-.00X	-.0X	XX.	-.00X	-	-	-	-	-.X	-	-.00X	+0X	-	-	+00X	-.0X	-	Be
-.0X	+0X	-.X.	-.00X	-	XX.	-.00X	-.000X	-	-.00X	-	-.X.	+X	-.X	+0X	-.0000X	-	+00X	-	-	Li
-	-.00X	-.0X	-	-	-.X	-	-	-	-	-	+X.	-	-	-.00X	-	-	-.00X	-	-	
-.0X	+0X	-.X.	-.00X	-	-.X.	-	-	-	-.00X	-	-.X	+X	+0X	+0X	-.000X	-.00X	+0X	-.00X	-	Be
-.0X	+0X	-.X.	-.00X	-	-.X.	-.00X	-.000X	-	-	-	-.X.	+X	+0X	+0X	+000X	-.00X	-.0X	-	-	
-	-.0X	-.X	-	+00X	+X	-	-	-	-	-	+X.	-.X	+0X	+0X	+000X	-	-.00X	-	-	
-	-.X	+X.	-.00X	-.0X	-.X.	-.00X	-	-	-	-	-.X.	-.X	+0X	+0X	-	-.0X	-.00X	-	-.00X	
-	-.0X	-.X	-.00X	-.00X	XX.	+0X	-.00X	-.X	-.X	+0X	+0X	-	-.00X	+0X	-	-	-.000X	-	-	Dy Er
-	-	-	-.00X	-	-	-	-	-	-	-	-	-	+0X	+0X	+0X	XX.	XX.	-	-	HgAuCdZnBi
-	-.0X	+0X	-	-.00X	-.X.	-	-	-	-	-	+X	-	-.00X	-.0X	-	-	-.00X	-	-	
-	-	-.00X	-	-.00X	-.X	-	-	-	-	-	-	-	XX.	-.0X	-	-	-.00X	-	-	
-.0X	+X	-.X.	-	-	-.X	-	-	-	-	-	-.X.	-.X.	-.X	+00X	-	-	+000X	-	-	Li
.005	.0007	.00003	.001	.0008	.01	.003	.0003	.03	.003	.006	.01	.3	.001	.001	.0001	.001	.00005	.004	.0005	

%=+.X, .1-.5%=.X, .05-.1%=+0X, .01-.05%=-.0X

%=+.000X, .0001-.0005%=-.000X, .00005-.0001%=+.0000X, .00001-.00005%=-.0000X

Analyst: Joseph Haffty,
U.S. Geological Survey
Washington, D.C.